# Novel Stimuli-Responsive Supramolecular Hydrogels toward Sophisticated Nano-Micro Biomaterials( Dissertation_全文 )

AUTHOR(S):

Matsumoto, Shinji

# Novel Stimuli-Responsive Supramolecular Hydrogels toward Sophisticated Nano-Micro Biomaterials

**Shinji Matsumoto**

**2008**

**Kyoto University**

## Table of Contents

## Preface and Acknowledgements

The studies presented in this thesis have been carried out under the direction of Professor Itaru Hamachi at the Department of Materials Science & Engineering, Kyushu University, during April 2003 to March 2005, and at the Department of Synthetic Chemistry and Biological Chemistry, Graduate School of Engineering, Kyoto University, during April 2005 to March 2008. This thesis is concerned with the development of the external-stimuli responsive supramolecular hydrogels and the applications toward nano/micro-sized smart biomaterials.

I wish to express my grateful acknowledgement to Professor Itaru Hamachi, whose encouragement and helpful suggestions have been indispensable to the completion of the present thesis. I extend my sincere gratitude to Assistant Prof. Satoshi Yamaguchi, Shun-ichi Tamaru, Masato Ikeda and Shigeki Kiyonaka for their valuable advices, guidance, and fruitful discussions. I am also deeply grateful to Associate Prof. Osamu Hayashida, Assistant Prof. Akio Ojida, and Dr. Shinya Tsukiji for their helpful advice, discussions, and encouragement.

I thanks Mr. Shan-Lai Zhou (Chapter 1), Mr. Koji Ishizuka, Ms. Yuko Iko, Assistant Prof. Kazuhito V. Tabata, Dr. Hideyuki Arata, Prof. Hiroyuki Fujita, Assistant Prof. Hiroyuki Aoki, Prof. Shinzaburo Ito (Chapter 3) for collaboration. I specially thank Prof. Hiroyuki Noji for their supreme advice and collaboration (Chapter 3).

I thank the past and present members of Professor Hamachi laboratory for their suggestions and cooperation, and with whom I shared an enjoyable time. In particular, I express my appreciation to Assistant Prof. Eiji Nakata, Hiroshi Tsutumi, Takayuki Hishiya and Dr. Kei Honda for technical supports and their encouragement. I am also grateful to Dr. Takashi Hiraoka, Dr. Noriyuki Kasagi, Ms. Yasuko Mito-oka, Mr. Hiroki Yamane, Dr. Masaaki Inoue, Mr. Hiroyuki Takemoto, Mr. Takahiro Kohira, Mr. Yoichiro Koshi and Mr. Yoshifumi Miyahara.

I also wish to express my gratitude to Ms. Yuko Aoyagi, Masami Shiozaki, and Ikuyo Miyamae for their help with official business, and I should thank the JSPS (Japan Society for the Promotion of Science) Young Scientist Fellowship for financial support during 2006-2007

Finally, I wish to express my deepest gratitude for my parents Tadashi and Tetsuyo Matsumoto and my brother Kenji Matsumoto, who have supported my education and encouraged my affectionately.

March, 2008

*Shinji Matsumoto*

# General Introduction

Hydrogels constructed by three-dimensional networks of polymer chains that swell in water have a semi-wet environment, an intermediate between liquid state and solid state. Using conventional top-down approaches, one can easily fabricate gels as one likes in the size ranging from centimeter to nanometer scale. The inner solvents are trapped by the 3D mesh-like structures so that they are kept from being dry. On these benefits, hydrogels are generally used in the prevalent commodities such as gelatin for food, soft contact lenses, paper diapers, cosmetic items or air freshener matrix, and etc.[1] In addition, from the viewpoint of the inner 3D matrix capable of thickly immobilizing various substrates and biomolecules, hydrogels are also applied as sensor matrixes, DDS carriers, and scaffold for culturing tissue-cell.[2] Among them, the functional gels, so called "smart gels",[3, 4] which can be a spatially and/or temporally controlled by external stimuli such as temperature, electric field, light, pH, and molecular recognitions, are believed to become one of the requisite soft-materials in chemical, biological, and medical fields.

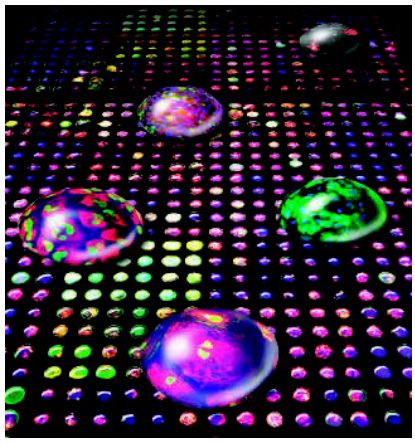

"Smart Biomaterials" excerpted from Science (2004)

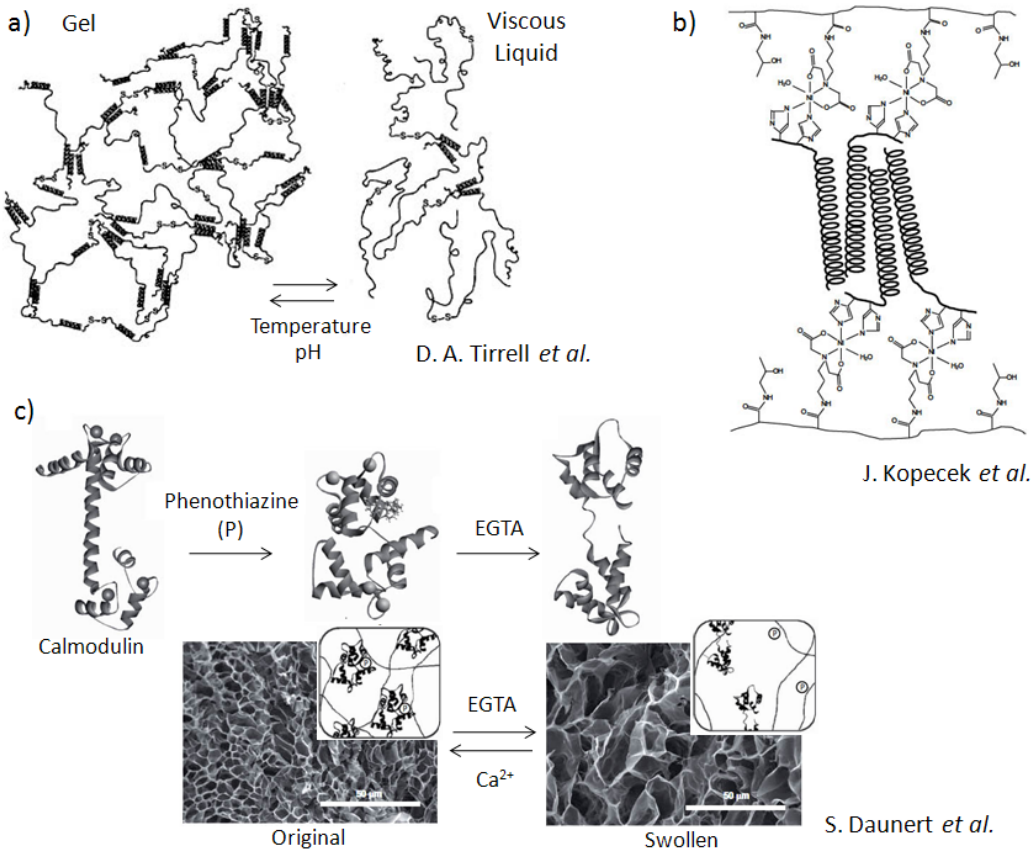


**Figure 1.** Hybrid hydrogels assembled from artificial protein domains.

However there are several factors that limit the broad application of hydrogels, such as their relatively slow response time.[5] For example, a swollen hydrogel might shrink quickly after exposure to a stimulus, but the re-swelling after reversal of the stimulus would happen much more slowly. Some of these limitations are due to how hydrogels are synthesized. As is often the case, naturally-occurring polymer gels such as agarose gel or conventional synthetic polymer gels are used. Traditional synthetic polymer gels, copolymeriazation with crosslinking of polymer precursors, don't perfectly permit the exact control of chain length, sequence or three-dimensional structure. To overcome these problems, several bio-hybrid polymer gels synthesized by genetic engineering methods were developed. For example, several researchers used coiled-coil proteins or calmodulin as a cross-linker between polymer chains instead of chemical cross-linkages (Figure 1).[6] T. J. Deming *et al.* designed and synthesized block copolypeptides containing hydrophobic and hydrophobic amino-acid sequences (Figure 5a).[7] These polymer gels, without additional chemical modification of functional groups, show the rapid "on-off" stimuli-response triggered by a folding/unfolding of the proteins or peptides. Moreover, the easy degradability of amino-acid based hydrogel structures *in vivo* is attractive for biomedical applications. Since there is a limited availability in proteins used as gel components and it is difficult to design and synthesize gels having various additional functions, other innovative approaches for developing the hydrogel are desired.

The supramolecular hydrogel,[8] which is distinguished from conventional polymer gels, has recently attracted much attention. Since the supramolecular hydrogel arises from hierarchical self-assembly of small organic molecules unlike conventional polymer, the functions, e.g. external stimuli responsive, can be rationally designed via designer monomers. In addition, the potential physical properties in biomaterials are also described by several researchers. Therefore, the supramolecular hydrogel is considered to be new semi-wet materials in the next generation.[8a] In this chapter, development and characteristic properties of the supramolecular hydrogels are reviewed.

## From the birth of supramolecualr polymers to the discovery of supramolecular gels

In 1978, J-M. Lehn propounded a groundbreaking concept for "supramolecular chemistry" embracing a philosophy about molecular self-assembly, and he described the importance on controlling weak noncovalent bonding interactions for intra- and intermolecular assemblies.[9] Since then, many researchers' interest has gradually sifted from 1 : 1 molecular interactions, a typical host/guest molecular recognition chemistry, to the higher-order molecular complexes. As the pioneer examples, "supramolecular polymers" were reported by J. Rebek, Jr and E. W. Meijer**.** J. Rebek, Jr *et al*, developed complexes (host : guest molecules = 2 : 1 complex).[10] Two calix[4]arenes was covalently connected at their lower rims, so that polymeric capsules (Figure 2a), $(2:1)_n$ (host/guest) complexes, formed having tensile strengths on the order of $10^8$ Pa, or 1 g/denier (commercial nylon fibers: ~5 g/denier).[11] Recently, E. W. Meijer *et al*. designed a 2-ureide-4-pyrimidon derivative, which formed a robust dimer ($Ka > 10^6$ $M^{-1}$) via multi-hydrogen bonding interactions.[12] On the benefit of the preprogrammed intermolecular hydrogen

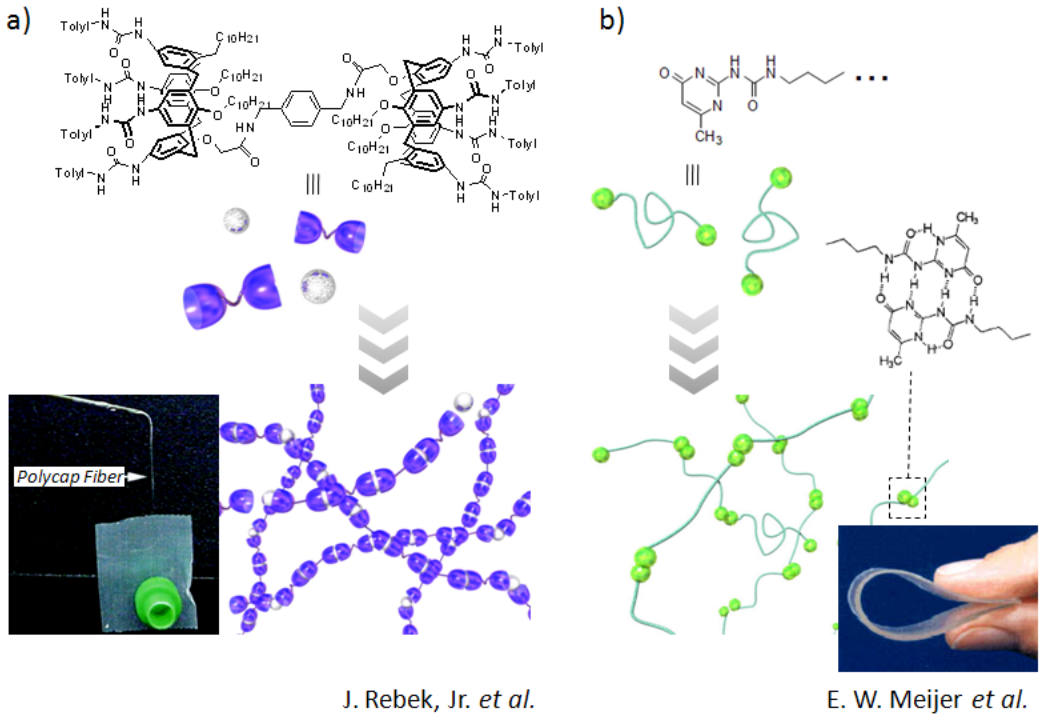


**Figure 2.** Supramolecular polymers; a) Polymer capsule (polycap) formation. Two calixarenes are covalently attached at their lower rims. Encapsulation of guests causes the formation of a linear polymer. b) Poly(ethylene/butylene) functionalized with 2-ureido-4-pyrimidone units.

bonding forces, these molecules self-assembled into one-dimensional polymeric $(1:1)_n$ aggregates having a high viscous property (Figure 2b). These results suggest that it is crucial to precisely control alignment of multi-noncovalent bonding forces, such as hydrogen bonding network, in order to construct the high-order supramoelcular architectures having polymeric behaviors.

One-dimensional fibril-like aggregates of small molecules, "supramolecular polymers", form into various secondary structures such as, tape, ribbon, rod and cylindrical structure depending on the molecular structure, preparation conditions (e.g. solvents and temperature), and concentration (Figure 3a, b).[13] The thick entanglements of the secondary structures formed mesh-like architecture that is able to capture solvents, resulting in gelling solvents ("supramolecular gels").[14] In order to construct stable supramolecular gels, it is critical to design gelator molecules which can assemble into the anisotropic molecular aggregations such as fibril-like architectures, instead of symmetric vesicles and micelles. In the case of development of organogelators that gelate organic solvents,[15] it is now clean that intermolecular hydrogen-bonding interactions act as a main force for the anisotropic and stable molecular assemblies.[16] Therefore, the organogelators can be rationally designed by the elaborate incorporation of hydrogen-bonding units. In contract, in the case of hydrogelators that gelate water,[8] intermolecular hydrophobic interaction is used as a main driving force for the molecular aggregations and the

intermolecular hydrogen bonding acts as an additional force.[17] Although the hydrogen bonding is prominent in controlling their anisotropic assemblies, it is rather tough to regulate the hydrogen bonding networks in aqueous medium because of the strong competition of water molecules. Thus, rational molecular designs of the hydrogelators which are controlled with these hydrophilic/hydrophobic forces are

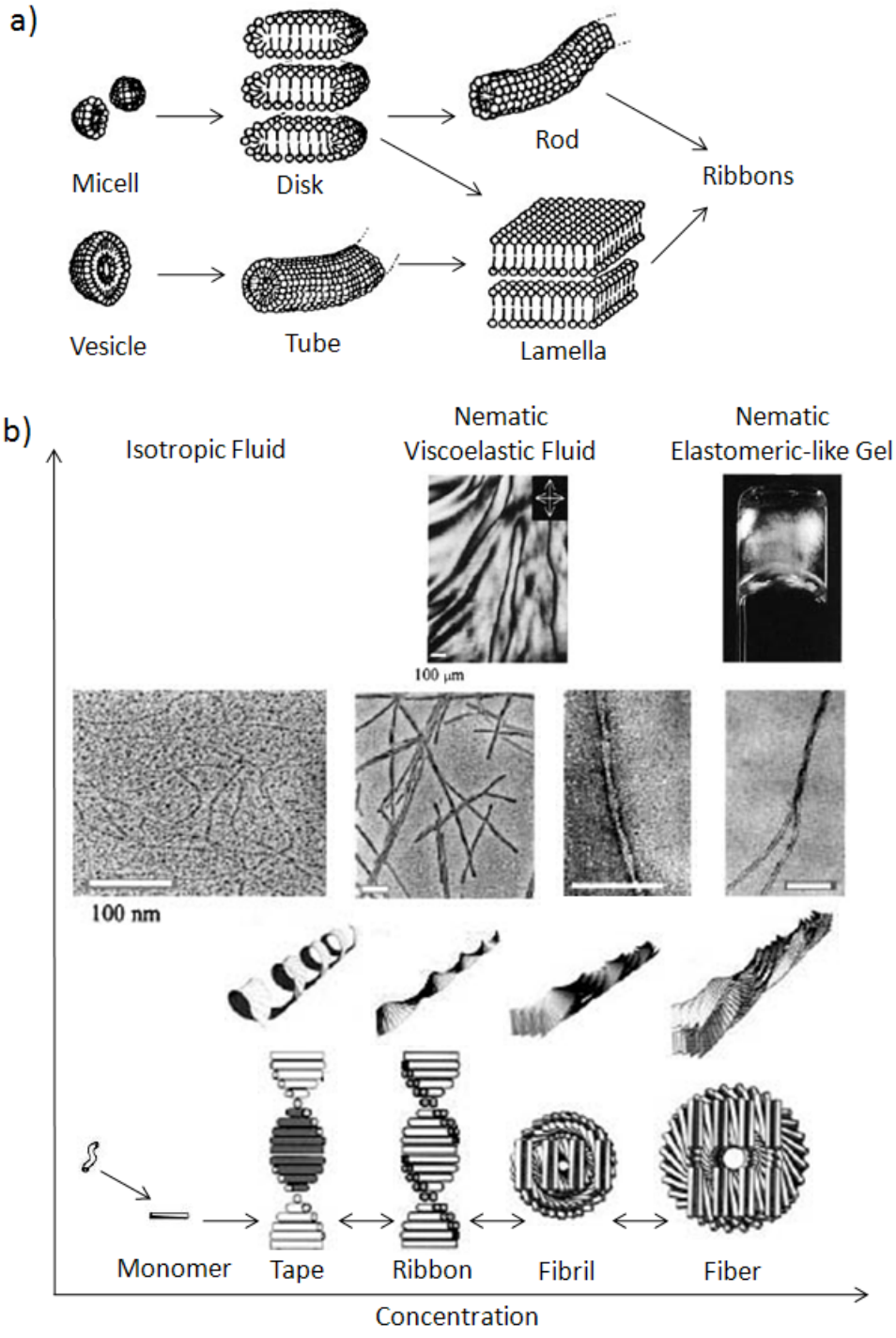


**Figure 3.** Schematic illustration of aggregates of amphiphilic molecules in aqueous solution.

much more difficult than one of the organogelators. In deed, most of surpamolecular hydrogelators so far came from an incidental discovery in organogelator libraries. Although rational molecular designs of the hydrogelators are not still established, the hydrogelators can be divided into several categories on molecular basic framework.

## Supramolecular hydrogelators

Various hydrogelators are categorized into three types based on their molecular structures and characteristics.

### I. Typical amphiphilic hydrogelator

Conventional amphiphiles containing a polar head group and one or two hydrophobic tail groups have been well-known to show with various aggregation morphologies in water, such as vesicle and micelle.[13, 17] Assembly of hydrophobic groups acts as a driving forces to cause aggregation in water media, and the hydrophilic groups interact solvents so that the solvated hydrophilic groups repulsively or attractively interact with one another. Controlling the interactions between the hydrophilic groups by introduction of hydrogen bonding units to the proper position, using suitable units such as urea and amide residues, leads to form the anisotropic molecular aggregation such as fibril-like architectures, instead of vesicle and micelle. Since these conventional amphiphiles are comprised of well-defined molecular modules, it is convenient on combinatorial screening for optimizing structures of hydrogelators (e.g. head-part can be replaced with various function groups, and lipid-chain length can be varied to fine tuning). Until now, three basic types of hydrogels (surfactant types,[18] Gemini-surfactant types,[19] Bolaamphiphile types[20]) have been reported as shown Figure 4.

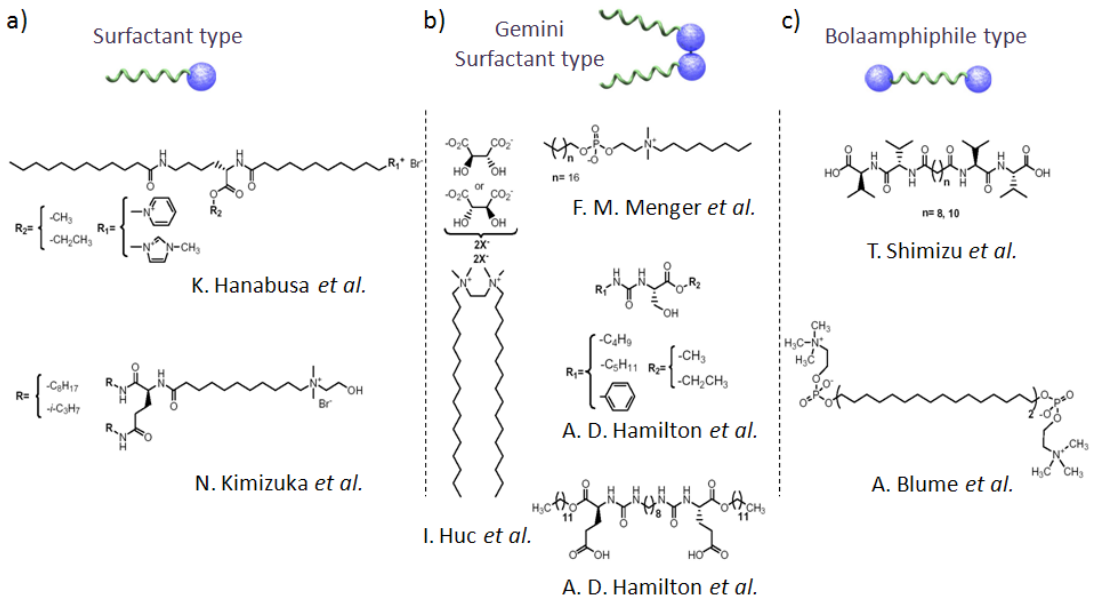


**Figure 4.** Typical amphiphilic hydrogelators; a) Surfactant based hydrogelators, b) Gemini surfactant based hydrogelators, c) Bolaamphiphile based hydrogelators.

## II. Biomolecule-based hydrogelator

Native proteins create a sophisticated higher-order molecular architecture by self-folding of well-defined peptide segments with preprogrammed noncovalent forces in water. De novo peptide/protein design based on mimicking these motifs in order to develop the hydrogelator has several advantages as follows:[8a, 21]

i) Well-defined motifs such as α-helix and β-sheet are preprogrammed for precise aggregation in water. In particular, β-sheet structure can align molecular aggregates precisely by well-developed hydrogen bonding networks, such as anti-parallel β-sheet formations.

ii) Library synthesis to optimize structure is easy by solid-support synthesis methods.

iii) High biodegradable and biocompatible properties in principle.

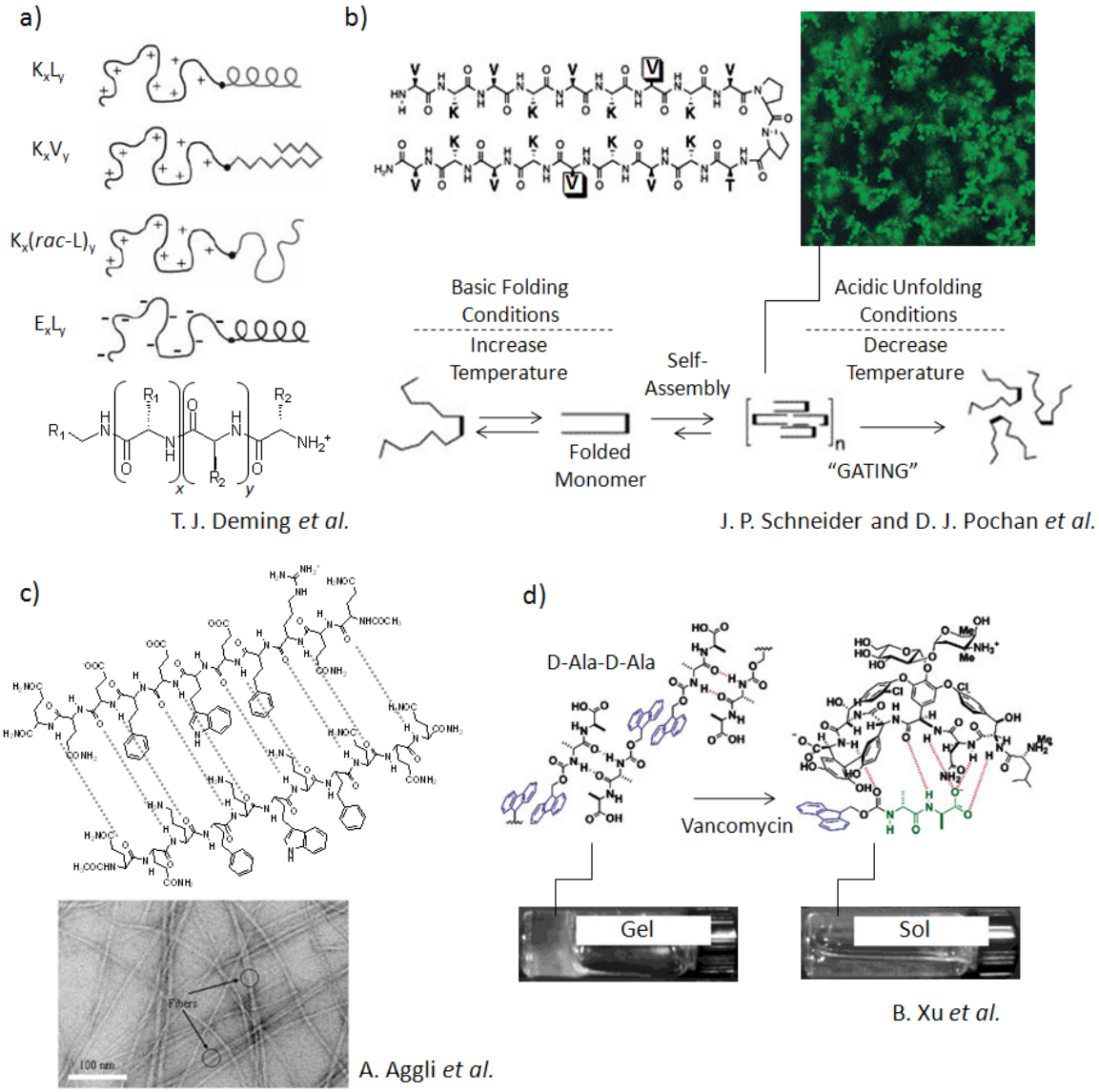


**Figure 5.** Biomolecule-based hydrogelators

As representative examples of peptide-mimic hydrogelators (Figure 5), di-block peptide-based gelator (by T. J. Deming *et al.*),[7] β-hairpin forming gelator (by J. P. Schneider and D. J. Pochan *et al.*),[22] and β-sheet forming gelator (by A. Aggli *et al.*)[23] are reported. Recently, B. Xu *et al.* have developed a very simple di-peptide hydrogelators consisting of *D*-Ala-*D*-Ala protected *N*-terminus with fluorenylmethoxy carbonyl (Fmoc), whose π-π intermolecular interactions act as a crucial factor upon molecular assembly to form stable gel fibers.[24]

### III. Semi-synthetic hydrogeletor comprised of bio/artificial molecular components.

Semi-artificial hydrogels inspired by native molecular segments of DNA, amino acids containing peptides, and sugars containing glycol-lipids have been intensively developed. By virtues of their simple and artificial segments of this gelator, fine-tuning of hydrogelators can be easily accomplished by combinatorial synthesis approaches (Figure 6).[25] As typical examples (Figure 7), there are DNA-lipid based gels (by T. Shimizu, B. H. Kim, *et al.*),[26] peptide-lipid based gels (by S. I. Stupp *et al.*),[27] and glycol-lipid based gels (by T. Shimizu, S. Shinkai, S. Bhattacharya, I. Hamachi, *et al.*).[28] I believe that the strategy mixed of

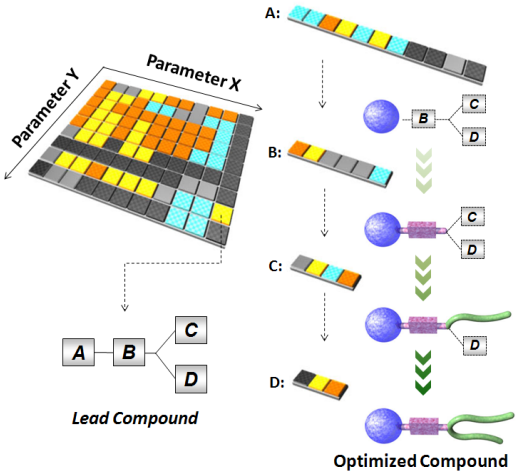


**Figure 6.** Combinatorial synthesis approaches to obtain the optimized hydrogelator

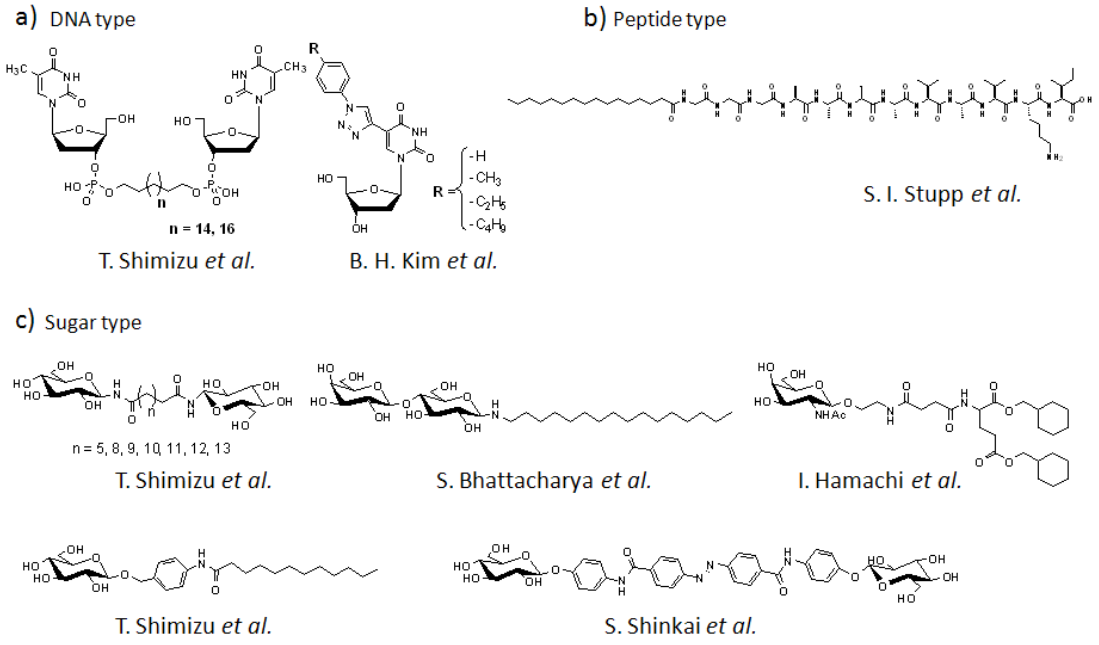


**Figure 7.** Semi-synthetic hydrogeletor comprised of bio/artificial molecular components.

**I** (a combinatorial approach) and **II** (the usage of biomolecules) should be the most convenient and general method for optimal design of supramolecular hydrogelators, which is applicable toward smart biomaterials.

### Supramolecular hydrogels as smart biomaterials

As shown in Figure 8, supramolecular hydrogels have unique features concerning their structures and physical properties.

i) Formation and de-formation of gel fibers constructed by the hierarchical self-assembly of monomer molecules are perfectly reversible.

ii) Since the high aspect ratio of the gel fibers, which have a few nm size in the width and more than several hundred μm size in the length, the surface of gel fibers and the entangling meshes can be applied as active soft-materials

iii) Due to the larger void of the supramolecular hydrogel meshes compared to that of polymer gel, free diffusion of substrates embedded in hydrogel is not hindered.

iv) Because the thermodynamic recombination of fluid fibers can occur, the meshes-like fiber networks distribute homogenously in contrast to the polymer gels meshes.

v) Supramolecular hydrogel have two opposite physical domains, that is, the hydrophilic domain containing much water molecules in the void space in the fiber networks and the hydrophobic domain in fiber inner space arose from self-assembly of hydrophobic moiety of monomer molecules.

This section summarizes various demonstrations by using above unique properties of supramoelcular hydrogels.

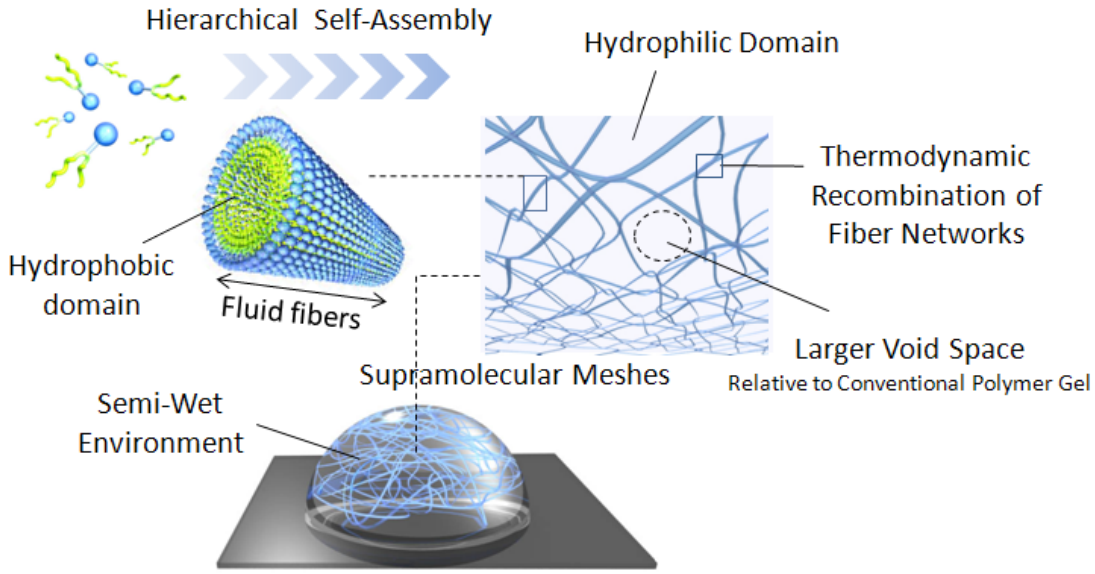


**Figure 8.** Schematic illustration of typical supramolecular hydrogel arising from hierarchal self-assembly of small organic molecules in water.

### Immobilization of biomolecules in supramolecular gels

### Read-out systems of biomolecular recognitions

In 2003, I. Hamachi *et al*. have reported the first demonstration of stable immobilization of a native protein, myoglobin (Mb: an oxygen-storage hemoprotein) in glycolipid-based supramolecular hydrogels without denaturation.[25] They used the oxidation rate indicating the lifetime of the active state of Mb since it is well known that the active state of Mb (i.e., oxy-Mb) gradually changes to the resting form (i.e., ferric-Mb) by a auto-oxidation reaction. The half lifetime of oxy-Mb was estimated to be 8.7 h in the hydrogel and 6.9 h in aqueous solution. These results indicated that the lifetime of the active state of Mb in the gel was comparable to or rather more stable than that of Mb in homogeneous aqueous solution.

Based upon this pioneering work, biochemical studies using inner space of semi-wet supramolecular hydrogel have attracted much attention. The same group, as other demonstration, have applied the supramolecular hydrogel as a protein microarray matrix with *in situ* read-out of the protein activity (Figure 9).[29] In a proof-of-principle experiment, lysyl-endopeptidase (LEP) was used as an enzyme catalyst. They designed a substrate for LEP, that hydrophilic Lys-based peptide bearing an environmental fluorescent DANSen dye at the peptide-terminal. When LEP cleaves the peptide bond between Lys and DNASen, the resultant DANSen shifts from the aqueous cavity of the hydrogel to the hydrophobic domain because of DANSen's strong hydrophobicity, causing the fluorescence increase and blue shift. This assay system could be minimized so that one could construct a supramolecular gel array including a peptide/protein in an active state. This system could be useful not only for screening inhibitors from non-inhibitors, but also for discriminating levels of the inhibition potency in a high-throughput manner. Previously developed protein/peptide chips involve inevitable chemical processes for covalently attaching the protein/peptide to a substrate.[30] In addition, the amount of immobilized protein/peptide is limited to a two-dimensional area, causing a low sensitivity and a low signal/noise level. Furthermore, as the conventional protein/peptide chip is a dry system, the denaturation of immobilized proteins is problematic. In contrast, the present supramolecular hydrogel entraps enzymes in three-dimensional and semi-wet cavities without substantial loss of activity. Although a polymer-based three-dimensional protein-gel chip

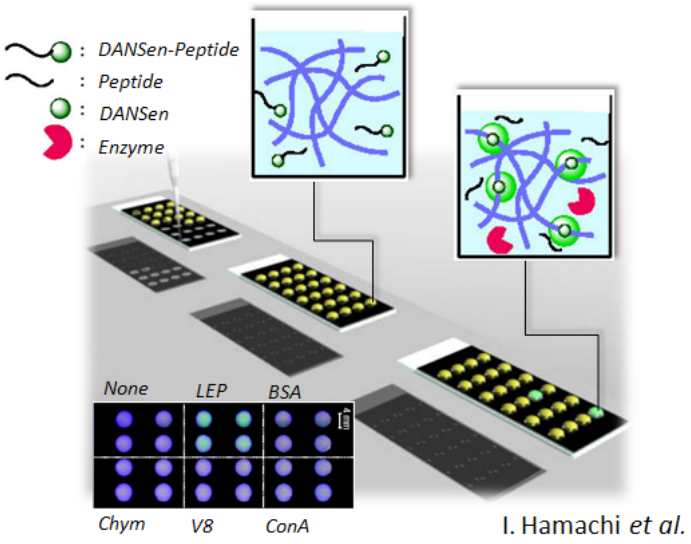


**Figure 9.** Semi-wet peptide/protein micro array using supramolecular hydrogel.

was reported very recently to improve sensitivity, the gel-preparation process, including the photo-polymerization of each spot, is tedious. The supramolecular gel formation reported here is completely spontaneous, and does not require the addition of any polymerization. In addition, the gel is sufficiently mechanically robust that it can be spotted on glass. This will probably permit a more densely packed protein-chip-array than that present 96-well plates. These unique features are intriguing for pharmaceutical and proteome research.

This semi-wet array system can be applied to assay not only protein activities but also molecular recognitions with artificial chemo-sensors. I. Hamachi *et al*. have successfully demonstrated that the cooperative action of artificial receptors with semi-wet supramolecular hydrogels may produce a unique and efficient molecular recognition device not only for the simple sensing of phosphate derivatives, but also for discriminating among phosphate derivatives.[31] These strategies are based on the usage of dynamic change of the location of fluorescent artificial receptors between the aqueous cavity and the hydrophobic fibers upon guest-binding under semi-wet conditions provided by the supramolecular hydrogel. Using a guest-dependent dynamic redistribution of the receptor molecules, a sophisticated tool for molecular recognition of phosphate derivatives can be rationally designed in the hydrogel matrix. That is, the elaborate utilization of the hydrophobic fibrous domains, as well as the water-rich hydrophilic cavities, enables us to establish three distinct signal transduction modes for phosphate sensing: the use of (i) a photo-induced electron transfer type of chemosensor, (ii) an environmentally sensitive probe, and (iii) an artificial receptor displaying a fluorescence resonance energy transfer type of fluorescent signal change. Thus, one can selectively sense and discriminate the various phosphate derivatives, such as phosphate, tyrosine phosphate, phenyl phosphate, and adenosine triphosphate, using a fluorescence wavelength shift and a seesaw type of ratiometric fluorescence change, as well as a simple fluorescence intensity change. This system is promising for the rapid and high-throughput sensing of these phosphate derivatives.

Other detection systems using analyte responsive hydrogel are recently reported. H. Kim *et al*. developed insulin-sensible hydrogelators consisting of a hydrophobic pyrene and a hydrophilic D-gluconolactone moiety (Figure 10a), which, D-glucose interacts strongly with insulin in biological systems.[32] Depending on increase of the insulin concentration, the fluorescence intensity of pyrene decreased and the gel fiber became more than two times thicker than that of initial state, indicating that insulin interacts the gel fiber surface. Since the other sugar-type derivatives did not respond to the insulin, it is confirmed that *D*-gluconolactone based hydrogel detected the specific interaction between insulin and glucose. There are many methods for estimation of insulin, e.g., glucose tolerance test (GTT), insulin tolerance test (ITT), insulin sensitivity test (IST), and continuous infusion of glucose with model assessment (CIGMA). Unfortunately all of these methods require multiple venipunctures, making them relatively impractical for office assessment. Even today, commonly used oral glucose tolerance test (OGTT) does involve several venipunctures and need 2 to 4 h of patient and technician time. By contraries, this supramolecular hydrogel system can simply and high-sensitively detect the insulin at the μg levels.

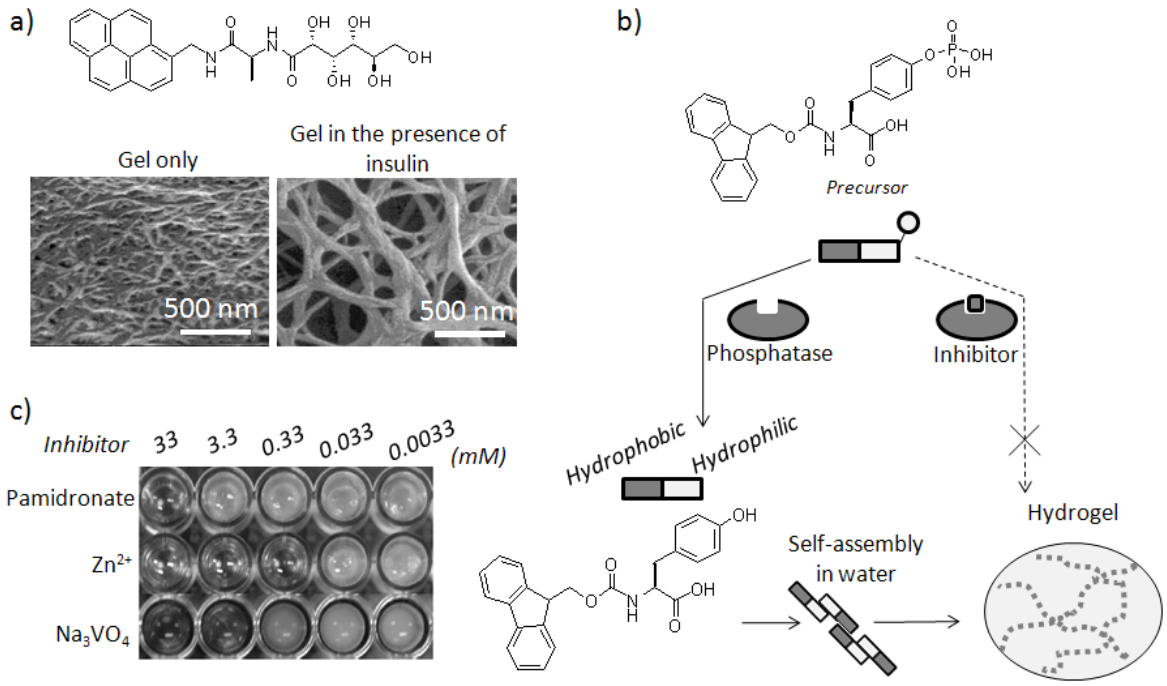


**Figure 10.** a) Insulin-sensitive hydrogelator (B. H. Kim *et al.*). b) The illustration of the design for identifying inhibitors of an enzyme by hydrogelation (B. Xu *et al.*). c) Activity assays of three inhibitors using panel b systems.

In another example, X. Bing and colleagues developed the peptide-based hydrogelators that showed sol-gel transition induced by specific enzymatic reaction (Figure 10b).[33] They successfully applied this system to an inhibitor screening using this hydrogel by macroscopic observation of light-scattering state of the gel and sol. They demonstrated that a non-gelling phosphorylated fluorenylmethoxycarbonyl (Fmoc)-Tyrosine, a precursor of hydrogelator, could gelate by dephosphorylation catalyzed by a phosphatase. Electrostatic repulsion of the negatively charged phosphate groups prevented the gelation of the precursors. Upon removal of the phosphate groups, π-stacking between the fluorenyl groups assisted self-assembly and the formation of a gel. Applying this trick, they have succeeded in development of a quantitative inhibitor assay system by determining the formation or de-formation of hydrogel under various inhibitor conditions (Figure 10c).

These reports suggest that their activities and functions of biomolecules and artificial molecules immobilized in supramolecular hydrogels remain intact and can be read out in situ with gelation properties.

### Additional functions to biomolecular activities

X. Bing *et al*. have found that the enzymes enclosed in the molecular hydrogel exhibited higher activity (e.g., up to eight times) in the organic media (e.g., toluene) than that of unconfined enzymes in water (Figure 11).[34] They suggest that it is likely that several factors contribute to the superactivity of enzymes. That is, (i) Hydrophilicity promotes the substrate to enter the hydrogel across the microinterface, similar to the case of reversed micelles. (ii) Amphiphilic character and/or the molecular superstructure of the self-assembled nanofibers in gel may assist the substrates to approach enzyme and the products to leave enzyme. This assumption agrees with the much lower activity of enzyme (i.e., enzyme immobilized by a randomly crosslinked poly(acrylamide) hydrogel) than that of enzyme in supramolecular hydrogel. (iii) The large pore sizes of the nanofibrous networks can facilitate the mass transport in gel.

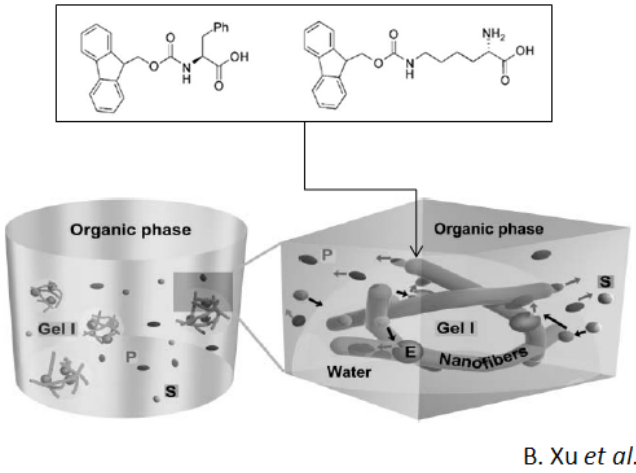


**Figure 11.** Illustration of the molecular hydrogel-immobilized enzymes that catalyze a reaction in organic media (E: enzymes; S: substrates; P: products).

S. I. Stupp *et al*. reported that neural progenitor cells were encapsulated in vitro within a three-dimensional network of nanofibers formed by self-assembly of peptide amphiphile molecules, which were designed to present to cells the neurite-promoting laminin epitope IKVAV. Cells survive during the growth of the nanofibers around them (Figure 12).[27, 35] Relative to laminin or soluble peptide, the artificial nanofiber scaffold induced very rapid differentiation of cells into neurons, while discouraging the development of astrocytes. They claimed that this rapid selective differentiation is linked to the amplification of bioactive epitope presentation to cells by the nanofibers.[36]

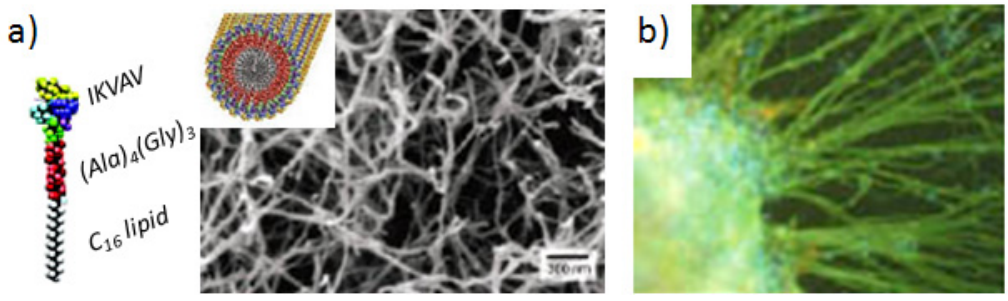


**Figure 12.** a) An IKVAV-containing peptide molecule and its self-assembly into nanofibers. b) Immunocytochemistry of a neural progenitor cell (NPC) neurosphere encapsulated in an IKVAV-PA nanofiber network at 7 days.

### External stimuli responsive functions

This section focuses on examples of external stimuli responsive hydrogels having intriguing responsive properties and prospective functions toward practical applications.

### Volume phase transition gels

Stimuli-responsive volume phase transition in polymer-based hydrogels was pioneered by T. Tanaka, and the potential use of such gels as soft materials in diverse applications has been anticipated.[3] In contrast, few studies of responsive volume change have been performed in supramolecular gels, although there are many reports on stimuli-responsive gel–sol transitions. This may be because noncovalent interactions, relative to covalent ones, are generally too weak to maintain stable polymeric chains prior to and following stimuli, and instead readily degrade into nonpolymeric units producing a sol state but no volume change. I. Hamachi *et al*. reported the first thermal shrinkage of a supramolecular hydrogel (Figure 13a).[28e] This phenomenon suggested that the robust hydrogen-bonding networks assisted by the hydrophobic packing maintain the well-developed fiber structures even at elevated temperature so that the gel shrinks instead of gel-sol transition. This volume phase transition could be applied to control not only the release of hydrophilic oligo-DNA from gel to bulk solution, but also catch hydrophobic substances (e.g. bisphenol A) in hydrophobic domain arising from assembly of lipid-moieties of gelators. This controlling catch and release depending on hydrophilicity/hydrophobicity of substrates is interesting functions, compared to conventional polymer gels without developed hydrophobic domains. However, the examples of stimuli responsive volume phase transition have limited in only two reports until now because the design concept have not yet been established (Figure 13a, b).[24]

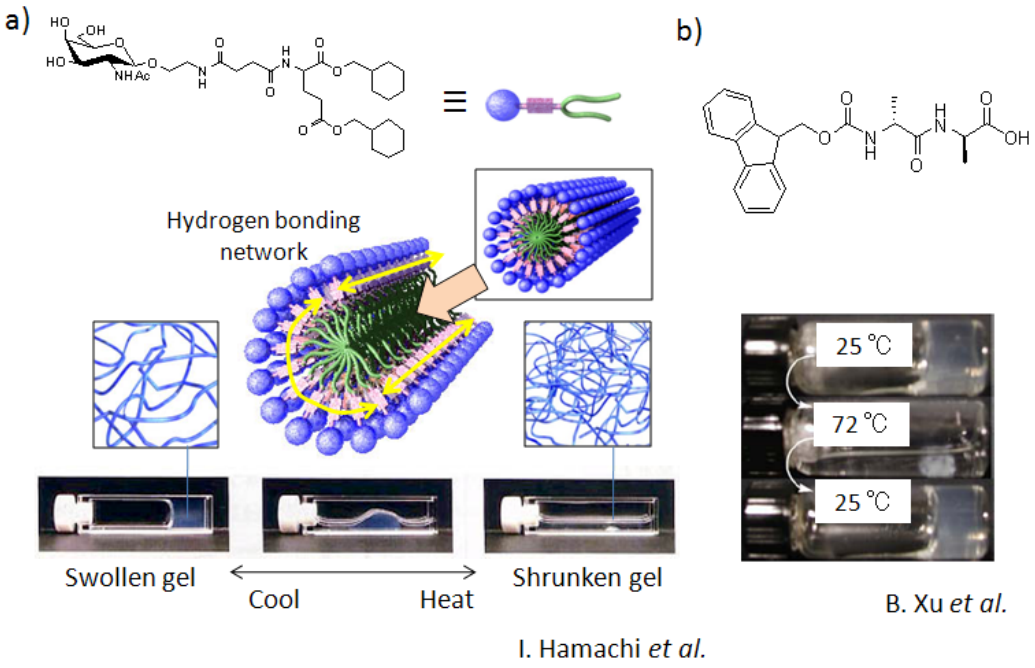


**Figure 13.** Thermal responsive volume phase transition of supramolecular hydrogels.

### Enzyme responsive gel (precursor hydrogelator)

Some precursor hydrogelators which show the sol-gel or gel-sol transition triggered by enzymatic reactions are reported. R. V. Ulijn *et al*. demonstrated the use of a protease to catalyze peptide synthesis (ligation) to produce amphiphilic fluorenylmethoxy carbonyl (Fmoc)-peptide hydrogelators that spontaneously form nanofibrous gel structures (Figure 14a, b).[37] By contraries, X. Bing *et al*. designed hydrogelators attached to protective groups which act as an inhibitor to aggregate *et*

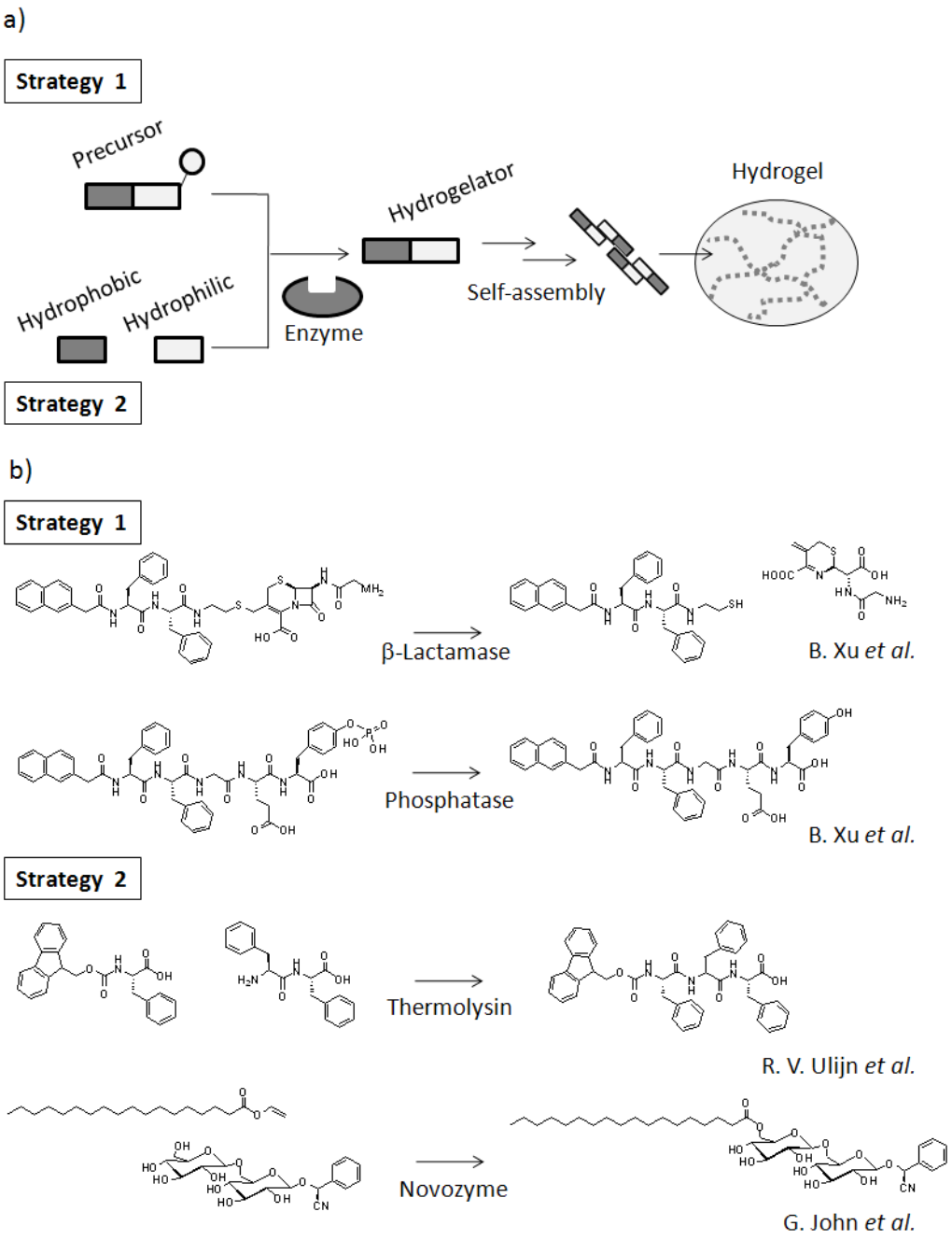


**Figure 14.** Enzymatic responsive gelation systems using precursor of hydrogelator.

*al*. designed hydrogelators attached to protective groups which act as an inhibitor to aggregate molecules (Figure 14a, b). The removal of the protection by enzymatic reactions induced to form gel fibers. They demonstrated that the usage of phosphatase,[38] or β-lactamase[39] are able to catalyze the formation of a supramolecular hydrogel. Moreover, both groups of X. Bing and G. John, *et al*. also reported that reversible sol-gel/gel-sol transitions could be regulated by enzymatic reactions (Figure 14b).[38, 40]

More interestingly, these enzymatic hydrogelation can be used inside *E. coli*. The overexpressed phosphatase in *E. coli* was found to catalyze the formation of the hydrogelator inside the bacterium, and the subsequent intracellular hydrogelation inhibited its growth (Figure 15a).[41] X. Bing *et al.* also tested the enzymatic hydrogelation in vivo: subcutaneous injection of precursor of gelator in mice leads to the formation of supramolecular hydrogel in vivo, and additional in vitro and in vivo tests also confirmed the biocompatibility of the gelator (Figure 15b).[38a] Since many diseases (e.g., cancer, diabetes, Alzheimer's disease, and multiple sclerosis) are associated with the abnormal activities of kinases and/or phosphatases,[42]

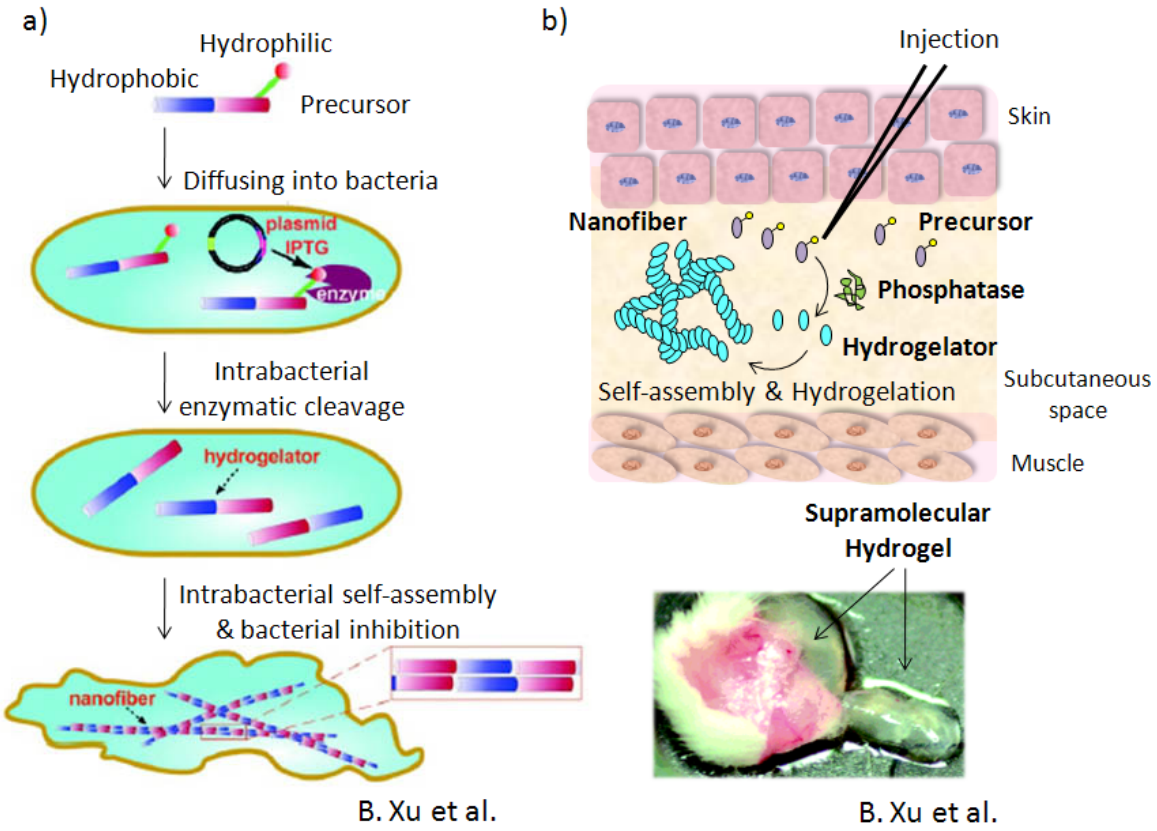


**Figure 15.** a) Schematic representation of intracellular nanofiber formation leading to hydrogelation and the inhibition of bacterial growth. b) Enzymatic hydrogelation in Vivo. Inset; Optical image of the hydrogel formed subsequently 1 h after injecting a peptide-based hydrogelator into the mice.

it is expected that the combination of the kinase/phosphatase switch with supramolecular hydrogelation promises a new way to make and apply biomaterials for therapeutic interventions.

This new methodology—enzyme-regulated self-assembly of small molecules for creating artificial nanostructures—could lead to not only one of the external stimuli responsive semi-matrixes but also a new technique for managing cellular processes, understanding cellular functions, and developing new therapeutics at the supramolecular level.

### Multi external stimuli responsive hydrogels

D. J. Pochan and J. P. Schneider *et al*. developed a β-hairpin peptide-based gelator having multi-stimuli (heat, pH, ionic strength, and light) responsiveness (Figure 16a).[22, 43] The peptide-based hydrogelator consists of alternating polar lysine and apolar valine residues either side of the turn-inducing residues, resulting in an amphiphilic hairpin structure, which is able to self-assemble and form a hydrogel. These lysine residues are protonated at physiological pH and the resulting charge-charge repulsion among the lysine residues inhibits β–hairpin and hydrogel formation. Gelation may be triggered either by increasing the pH to 9.0 to neutralize the lysine residues, or at pH 7.0 by increasing the ionic strength of the solution to 150 mM to screen their charges. Hairpin formation and assembly of the gelator were also

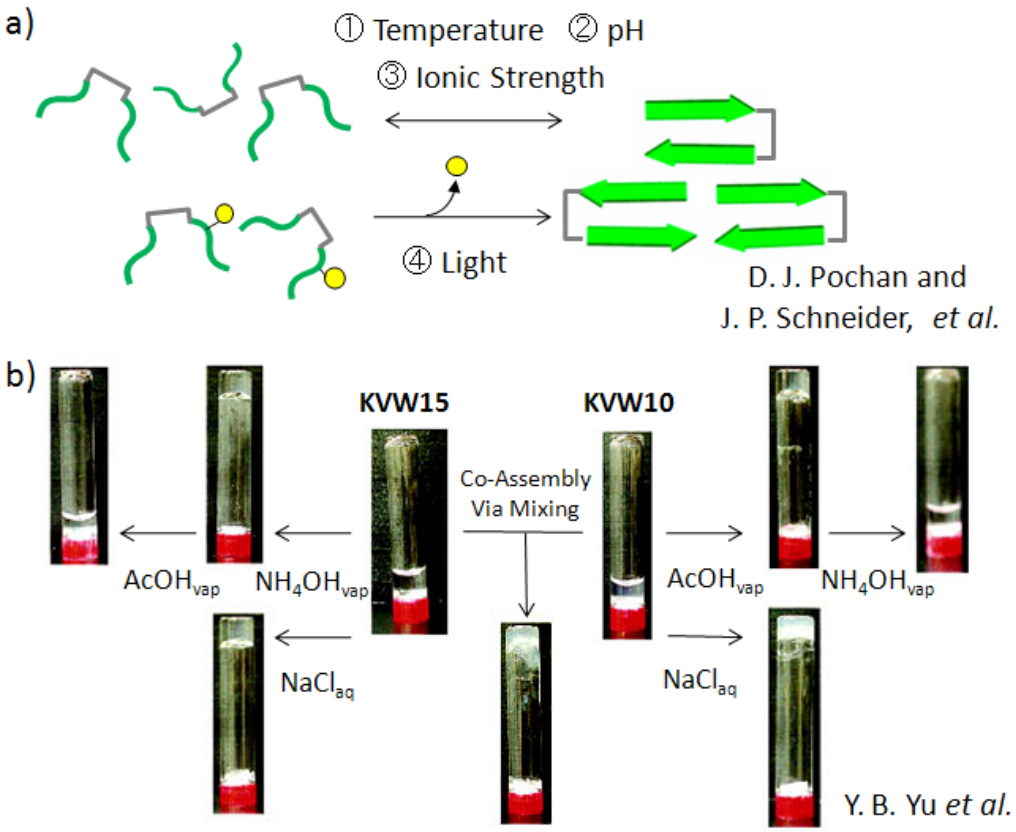


**Figure 16.** Multi-external responsive supramolecular hydrogels.

triggered by elevated temperatures. A modified version of the gelator, where a cysteine residue was incorporated in place of a valine and decorated α-carboxy-2-nitrobenzyl molecule, resulted in photosensitive hydrogelation.

Y. B. Yu, *et al* also develop multi-stimuli responsive hydrogelator, such as pH, ionic, strength, and two-components mixing (Figure 16b).[44] A. Banerjee, *et al* describes the gelation of bola-amphiphiles by a selection of divalent metal ions, to form hydrogels depending on the pH and heat.[45] Sophisticated gel-sol/sol-gel transition regulated by various orthogonal stimuli is potentially intriguing and can facilitate the development of elaborated smart soft materials.

### Photo-responsive hydrogels

Photo-responsive hydrogels are regarded as one of the intriguing biomaterials applicable to biological and medical fields. This is because light is one of the ideal stimuli for fabricating and manipulating various properties of semi-wet materials due to its clean, fast, and spatio-and-temporarily controllable features. However, hydrogels having an efficient photo-responsive property have not been sufficiently developed,[46] compared to other types of hydrogels responsive to physical stimuli such as pH or heat. It is now crucial to explore the capability and investigate the limitation of photo-responsive hydrogels as potential biomaterials.

S. Shinkai and S. Bhattacharya, *et al*. designed several photo-responsive candidate gelators substituted an azobenzen as a photo-sensitive moiety at hydrophobic part.[28c, 47] However, photo-responsive function did not occur because the photo-isomerization of azobenzen could not efficiently perform in the assembled gel fibers where hydrophobic azobenzen groups densely stacked, relative to in the dispersed monomeric state. To overcome this problem, K. Kim *et al*. described a guest-induced stimuli-responsive gel-sol system that photosensitive substances as an additive functional component was mixed to existing supramoelcular gels by applying host/guest molecular recognition (Figure 17a).[48] They demonstrated that cucurbit[7]uril hydrogelator mixed with a azobenzen derivative, which is well known as a guest molecule of a cucurbit[7]uril, showed the gel-sol transition induced by visible light. The gel-sol/sol-gel transition can be repeated many times with alternating UV irradiation and heat treatment. But this preparation conditions (irradiation with UV light (365 nm) for 2 h, heating at 60 ºC for 12 h, under 1.0 N $H_2SO_4$ solution) are impractical for application as biomaterials.

M. Zinic *et al*. developed a photo-responsive hydrogelator based on the molecular maleic acid amide to fumaric acid amide photoisomerization with presence of a small amount of bromine, and presented the evidence that the configurational isomerization induced the morphological transition at the molecular level, exemplified by the conversion of microspheres (maleic-formed) to gel fibers (fumaric-formed) (Figure 17b).[49] J. P. Schneider *et al*. developed a simple light-activated hydrogelation system that employs a designed photocaged peptide (Figure 16a). It remains unfolded and is unable to self-assemble, whereas light irradiation removed the photocage and peptide folding occurred, resulting in

self-assembly of amphiphilic β-hairpins peptide into hydrogel formation.[43b] However, in these two examples, there are concerns about denaturation and toxicity to biomolecules by treatment of bromine or removal cage-residues.

The development of a sophisticated photo-responsive hydrogel are, therefore, desired as temporal and spatial bio-manipulable materials.

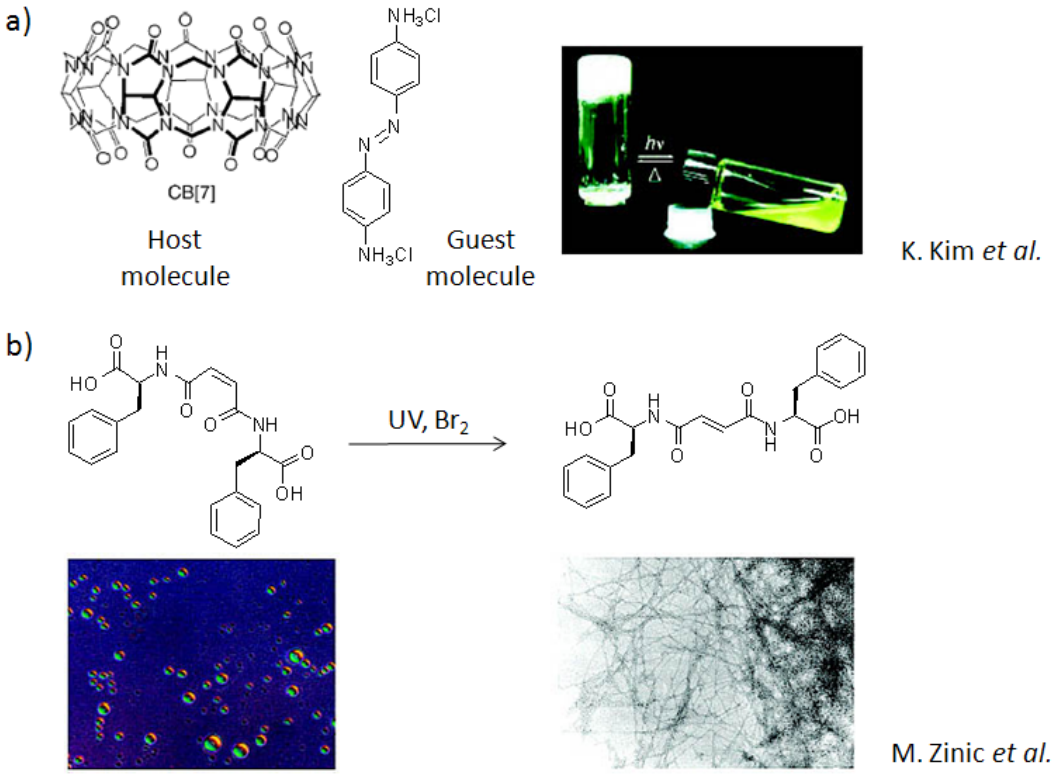


**Figure 17.** Photo-responsive supramolecular hydrogels.

### Supramolecular gels bearing pharmacological activities

J. C. Tiller *et al*. reported that gelation ability of an anionic hydrogelator on the cationic surface was even 50-fold increased (Figure 18a).[50] The same phenomenon was reported by X. Bing's group, exemplified by anitimicrobial hydrogelator based on the anitibiotic vancomycin which surprisingly shows an up to ten times greater antibacterial activity than the unmodified drug (Figure 18b).[51] Although these mechanisms have not been clarified, they indicated that enhanced functions are ascribed to the concentrated function and larger surface of supramolecular nano-micro gel fibers.

X. Bing's group developed a multifunctional hydrogel that employs three small molecules as its structural components—two amino acid derivatives that can reduce inflammation and a bisphosphonate that coordinates with $UO_2^{2+}$ and lowers the toxicity of $UO_2^{2+}$.[52] They administered the hydrogel topically

on wound sites that had been contaminated with (non-radioactive) uranyl nitrate on the skin of mice, so that the mice recovered to normal (Figure 18c). Suprmoalecular hydrogels assembled of pharmacologically active gelators is expected for a synergistic healing material having pharmacological effects, a moisture-rich environment and skin permeabilities (Figure 18d).[53]

There are also some prodrug-type hydrogelators reported by J. van Esch and H. Kim, *et al.*.[54] For example, J. van Esch *et al.* described a two-stage release system (Figure 18e),[54a] where a drug mimic was

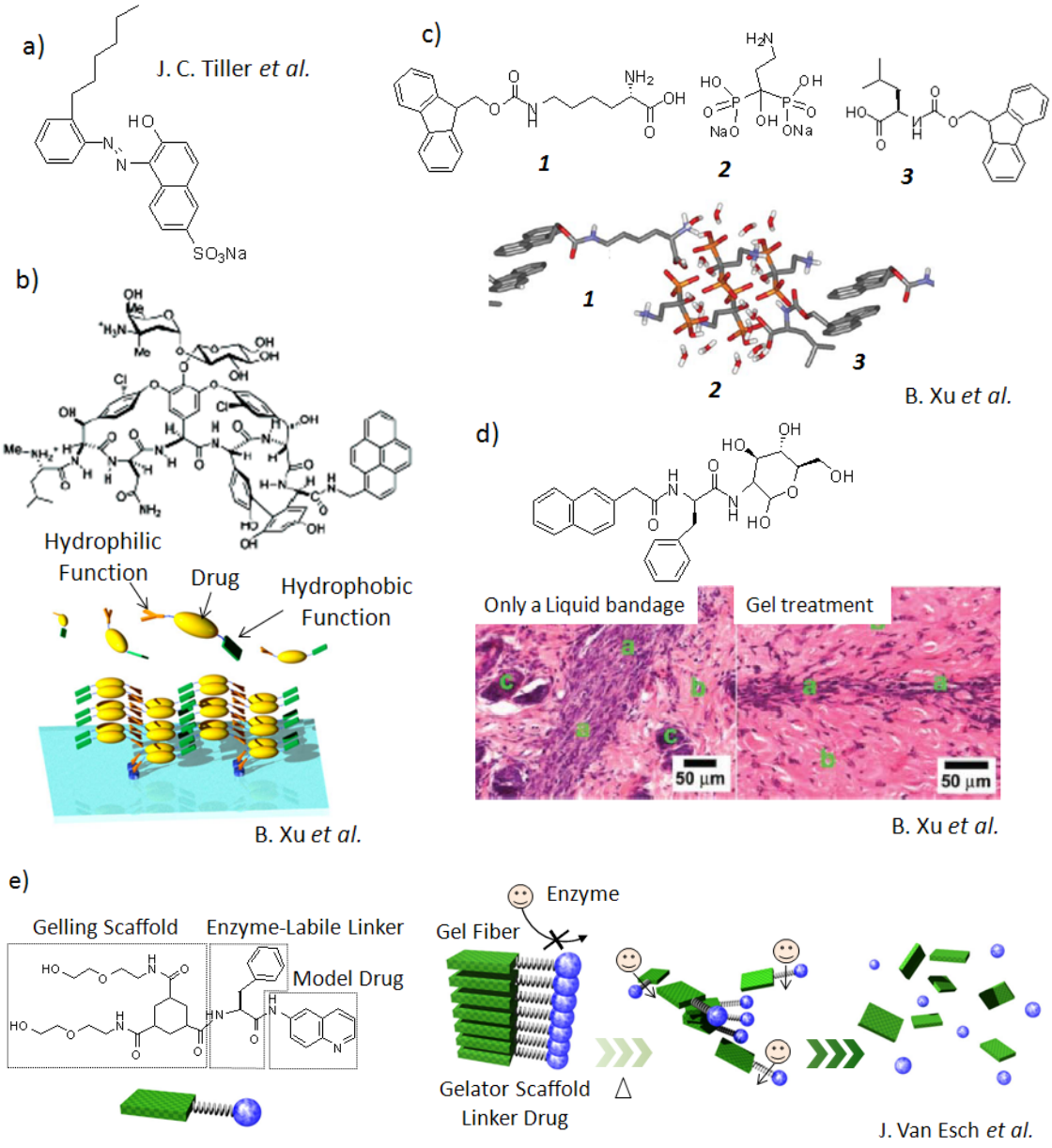


**Figure 18.** Pharmacological supramolecular hydrogelators.

incorporated, via an α-chymotrypsin-sensitive linker, into a hydrogelatior. In the assembled state, enzymes could not access the cleavable linker. Upon application of a stimulus (pH or temperature change), the gel fibers were found to dissociate into individual molecules that could be cleaved by α-chymotrypsin, resulting in the release of a model drug compound.

### Supramolecular hydrogels having inorganic-organic hybrid composites

Supramolecular gels are known to form various exotic nanoaggregates such as fibers, thin sheets, helical, and lamellar structures, so that the morphologies of gel fibers and the surface or the inner space are attractive as template materials for hard materials.

G. John *et al.* reported that urea-based hydrogels stabilized gold nanoparticles by *in situ* reduction (Figure 19a).[55] M. Zinic *et al.* described that incorporation of the $Ru(bpy)_2(dppz)^{2+}$ complex into gel fibers that act as a shield of the emission of the complex from quenching by water molecules, resulting in "switching on/off" behavior (Figure 19b).[56] S. I. Stupp *et al.* described that the fibers are able to direct mineralization of hydroxyapatite to form a composite material (Figure 19c).[57] This alignment is the same as that observed between collagen fibrils and hydroxylapatite crystals in bone. S. Mann *et al.* also reported that nucleation of calcium phosphate occurs specifically on the supramolecular fibers to produce hybrid gels that exhibit enhanced thermal stability, stiffness, and critical stress for breakage by controlling the levels of calcium and phosphate ions associated with a supramolecular fibrous structure (Figure 19d).[58]

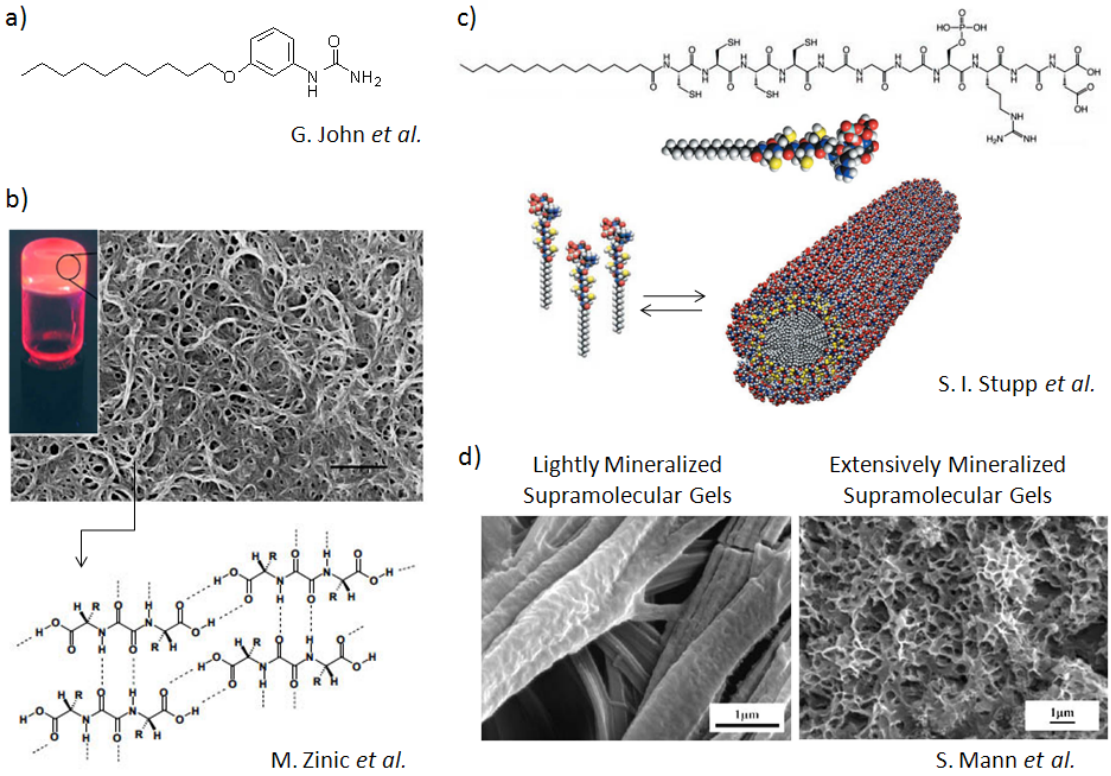


**Figure 19.** Inorganic-organic hybrid supramolecular hydrogels.

## Summary of thesis

Although supramolecular hydrogels have been one of the intriguing soft-matters precisely controllable in molecular level, there is still not any established rational design of functional hydrogel. In this thesis, I describe the molecular design concepts of the functional hydrogelator, exemplifying developments of some novel external responsive hydrogels, conferring pH-resposnvie volume phase transition or photo-resopnsive gel-sol functions, by a combination of rational design and combinatorial synthesis based on detailed molecular structural characteristic of glycol-lipid type hydrogelator. In addition, using these functional hydrogels, the author tried to construct novel bio-gel hybrid systems that the gel functions are induced by biomolecules activities and/or the biomolecular functions are controlled by supramolecular hydrogels.

Chapter 1 described the first pH responsive volume phase transition of supramoleular hydrogels comprised of the two amphiphilic small components. This is called as “supramolecular copolymerization”, in which a hydrogelator is mixed with the non-gelling derivative appending carboxyl- or pyridine-terimnation as pH-sensitive moieties. These two-components gels showed the swelling/shrinkage transition depending on external pH-changes. From investigations at a molecular level, it was obvious that protonation and deprotonation of carboxyl- or pyridine- terminus of the additives contributed to the pH-response. Using these gels, the author have succeeded in controllable drug release depending on pH-changes and difference of hydrophilicity/hydrophobicity of drug substances. In addition, the author has constructed the gel-to-gel communication systems regulated by enzymatic reactions embedded in gels via transporting molecules as well as proton signals.

In Chapter 2, the author designed a photo-responsive supramolecular hydrogel bearing fumaric amide as a trans-cis photo-switching module, showing a gel-sol transition induced by UV light. The trans-cis photo-isomerization of the fumaric-acid moiety effectively caused the formation and deformation of the self-assembled supramolecular fibers, so as to yield the macroscopic hydrogel and the corresponding sol, respectively. And this chapter described that a photo-responsive supramolecular gel droplet with nano- or pico-L volume was prepared in hexadecane. The inter-droplet mass transport and the subsequent enzymatic reactions confined in the interior of the gel droplets were effectively photo-controlled.

Chapter 3 described a library of the pseudo reversible photo-responsive hydrogels by light irradiation and discussed a variety of photo-responsive phenomena. Using the photolithographic technologies, the gels could be fabricated to micro-sized gel-sol pattern, and these limited gel/sol area, where formation/de-formation of supramolecular mesh-like structures occurred, were comfortable to regulate motilities of *E. Coli* bacteria and rotational motion of micro-beads tethered $F_1$-ATPase at a single molecular levels.

The author believes that this present molecular design are valuable for construction of various functional hydrogels and the conceptual system using these hydrogels will be promising strategies on the development of frontier smart biomaterials.

## References and Notes


1. Osada, Y.; Kajiwara, K. *Gel Handbook*; NTS: Tokyo, Japan, **1997**.
2. (a) Lee, K. Y.; Mooney, D. J. *Chem. Rev.* **2001**, *101*, 1869-1879. (b) Luo, Y.; Shoichet, M. S. *Nat. Mater.* **2004**, *3*, 249-253. (c) Lutolf, M. P.; Hubbell, J. A. *Nat. Biotechnol.* **2005**, *23*, 47-55. (d) Ulijn, R. V.; Bibi, N.; Jayawarna, V.; Thornton, P. D.; Todd, S. J.; Mart, R. J.; Smith, A. M.; Gough, J. E. *Materials Today* **2007**, *10*, 40-48.
3. (a) Tanaka, T. *Phys. Rev. Lett.* **1978**, *40*, 820-823. b) Tanaka, T. *Sci. Am.* **1981**, *244*, 124-136. c) Suzuki, A.; Tanaka, T. *Nature* **1990**, *346*, 345-347. d) Annaka, M.; Tanaka, T. *Nature* **1992**, *355*, 430-432. e) Oya, T.; Enoki, T.; Grosberg, A. Y.; Masamune, S.; Sakiyama, T.; Takeoka, Y.; Tanaka, K.; Wamg, G.; Yilmaz, Y.; Feld, M. S.; Dasari, R.; Tanaka, T. *Science* **1999**, *286*, 1543-1545. f) Enoki, T.; Tanaka, K.; Watanabe, T.; Oya, T.; Sakiyama, T.; Takeoka, Y.; Ito, K.; Wang, G.; Annaka, M.; Hara, K.; Du, R.; Chuang, J.; Wasserman, K.; Grosberg, A. Y.; Masamune, S.; Tanaka, T. *Phys. Rev. Lett.* **2000**, *85*, 5000-5003.
4. (a) Irie, M.; Kunwatchakun, D. *Macromol.* **1986**, *19*, 2476-2480. (b) Kwon, I. C.; Bae, Y. H.; Kim, S. W. *Nature* **1991**, *354*, 291-293. (c) Osada, Y.; Matsuda, A. *Nature* **1995**, *376*, 219-219. (d) Osada, Y.; Gong, J. P. *Adv. Mater.* **1998**, *10*, 827-837. (e) Beebe, D. J.; Moore, J. S.; Bauer, J. M.; Yu, Q.; Liu, R. H.; Devadoss, C.; Jo, B. H. *Nature* **2000**, *404*, 588-590. (f) Miyata, T.; Uragami, T.; Nakamae, K. *Adv. Drug Deliv. Rev.* **2002**, *54*, 79-98. (g) Eddington, D. T.; Beebe, D. J. *Adv. Drug Deliv. Rev.* **2004**, *56*, 199-210. (h) Anderson, D. G.; Burdick, J. A.; Langer, R. *Science* **2004**, *305*, 1923-1924. (i) Behl, M.; Lendlein, A. *Materials Today* **2007**, *10*, 20-28.
5. (a) Kajiwara, K.; Ross-Murphy, S. B. *Nature* **1992**, *355*, 208-209. (b) Kopecek, J. *Nature* **2002**, *417*, 388-391.
6. (a) Petka, W. A.; Harden, J. L.; McGrath, K. P.; Wirtz, D.; Tirrell, D. A. *Science* **1998**, *281*, 389-392. (b) Wang, C.; Stewart, R. J.; Kopecek, J. *Nature* **1999**, *397*, 417-420. (c) Jeong, B.; Gutowska, A. *Trends Biotechnol.* **2002**, *20*, 305-311. (d) Jeong, B.; Kim, S. W.; Bae, Y. H. *Adv. Drug Deliv. Rev.* **2002**, *54*, 37-51. (e) Ehrick, J. D.; Deo, S. K.; Browning, T. W.; Bachas, L. G.; Madou, M. J.; Daunert, S. *Nat. Mater.* **2005**, *4*, 298-302.
7. Nowak, A. P.; Breedveld, V.; Pakstis, L.; Ozbas, B.; Pine, D. J.; Pochan, D.; Deming, T. J. *Nature* **2002**, *417*, 424-428.
8. (a) Zhang, S. G. *Nat. Biotechnol.* **2003**, *21*, 1171-1178. (b) Estroff, L. A.; Hamilton, A. D. *Chem. Rev.* **2004**, *104*, 1201-1217. (c) de Loos, M.; Feringa, B. L.; van Esch, J. H. *Eur. J. Org. Chem.* **2005**, *17*, 3615-3631. (d) Sangeetha, N. M.; Maitra, U. *Chem. Soc. Rev.* **2005**, *34*, 821-836.
9. Lehn, J.-M. *Supramolecular Chemistry; Concepts and Perspective*; VCH: Weinheim, Germany, **1995**.
10. Hamann, B. C.; Shimizu, K. D.; Rebek, J. Jr. *Angew. Chem. Int. Ed.* **1996**, *35*, 1326-1329.
11. (a) Castellano, R. K.; Rudkevich, D. M.; Rebek, J. Jr. *Proc. Natl. Acad. Sci, USA* **1997**, *94* 7132-7137. (b) Castellano, R. K.; Clark, R.; Craig, S. L.; Nuckolls, C.; Rebek, J. Jr. *Proc. Natl. Acad. Sci, USA* **2000**, *97*, 12418-12421.

12. (a) Sijbesma, R. P.; Beijer, F. H.; Brunsveld, L.; Folmer, B. J. B.; Hirschberg, J. H. K. K.; Lange, R. F. M.; Lowe, J. K. L.; Meijer, E. W. *Science* **1997**, *278*, 1601-1604. (b) Folmer, B. J. B.; Sijbesma, R. P.; Versteegen, R. M.; van der Rijt, J. A. J.; Meijer, E. W. *Adv. Mater.* **2000**, *12*, 874-878.

13. (a) Kunitake, T.; Okahata, Y.; Shimomura, M.; Yasunami, S.-I.; Takarabe, K. *J. Am. Chem. Soc.* **1981**, *103*, 5401-5413. (b) Schnur, J. M. *Science* **1993**, *262*, 1669-1676. (c) Aggeli, A.; Nyrkova, I. A.; Bell, M.; Harding, R.; Carrick, L.; McLeish, T. C. B.; Semenov, A. N.; Boden, N. *Proc. Natl. Acad. Sci, USA* **2001**, *98*, 11857-11862.

14. (a) Pasini, D.; Kraft, A. *Curr. Opin. Sol. Mater. Sci.* **2004**, *8*, 157-163. (b) Sakurai, K.; Jeong, Y.; Koumoto, K.; Friggeri, A.; Gronwald, O.; Sakurai, S.; Okamoto, S.; Inoue, K.; Shinkai, S. *Langmuir* **2003**, *19*, 8211-8217. (c) Wang, R.; Geiger, C.; Chen, L. H.; Swanson, B.; Whitten, D. G. *J. Am. Chem. Soc.* **2000**, *122*, 2399-2400.

15. (a) Terech, P.; Weiss, R. G. *Chem. Rev.* **1997**, *97*, 3133-3159. (b) Abdallah, D. J.; Weiss, R. G. *Adv. Mater.* **2000**, *12*, 1237-1247. (c) van Esch, J. H.; Feringa, B. L. *Angew. Chem. Int. Ed.* **2000**, *39*, 2263-2266.

16. Fenniri, H.; Packiarajan, M.; Vidale, K. L.; Sherman, D. M.; Hallenga, K.; Wood, K. V.; Stowell, J. G. *J. Am. Chem. Soc.* **2001**, *123*, 3854-3855.

17. Israelachvili, J. N. *Intermolecular and Surface Forces*, 2nd ed.; Academic Press: New York, **1991**.

18.(a) Suzuki, M.; Yumoto, M.; Kimura, M.; Shirai, H.; Hanabusa, K. *Chem. Commun.* **2002**, 884-885. (b) Suzuki, M.; Yumoto, M; Kimura, M.; Shirai, H.; Hanabusa, K. *Chem. Eur. J.* **2003**, *9*, 348-354. (c) Nakashima, T.; Kimizuka, N. *Adv. Mater.* **2002**, *14*, 1113-1116.

19. (a) Menger, F. M.; Peresypkin, A. V. *J. Am. Chem. Soc.* **2003**, *125*, 5340-5345. (b) Oda, R.; Huc, I.; Candau, S. J. *Angew. Chem. Int. Ed.* **1998**, *37*, 2689-2691. (c) Wang, G. J.; Hamilton, A. D. *Chem. Commun.* **2003**, 310-311. (d) Estroff, L. A.; Hamilton, A. D. *Angew. Chem. Int. Ed.* **2000**, *39*, 3447-3450.

20. (a) Kogiso, M.; Hanada, T.; Yase, K.; Shimizu, T. *Chem. Commun.* **1998**, 1791-1792. (b) Kohler, K.; Forster, G.; Hauser, A.; Dobner, B.; Heiser, U. F.; Ziethe, F. Richter, W.; Steiniger, F.; Drechsler, M.; Stettin, H.; Blume, A. . *J. Am. Chem. Soc.* **2004**, *126*, 16804-16813. (c) Fuhrhop, J. -H, Wang, T. *Chem. Rev.* **2004**, *104*, 2901-2937.

21. (a) Zhang, S.; Marini, D. M.; Hwang, W.; Santoso, S. *Curr. Opin. Chem. Biol.* **2002**, *6*, 865-871. (b)Rajagopal, K.; Schneider, J. P. *Curr. Opin. Struct. Biol.* **2004**, *14*, 480-486.

22. (a) Schneider, J. P.; Pochan, D. J.; Ozbas, B.; Rajagopal, K.; Pakstis, L.; Kretsinger, J. *J. Am. Chem. Soc.* **2002**, *124*, 15030-15037. (b) Pochan, D. J.; Schneider, J. P.; Kretsinger, J.; Ozbas, B.; Rajagopal, K.; Haines, L. *J. Am. Chem. Soc.* **2003**, *125*, 11802-11803.

23. Aggeli, A.; Bell, M.; Boden, N.; Carrick, L. M.; Strong, A. E. *Angew. Chem. Int. Ed.* **2003**, *42*, 5603-5606.

24. Zhang, Y.; Gu, H. W.; Yang, Z. M.; Xu, B. *J. Am. Chem. Soc.* **2003**, *125*, 13680-13681.

25. Kiyonaka, S.; Shinkai, S.; Hamachi, H. *Chem. Eur. J.* **2003**, *9*, 976-983.

26. (a) Iwaura, R.; Yoshida, K.; Masuda, M.; Yase, K.; Shimizu, T. *Chem. Mater.* **2002**, *14*, 3047-3053. (b) Iwaura, R.; Yoshida, K.; Masuda, M.; Ohnishi-Kameyama, M.; Yoshida, M.; Shimizu, T. *Angew. Chem. Int. Ed.* **2003**, *42*, 1009-1012. (c) Park, S. M.; Lee, Y. S.; Kim, B. H. *Chem. Commun.* **2003**, 2912-2913.

27. Silva, G. A.; Czeisler, C.; Niece, K. L.; Beniash, E.; Harrington, D. A.; Kessler, J. A.; Stupp, S. I. *Science*, **2004**, *303*, 1352-1355.

28. (a) Nakazawa, I.; Masuda, M.; Okada, Y.; Hanada, T.; Yase, K.; Asai, M.; Shimizu, T. *Langmuir* **1999**, *15*, 4757-4764. (b) Jung, J. H.; John, G.; Masuda, M.; Yoshida, K.; Shinkai, S.; Shimizu, T. *Langmuir* **2001**, *17*, 7229-7232. (c) Kobayashi, H.; Friggeri, A.; Koumoto, K.; Amaike, M.; Shinkai, S.; Reinhoudt, D. N. *Org. Lett.* **2002**, *4*, 1423-1426. (d) Bhattacharya, S.; Acharya, S. N. G. *Chem. Mater.* **1999**, *11*, 3504-3511. (e) Kiyonaka, S.; Sugiyasu, K.; Shinkai, S.; Hamachi, I. *J. Am. Chem. Soc.* **2002**, *124*, 10954-10955.

29. (a) Kiyonaka, S.; Sada, K.; Yoshimura, I.; Shinkai, S.; Kato, N.; Hamachi, I. *Nat. Mater.* **2004**, *3*, 58-64. (b) Zhang, S. *Nat. Mater.* **2004**, *3*, 7-8. (c) Tamarum, S.-I.; Kiyonaka, S.; Hamachi, I. *Chem. Eur. J.* **2005**, *11*, 7294-7304. (d) Koshi, Y.; Nakata, E.; Yamane, H.; Hamachi, I. *J. Am. Chem. Soc.* **2006**, *128*, 10413-10422.

30. (a) Zhu, H.; Snyder, M. *Curr. Opin. Chem. Biol.* **2001**, *5*, 40-45. (b) Zhu, H.; Snyder, M. *Curr. Opin. Chem. Biol.* **2003**, *7*, 55-63.

31. (a) Yoshimura, I.; Miyahara, Y.; Kasagi, N.; Yamane, H.; Ojida, A.; Hamachi, I. *J. Am. Chem. Soc.* **2004**, *126*, 12204-12205. (b) Yamaguchi, S.; Yoshimura, I.; Kohira, T.; Tamaru, S.-I.; Hamachi, I. *J. Am. Chem. Soc.* **2005**, *127*, 11835-11841.

32. Bhuniya, S.; Kim, B. H. *Chem. Commun.* **2006**, 1842-1844.

33. Yang, Z.; Xu, B. *Chem. Commun.* **2004**, 2424-2425.

34. (a) Wang, Q.; Yang, Z.; Wang, L.; Ma, M. L.; Xu, B. *Chem. Commun.* **2007**, 1032-1034. (b) Wang, Q. G.; Yang, Z.; Zhang, X.; Xiao, X.; Chang, C. K.; Xu, B. *Angew. Chem. Int. Ed.* **2007**, *46*, 4285-4289.

35. For other functional peptide fibers, see: (a) Guler, M. O.; Soukasene, S.; Hulvat, J. F.; Stupp, S. I. *Nano Lett.* **2005**, *5*, 249-252. (b) Guler, M. O.; Hsu, L.; Soukasene, S.; Harrington, D. A.; Hulvat, J. F.; Stupp, S. I. *Biomacromolecules* **2006**, *7*, 1855-1863. (c) Guler, M. O.; Stupp, S. I. *J. Am. Chem. Soc.* **2007**, *129*, 12082-12083.

36. Toh, Y.-C.; Ng, S.; Khong, Y. M.; Zhang, X.; Zhu, Y.; Lin, P.-C.; Te, C.-M.; Sun, W.; Yu, H. *Nanotoday* **2006**, *1*, 34-43.

37. (a) Toledano, S.; Williams, R. J.; Jayawarna, V.; Ulijn, R. V. *J. Am. Chem. Soc.* **2006**, *128*, 1070-1071. (b) Ulijn, R. V. *J. Mater. Chem.* **2006**, *16*, 2217-2225. (c) Mart, R. J.; Osborne, R. D.; Stevens, M. M.; Ulijn, R. V. *Soft. Matter.* **2006**, *2*, 822-835.

38. (a) Yang, Z.; Liang, G.; Wang, L.; Xu, B. *J. Am. Chem. Soc.* **2006**, *128*, 3038-3043. (b) Yang, Z.; Xu, B. *Adv. Mater.* **2006**, *18*, 3043-3046. (c) Yang, Z. M.; Liang, G. L.; Xu, B. *Soft Matter* **2007**, *3*, 515-520.

39. Yang, Z.; Ho, P.-L.; Liang, G.; Chow, K. H.; Wang, Q.; Cao, Y.; Guo, Z.; Xu, B. *J. Am. Chem. Soc.* **2007**,

*129*, 266-267.

40. (a) Vemula, P. K.; Li, J.; John, G. *J. Am. Chem. Soc.* **2006**, *128*, 8932-8938. (b) John, G.; Vemula, P. K. *Soft Matter* **2006**, *2*, 909-914.
41. Yang, Z.; Liang, G.; Guo, Z.; Guo, Z.; Xu, B. *Angew. Chem. Int. Ed.* **2007**, *46*, 1-5.
42. den Hertog, J. *EMBO Rep.* **2003**, *4*, 1027-1031.
43. (a) Ozbas, B.; Kretsinger, J.; Rajagopal, K.; Schneider, J. P.; Pochan, D. J. *Macromolecules* **2004**, *37*, 7331-7337. (b) Haines, L. A.; Rajagopal, K.; Ozbas, B.; Salick, D. A.; Pochan, D. J.; Schneider, J. P. *J. Am. Chem. Soc.* **2005**, *127*, 17025-17029.
44. Rarnachandran, S.; Flynn, P.; Tseng, Y.; Yu, Y. B. *Chem. Mater.* **2005**, *17*, 6583-6588.
45. Ray, S.; Das, A. K.; Banerjee, A. *Chem. Mater.* **2007**, *19*, 1633-1639.
46. (a) Irie, M.; Kunwatchakun, D. *Macromolecules*, **1986**, *19*, 2476-2480. (b) Mamada, A.; Tanaka, T.; Kungwatchakun, D.; Irie, M. *Macromolecules*, **1990**, *23*, 1517-1519. (c) Frkanec, L.; Jokic, M.; Makarevic, J.; Wolsperger, K.; Zinic, M. *J. Am. Chem. Soc.*, **2002**, *124*, 9716-9717. (d) Haines, L. A.; Rajagopal, K.; Ozbas, B; Salick, D. A.; Pochan, D. J.; Schneider, J. P. *J. Am. Chem. Soc.* **2005**, *127*, 17025-17029. (e) Tomatsu, I.; Hashidzume, A.; Harada, A. *Macromolecules*, **2005**, *38*, 5223-5227
47. Srivastava, A.; Ghorai, S.; Bhattacharjya, A.; Bhattacharya, S. *J. Org. Chem.* **2005**, *70*, 6574-6582.
48. Hwang, I.; Jeon, W. S.; Kim, H. -J.; Kim, D.; Kim, H.; Selvapalam, N.; Fujita, N.; Shinkai, S.; Kim, K. *Angew. Chem. Int. Ed.* **2007**, *46*, 210-213.
49. Frkanec, L.; Jokic, M.; Makarevic, J.; Wolsperger, K.; Zinic, M. *J. Am. Chem. Soc.* **2002**, *124*, 9716-9717.
50. Bieser, A. M.; Tiller, J. C. *Chem. Commun.* **2005**, 3942-3944.
51. Xing, B.; Yu, C.-W.; Chow, K.-H.; Ho, P.-L.; Fu, D.; Xu, B. *J. Am. Chem. Soc.* **2002**, 124, 14846-14847.
52. Yang, Z.; Xu, K.; Wang, L.; Gu, H.; Wei, H.; Zhang, M.; Xu, B. *Chem. Commun.* **2005**, 4414-4416.
53. (a) Kang, L.; Liu, X. Y.; Sawant, P. D.; Ho, P. C.; Chan, Y. W.; Chan, S. Y. *J. Controlled Release* **2005**, *106*, 88-98. (b)Yang, Z.; Liang, G.; Ma, M.; Abbah, A. S.; Lu, W. W.; Xu, B. *Chem. Commun.* **2007**, 843-845.
54. (a) van Bommel, K. J. C.; Stuart, M. C. A.; Feringa, B. L.; van Esch, *J. Org. Biomol. Chem.* **2005**, *3*, 2917-2920. (b) Friggeri, A.; Feringa, B. L.; van Esch, J. *J. Controlled Release* **2004**, *97*, 241-248. (b) Bhuniya, S.; Seo, Y. J.; Kim, B. H. *Tetrahedron Lett.* **2006**, *47*, 7153-7156.
55. Vemula, P. K.; John, G.. *Chem. Commun.* **2006**, 2218-2220.
56. De Paoli, G.; Dzolic, Z.; Rizzo, F.; De Cola, L.; Vogtle, F.; Muller, W. M.; Richardt, G.; Zinic, M. *Adv. Funct. Mater.* **2007**, *17*, 821-828.
57. Hartgerink, J. D.; Beniash, E.; Stupp, S. I. *Science* **2001**, *294*, 1684-1688.
58. Schnepp, Z. A. C.; Gonzalez-McQuire, R.; Mann, S. *Adv. Mater.* **2006**, *18*, 1869-1872.

# Chapter 1

## pH-Responsive Shrinkage/Swelling of Supramolecular Hydrogel Composed of Two Small Amphiphilic Molecules

**Abstract**

**A pH-responsive volume change function was successfully introduced into a supramolecular hydrogel that contained GalNAc-appended (GalNAc = *N*-acetylgalactosamine) glutamate ester 1 by the simple mixing of it with an appropriate amount of 2a or 2b amphiphilic carboxylic acid. In the 1:1 mixture (1:2), the hydrogel swelled under neutral pH conditions, but shrank to almost half of its original volume under acidic pH conditions. The structure and pH response of the mixed hydrogel were characterized by using X-ray diffraction (XRD), confocal laser scanning microscopy (CLSM), transmission or scanning electron microscopy (TEM, SEM), and Fourier transform IR (FTIR) spectroscopy. Well-developed fibers formed a stable hydrogel by self-assembly, and under acidic conditions the charge of the carboxylic acid terminal (from the carboxylate anion) was neutralized and then these fibers became densely packed. This macroscopic pH response was also applied to the pH-triggered release of bioactive substances and furthermore to a novel communication system between gels triggered by enzymatic pH changes. In this mixed supramolecular hydrogel, the hydrogelator 1 provides a stable hydrogel structure and the additive 2 acts as a commander that is sensitive to an environmental pH signal. Using the present supramolecular copolymerization strategy, we were also able to rationally design a basic pH responsive gel composed of 1 and 3 amphiphilic pyridine. This strategy should be useful principle for the construction of novel, stimuli-responsive, soft materials.**

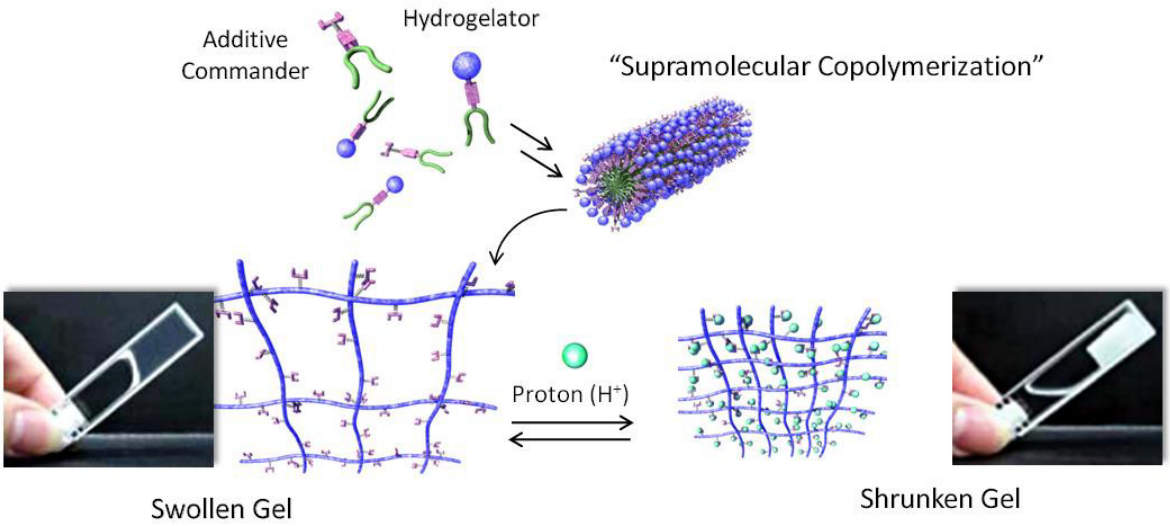

## 1-1. Introduction

The development of stimuli-responsive, synthetic molecules for the construction of molecular memories, switches, and machines has been ongoing for more than two decades.[1–3] Nevertheless, substantial discrepancies between sophisticated molecules in solution and macroscopic materials displaying a macroscopic response have been recognized and investigated. In a pioneering approach, Stoddart and co-workers created a monolayer assembly consisting of catenanes or rotaxanes, which could operate as a switch device to regulate macroscopic electric capacity.[4] Further efforts are, however, required before these small molecules can be applied to molecularly defined macroscopic devices. Most stimuli-responsive macroscopic materials are synthesized from polymers,[5] even though precise manufacturing is generally difficult in polymer-based materials. Supramolecular polymers (noncovalently assembled polymeric molecules) are regarded as intermediates between molecules and conventional polymers. Therefore, it is envisioned that molecularly defined intelligent materials may be constructed by using the supramolecular concept.[6] We recently discovered a supramolecular polymer in the form of a new hydrogel consisting of a low-molecularweight glycosylated amino acetate (a so-called supramolecular hydrogel) that displayed a unique property of thermally induced volume phase transition.[7] Stimuli-responsive macroscopic shrinkage/swelling in polymer-based hydrogels was pioneered by T. Tanaka, and the potential use of such gels as soft materials in diverse applications has been anticipated.[8] In contrast, few studies of responsive volume change have been performed in supramolecular hydro- or organogels although there are many reports of responsive gel–sol transitions.[9, 10] This may be because noncovalent interactions relative to covalent ones are generally too weak to maintain stable polymeric chains prior to and following stimuli, and instead readily degrade into nonpolymeric units producing a sol state but no volume change (Figure 1). Our report of the thermal shrinkage of a supramolecular hydrogel suggested, however, that a thermally stable noncovalent polymer chain composed of multiply accumulated interactions can display thermal

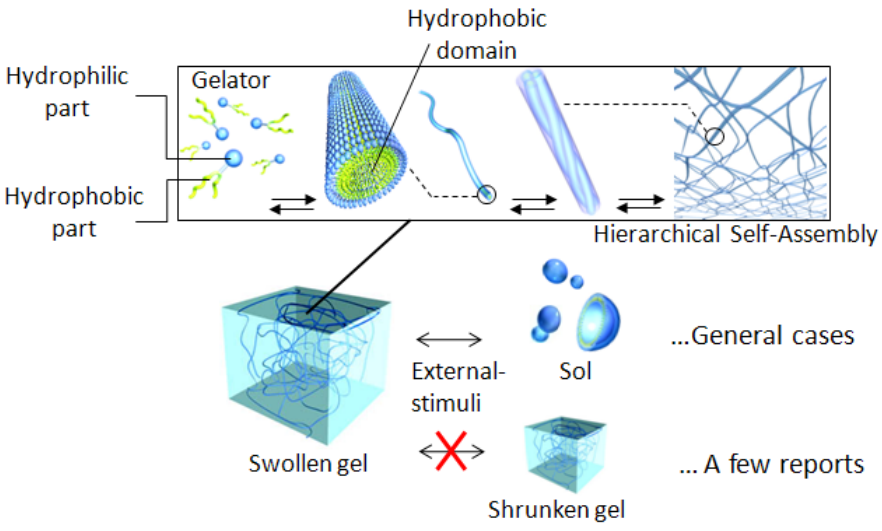


**Figure 1.** Schematic illustration of hierarchical self-assembly process of supramolecular hydrogelators.

shrinkage instead of simply dissolving.[7a, 11] The design at the molecular level of such a unique feature will provide a new category of supramolecular materials. From this perspective, we have investigated supramolecular systems that exhibit various stimuli-responsive volume changes. We recently reported the addition of a carboxylic acid derivative to the supramolecular gelator matrix to form a highly stable self-assembled nanofiber in small amounts. This matrix revealed pH-dependent thermal behavior of the mixed hydrogel, that is, gel–sol transition at neutral pH and volume phase transition at acidic pH.[9n] Here we describe the successful pH-triggered shrinkage or swelling of a supramolecular hydrogel, which was produced by mixing optimized structures and amounts of amphiphilic carboxylic acids with the hydrogelator. This supramolecular copolymerization strategy is widely applicable for the production of novel stimuli-responsive supramolecular materials (Figure 2).[12]

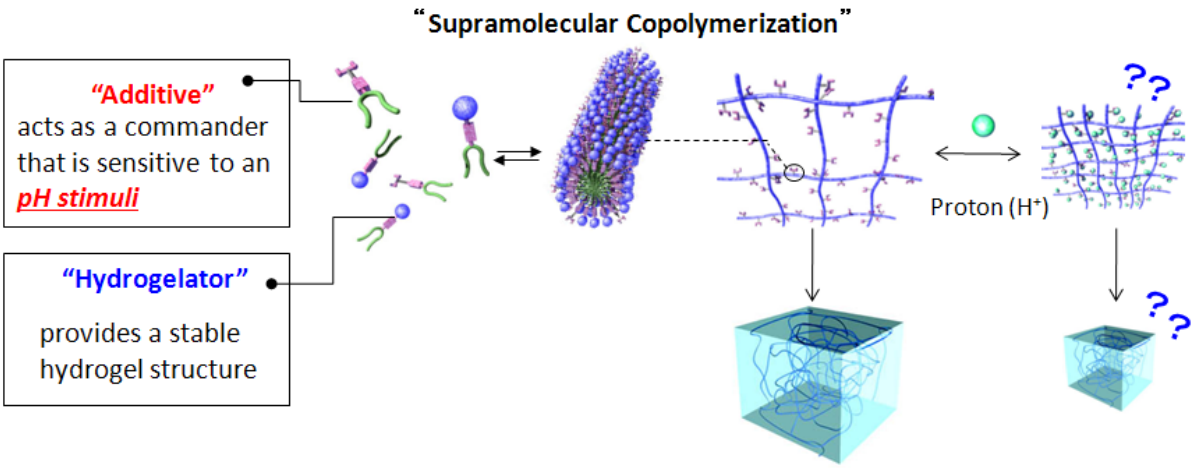


**Figure 2.** Schematic illustration of "Supramolecular copolymerization" strategy to confer pH-responsive functions to supramolecular hydrogel.

## 1-2. Results and Discussion

### 1-2-1. Molecular design and gelation screening

GalNAc-appended (GalNAc = *N*-acetylgalactosamine) glutamate ester **1** (which was found by using a combinatorial approach to be an excellent low-molecular-weight hydrogelator) was used as the fundamental gel matrix because of its stable nanofiber formation.[11, 13] As an additional component, three amphiphilic carboxylic acid derivatives bearing different lengths of methylene chains (**2a**–**c**) were designed and synthesized on the basis of their structural similarity to the hydrophobic parts of **1**. Figure 3 shows the gelation capabilities of the mixed gels under neutral pH conditions. A single component of **2a**–**c** (i.e., molar

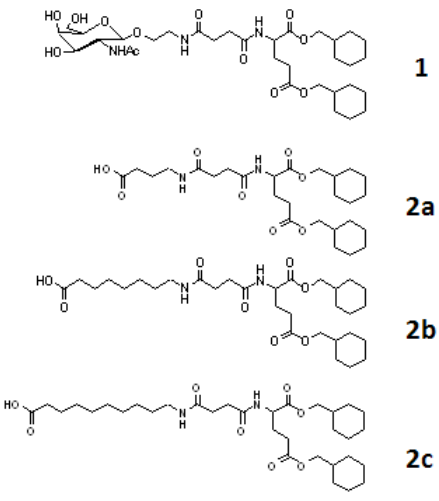

ratio **1**/**2** = 0:10) is quite soluble in water and, therefore, has no gelation capability with water. On the other hand, a single component of **1** (i.e., molar ratio **1**/**2** = 10:0) forms a stable hydrogel. The mixing of these components in various ratios produces solutions with distinct macroscopic phases such as a homogeneous solution, an unstable hydrogel and a stable hydrogel depending on the ratio of mixing. Stable gels were formed following the mixing of a single component of **1** and an almost equimolar amount of **2**. The gelation capability of the mixed hydrogel is also influenced by the molecular structure of **2**. The mixture of **2b** and **1** gelates neutral water over the widest ratio range among the three derivatives (**1**/**2b** = 10:0-6:10). The addition of excess **2** (**1**/**2a** > 8:10, **1**/**2b** > 6:10, **1**/**2c** > 8:10) produces a homogeneous solution instead of a hydrogel. In the case of **2c**, which has the longest methylene chain, the almost equimolar mixture ratios (**1**/**2c** = 10:6-8:10) produced unstable hydrogels.

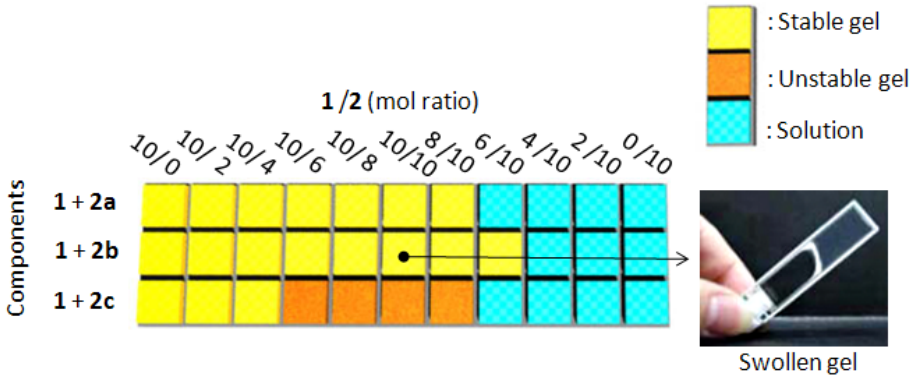


**Figure 3.** Gelation screening of the mixed hydrogels consisting of **1** and **2a**, **b** or **c** under neutral-pH condition (pH 7.0 phosphate buffer).

### 1-2-2. pH-induced shrinkage of the two-component hydrogel

The hydrogels were exposed to an acidic atmosphere (HCl vapor) and changes in their macroscopic morphology were observed. A typical example is shown in Figure 4a. Clearly, shrinkage of the hydrogel takes place upon exposure to an acidic vapor. Half of the volume of water was expelled from the original hydrogel. In addition, the hydrogel changes from almost transparent to opaque and the shrunken gel becomes stiffer than the original swollen gel. Such a change was examined by rheological study. Figure 4b shows the dependence of storage (*G'*) and loss (*G"*) moduli of the mixed hydrogel with equimolar ratios of **1** and **2b** on the angular frequency at neutral pH and acidic pH. Under acidic condition, a broad plateau region appeared for both *G'* and *G"* in the frequency range of 100-0.1 rad $sec^{-1}$ and then the values of both *G'* and *G"* dramatically increased by $10^3$-fold relative to those of the initial swollen gel state at 0.1 rad $sec^{-1}$, clearly indicating that shrunken gel formed into a rheologically stable and stiff gel. As shown in Figure 4a, such gel-shrinkage occurs only in those mixed hydrogels with almost equimolar ratios of **1** and **2**, and was not observed in the single component of **1** or in mixtures containing the small amounts of **2**. This implies that the pH response requires both components to be present in an optimal ratio. Interestingly, the pH-responsive volume change was also sensitive to the molecular structure of the additive **2**. The addition

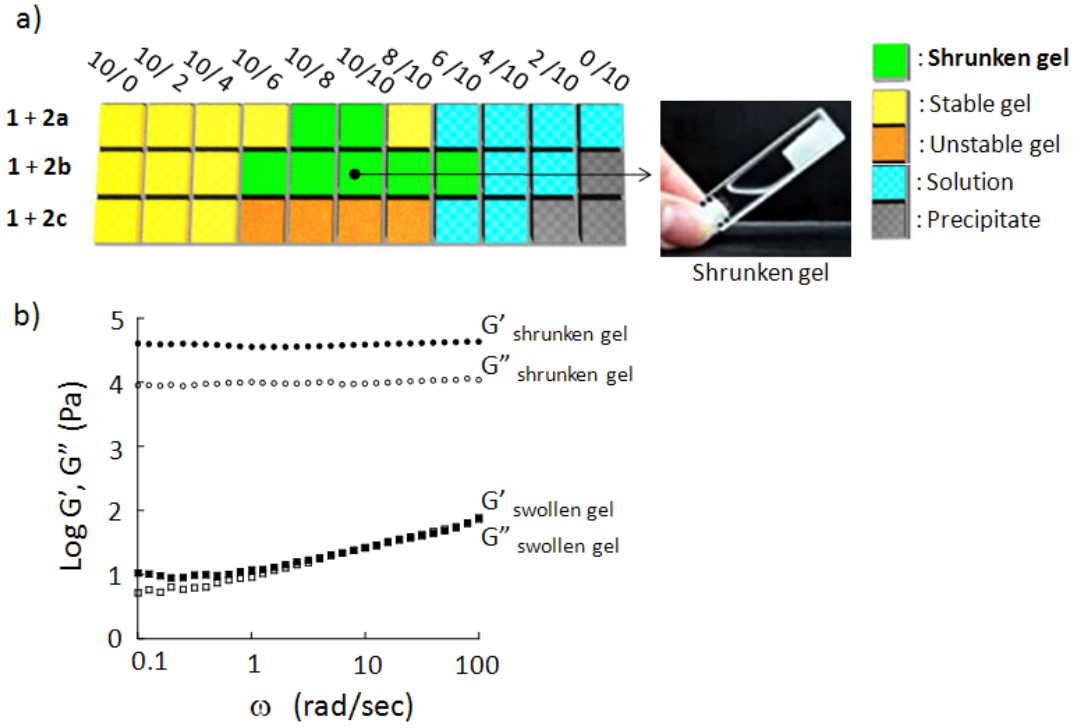


**Figure 4.** a) Screening of the acidic-pH responsive volume-change function of the mixed hydrogel performed as in Figure 3. b) Dynamic viscoelastic properties of swollen and shrunken hydrogel. *G'* (■: under neutral-pH, ●: under acidic-pH), *G"* (□: under neutral-pH,○: under acidic-pH).

of **2b** affords pH-responsive gel shrinkage over the widest ratio range among the three additives (10:6–6:10), whereas **2a**, which bears the shortest methylene unit, causes a macroscopic pH response of the hydrogel within a rather limited range (10:8–10:10), and **2c**, with the longest methylene chain, confers no pH-sensitive gel shrinkage at all. This trend is in good agreement with the data obtained for the gelation capability (Figure 3). By using molecular modeling to compare the molecular lengths of **1** and **2**, it is suggested that the hydrophilic carboxylic acid group in the case of **2b** is slightly exposed at its interface with the hydrophilic GalNAc groups of **1**, but slightly buried in the case of **2a**, and very exposed in the case of **2c** (Figure 5).[14] It is interesting that such a subtle structural difference appears to significantly influence not only the gelation capability but also the

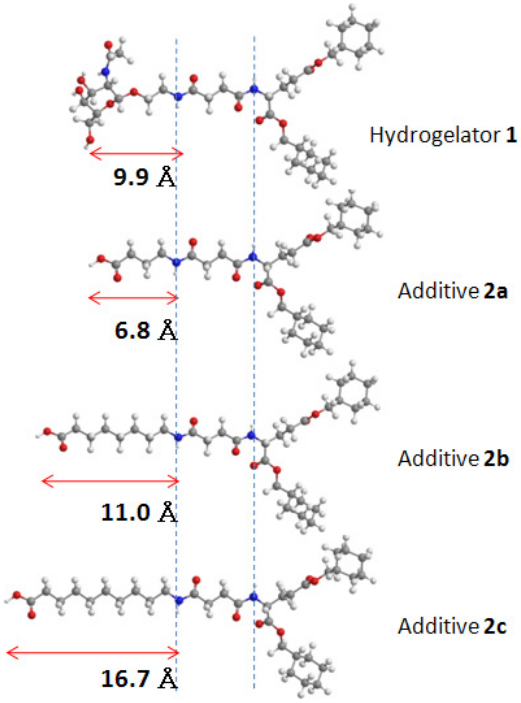


**Figure 5.** Molecular modeling to compare the molecular lengths of **1** and **2**.

resultant pH response of the mixed hydrogel. Another control sample, in which the methyl ester of **2b** was mixed with **1** in an equimolar ratio, displayed no pH-responsive volume change. We also tested the formation of a **1**/**2b** (1:1 ratio) hydrogel under acidic pH conditions (pH 4.0), which resulted in a shrunken, opaque gel comparable to the pH-triggered shrunken gel. These results suggest that the charge alteration (from negative to neutral) at the interface is crucial for the pH-responsive volume change. The shrunken hydrogel was re-swelled and became almost transparent by neutralization with neutral buffer solution (pH 7), followed by slight warming (40 ℃). The shrinkage/swelling cycle can be repeated at least six times (Figure 6), as monitored by the change in transparency. The ability to repeat the cycle indicates that the pH-induced gel shrinkage is not caused by the chemical decomposition of the component but by a reversible, physicochemical property change in the mixed hydrogel. $^{1}$H NMR and MALDI-TOF-Mass studies as shown in Figure 7 supported that any remarkable decompositions of the gelator **1** did not occur during the cycles.

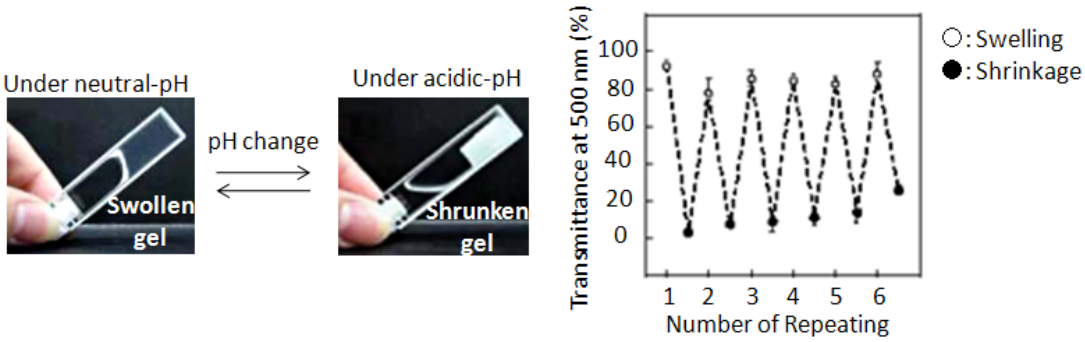


**Figure 6.** Repeated shrinkage/swelling cycles resulting from a change in pH and monitored by measuring gel transparency. The average values and experimental errors from three independent experiments were plotted.

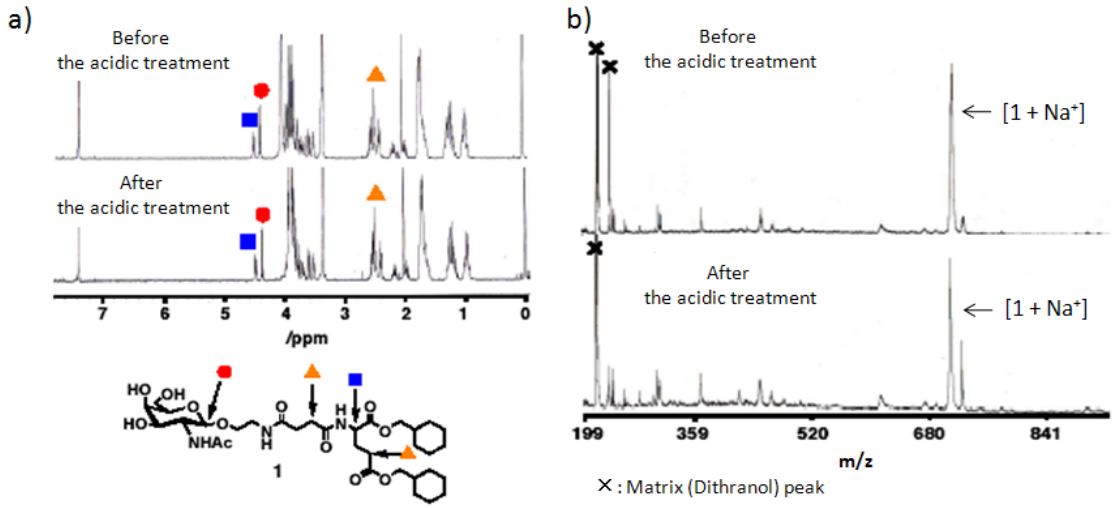


**Figure 7.** a) The $^{1}$H NMR spectrum and b) MALDI TOF Mass spectra (b) of **1** before or after the acid treatment.

### 1-2-3. Structural analyses of the two-component hydrogel

The structure of the mixed supramolecular hydrogel was examined by using several microscopy and spectroscopy techniques. The X-ray diffraction pattern (XRD, Figure 8a) of the mixed hydrogel displayed two peaks corresponding to 3.7 nm (2.40º) and 0.4 nm (19.8º), values that are almost comparable to those obtained for the single-component hydrogel of **1**. From our previous study of **1**, based on XRD data (Figure 8b) and single crystal analysis, these values can be reasonably assigned to the interdigitated bimolecular layer of **1** (3.8 nm) and the van der Waals packing distance of the cyclohexyl rings of the hydrophobic core (0.4 nm).[11] Interestingly, good agreement between the long spacing in the mixed hydrogel with that of the single-component hydrogel **1** indicates that the two-component hydrogel of **1** and **2b** has a fundamental, bilayer-like structure comparable to the single-component hydrogel **1**.[15] Significantly, similar XRD peaks appear in the spectra for the shrunken gel, suggesting that the fundamental packing mode is not significantly disturbed by the pH-induced volume change. Confocal laser scanning microscopy (CLSM)

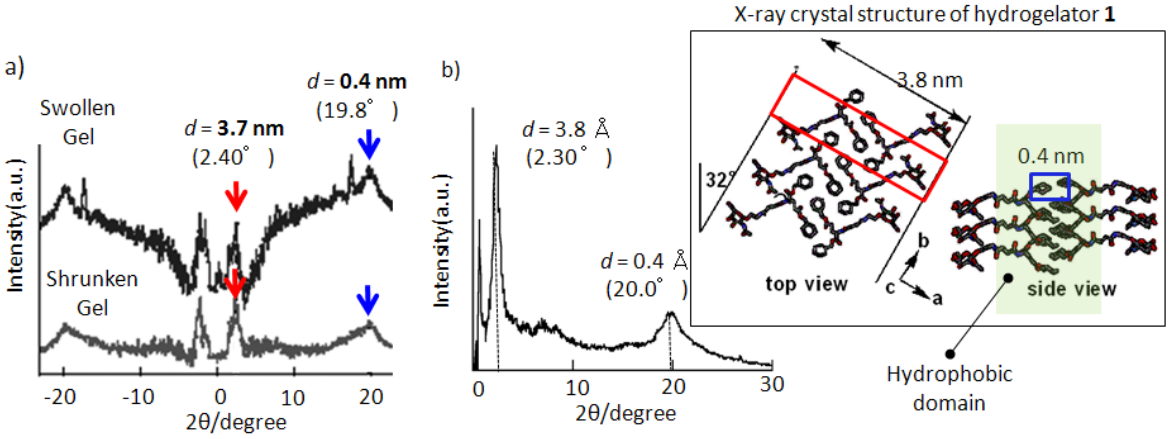


**Figure 8.** XRD profiles of a) the mixed hydrogel (**1**/**2b** = 10:10) before and after acidic treatment. There is an additional peak in XRD of the swollen gel (in panel a, upper data), which may be due to the contained phosphate salt. b) XRD profiles and X-ray crystal structure of hydrogel **1**.

produces a wet gel morphology without a drying process. Figure 9a shows a typical image of the mixed hydrogel that has been stained by a nitrobenzoxadiazole derivative (HANBD), an environmentally sensitive fluorophore that emits a strong fluorescence with a blue-shifted wavelength in less polar environments. Long fibers with green fluorescence were observed. The fluorescence spectrum of the area proximal to a fiber (circled in Figure 9a) shows the stronger peak at 530 nm with a shoulder at 550 nm (Figure 9b). Compared to the maximum peak of HANBD in aqueous solution (550 nm), the presence of the mixed hydrogel causes a blue shift of 20 nm, which strongly suggests that HANBD is incorporated into a hydrophobic domain of the hydrogel fibers, resulting in a strong emission. The shoulder peak at 550 nm implies that HANBD molecules partially distribute in the aqueous region of the hydrogel. The continuous

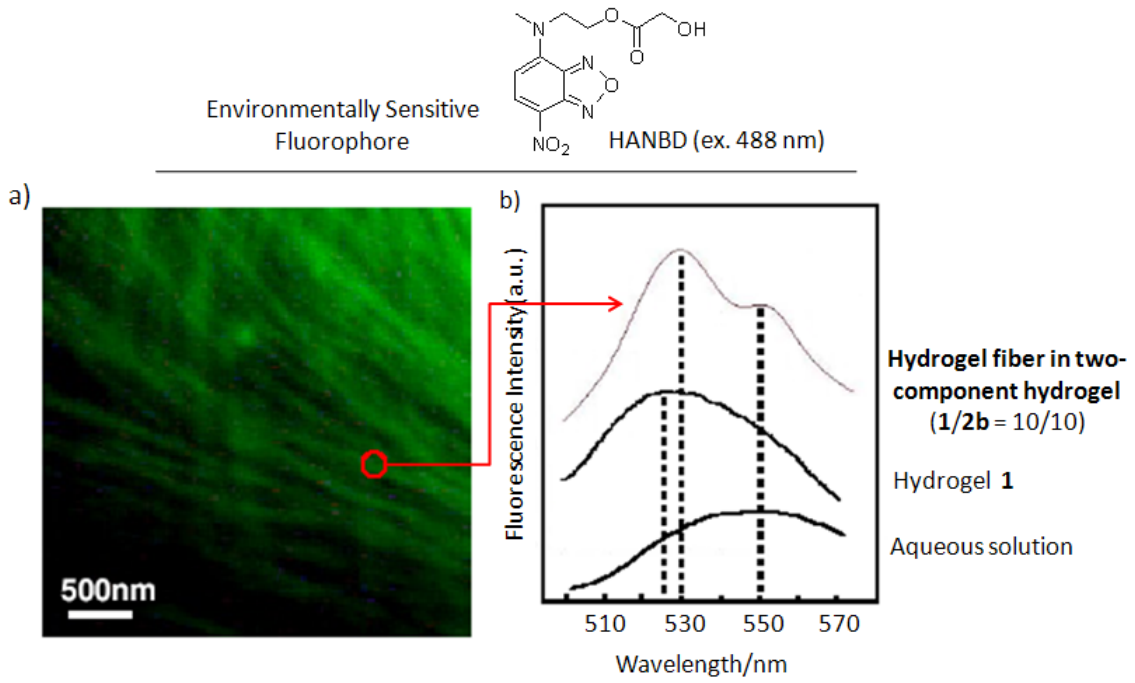


**Figure 9.** a) CLSM image of the hydrogel (**1**/**2b** = 10:10, 0.5 wt%) containing 20 μM HANBD under neutral pH conditions (in pH 7.0 phosphate buffer). The scale bar represents a distance of 500 nm. b) Fluorescence spectra of the hydrogel fibers circled in panel a (measured by using CLSM), the single-component hydrogel **1** (**1**/**2b** = 10:0, 0.5 wt%) staining with HANBD and the spectrum of HANBD in aqueous solution using the conventional fluorescence spectrophotometer.

hydrophobic region is consistent with the mixed hydrogel structure suggested by the XRD data described above. A greater blue shift in the single component hydrogel **1** is observed at 525 nm, indicating that the well-developed hydrophobic domains are slightly disturbed by **2b** in the mixed hydrogel. Thin fibers (10–100 nm diameter) of the mixed hydrogel (**1**/**2b** = 10:10), under both neutral and acidic conditions, were also observed by using transmission electron microscopy (TEM, Figure 10a and c, respectively). This fibrous morphology is almost the same as that of the single-component hydrogel **1**, indicating that the original self-assembly characteristics are not disrupted by the additive **2b**. Interestingly, the fibers in acidic pH become more densely entangled than those in neutral pH. Entangled fibrous three-dimensional networks were observed by using scanning electron microscopy (SEM, Figure 10b and d). Consistent with TEM observations, fibers in acidic pH conditions become thicker than those in neutral conditions. These results suggest that the macroscopic opaqueness of the hydrogel may be ascribed to a thickening of the pH-induced fibrils, caused by the dense packing of the self-assembled fibers.

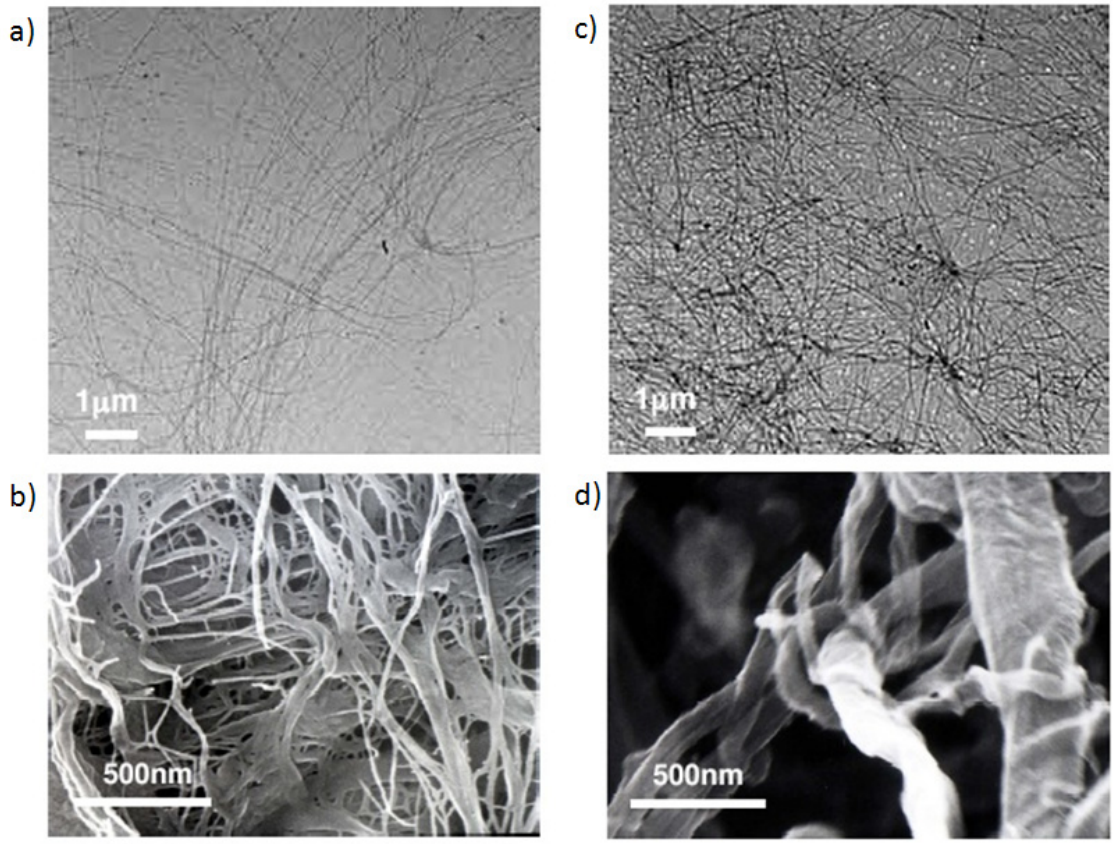


**Figure 10.** a) TEM and b) SEM images of swollen gel under pH 7.0. c) TEM and d) SEM images of shrunken gel under acidic-pH.

FT-IR measurements of the mixed hydrogel before and after shrinkage show a significant change in the equilibrium between the carboxylic acid (COOH) and the carboxylate ion ($COO^-$) (Figure 11). In the shrunken gel, a shoulder peak at 1713 $cm^{-1}$ appears which originates from the stretching of the dimeric COOH, whereas a strong peak at 1555 $cm^{-1}$ due to $COO^-$ disappears.[16] This result indicates that the charged carboxylate state of **2b** shifts to the neutral carboxylic acid state by exposure of the hydrogel to the acidic atmosphere. It may be reasonable to propose that in addition to increased osmotic pressure caused by the incorporation of a counter cation, the charged gel fiber causes an inter fibrous repulsion to yield a swollen gel. In contrast, suppression of such electrostatic repulsion and the decrease in osmotic pressure caused by the release of counterions in the neutral fiber, results in hydrogel shrinkage upon charge neutralization.[8a,d] This explanation is supported by the observation that the inclusion of the methyl ester of **2b** induced no pH response in the mixed hydrogel.

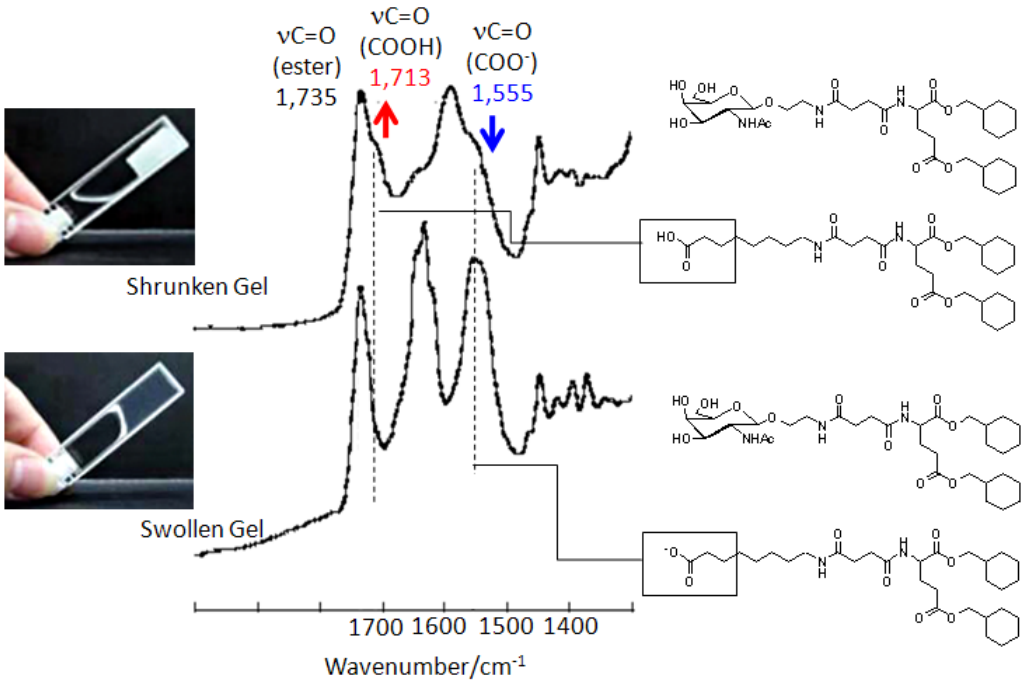


**Figure 11.** FT-IR (ATR) spectra of the mixed hydrogel (**1**/**2b** = 10:10, 0.5 wt%). a) Swollen gel and b) shrunken gel.

### 1-2-4. Basic pH responsive hydrogel using the supramolecular copolymerizaiton strategy

According to the present supramolecular copolymerization strategy, an additive component **3** bearing a pyridine residue responsive to an external basic pH with an analogous size to the hydrogelator **1** was rationally designed (Figure 12a). It is expected that the protonation/deprotonation of the pyridine unit of **3** modulated the electric-charge of the gel fiber surface, resulting in the swollen/shrunken type of morphological change of the hydrogel. When the additive **3** and the hydrogelator **1** were mixed with each other in various ratios under pH 4, distinct macroscopic phases of the mixed solution such as a homogeneous solution, unstable hydrogel and stable hydrogel were observed depending on the ratio (Figure 12b). Between the ratio of **1**:**3** = 10:0 and 8:10, in particular, the mixture formed transparent and stable hydrogel. Subsequently, these hydrogels were exposed to basic vapor diffusion of conc. $NH_3$ (25%), in order to monitor any changes in the macroscopic morphology. The hydrogels in the mixture of **1**:**3b** = 10:8-8:10 clearly displayed the shrinkage induced by basic pH (Figure 12b, c). By rheological measurement, the shrunken gel showed the $10^2$-fold stiffer than the initial swollen gel (Figure 13a). Whereas the dispersed thin fibers (*ca*. 100 nm-diameter) were observed in swollen gel with TEM, similar sized fibers more thickly assembled in shrunken gel (Figure 13b). The X-ray diffraction patterns (XRD, Figure 14) of the mixed hydrogel displayed two peaks corresponding to 4 nm (2.2º) and 0.4 nm (20.4º),

values that were almost comparable to those obtained for the single-component hydrogel of **1**.[11] In good agreement with pH responsive results of the acidic responsive hydrogel (**1**/**2b**). It was suggested that the stiffness of the shrunken hydrogel (**1**/**3**) might be ascribed to the pH-induced fibrils thickening by the dense packing of the self-assembled fibers.

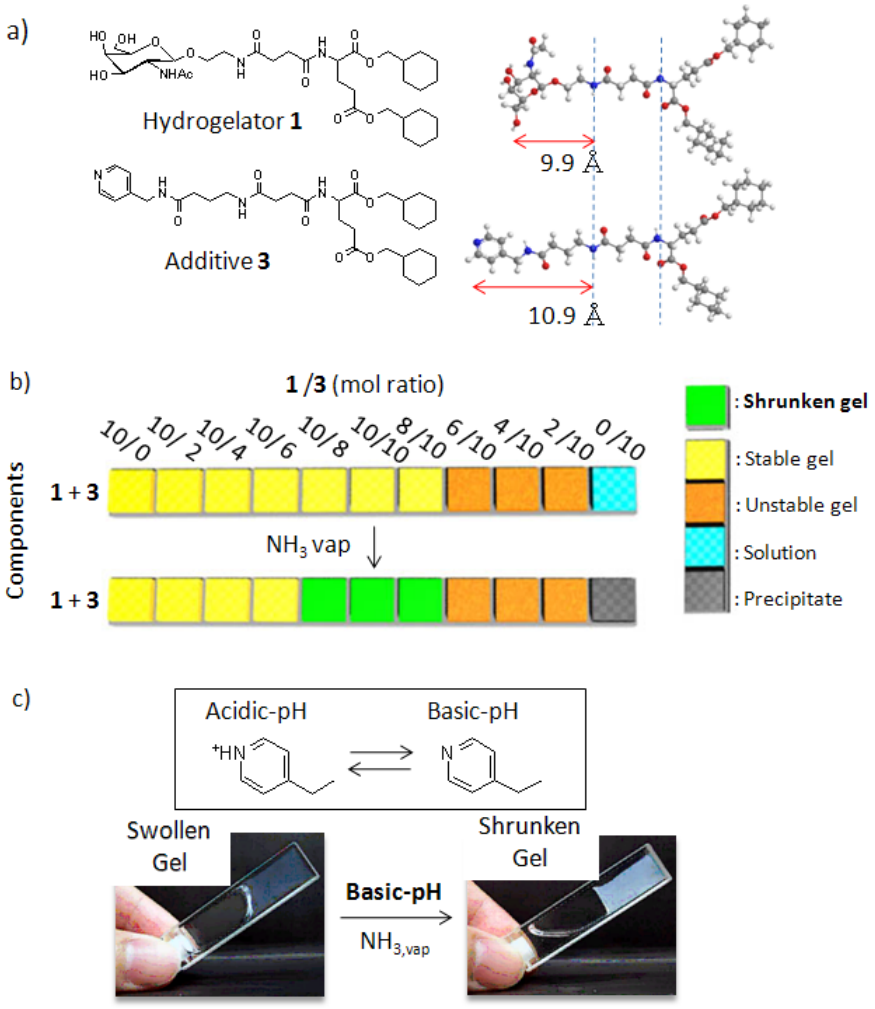


**Figure 12.** Gelation screening of the mixed hydrogels consisting of **1** and **3** a) before and b) after exposing to basic $NH_3$ vapor. c) Photographs showing swelling/shrinkage transition of the mixed hydrogel **1**/**3** = 10/10, red squares in panel a and b.

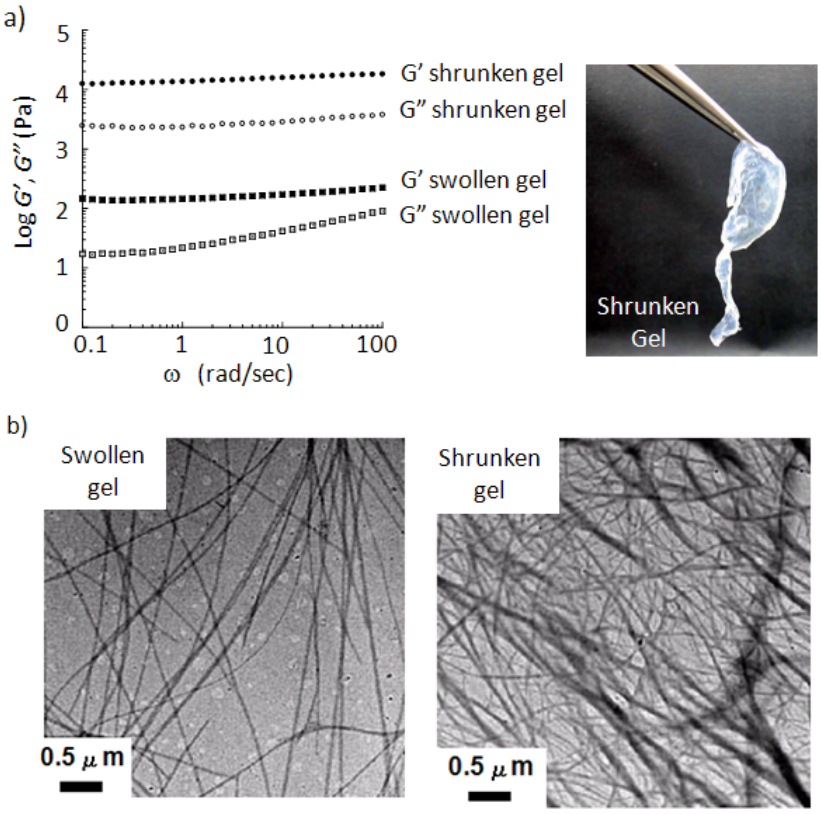


**Figure 13.** a) Dynamic viscoelastic properties of the mixed hydrogel (**1**/**3** = 10/10). *G'* (■: swollen gel, ●: shrunken gel), *G''* (□: swollen gel, ○: shrunken gel) b) TEM images of swollen gel (left) and shrunken gel (right), **1**/**3** = 10/10.

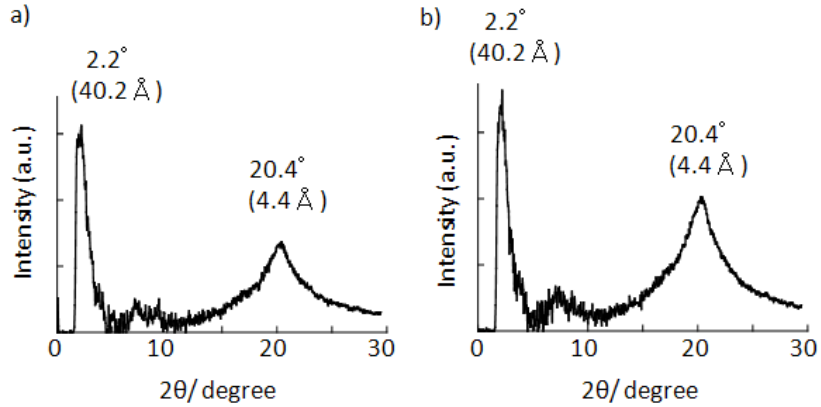


**Figure 14.** XRD profiles of the mixed hydrogel (**1**/**3** = 10:10) a) swollen gel (pH 4.0) and b) shrunken gel (basic-pH after treatment of $NH_3$ vapor diffusion).

### 1-2-5. pH-responsive drug release of the supramolecular hydrogel

Next, we investigated the pH-triggered release of bioactive substances.[17] Water-soluble vitamins, such as vitamins $B_1$, $B_6$, and $B_{12}$, were entrapped in the mixed hydrogel (**1**/**2b** = 10:10) as hydrophilic guest molecules during the gel preparation process, and the environmental pH was gradually acidified. The time course of vitamin $B_{12}$ release upon acidification was quantitatively determined by using UV-Vis spectroscopy (Figure 15a). Under neutral conditions, no release was observed due to the absence of gel shrinkage. Vitamin $B_{12}$ was released concurrent with gel shrinkage in an acidic atmosphere of HCl vapor. The vitamin $B_{12}$-entrapped hydrogel shrank by up to one half of its initial volume (see Figure 4a), and almost 50% of the vitamin $B_{12}$ was released within 60 min. The other two vitamin Bs (Figure 15a and b) exhibited release behavior similar to that of vitamin $B_{12}$. These results indicate that, in pH-triggered release, the vitamins are released in the expelled water. In contrast, the rather hydrophobic flavone derivatives, such as myricetin and quercetin, were less efficiently released, in spite of gel shrinkage (Figure 15a and b). This

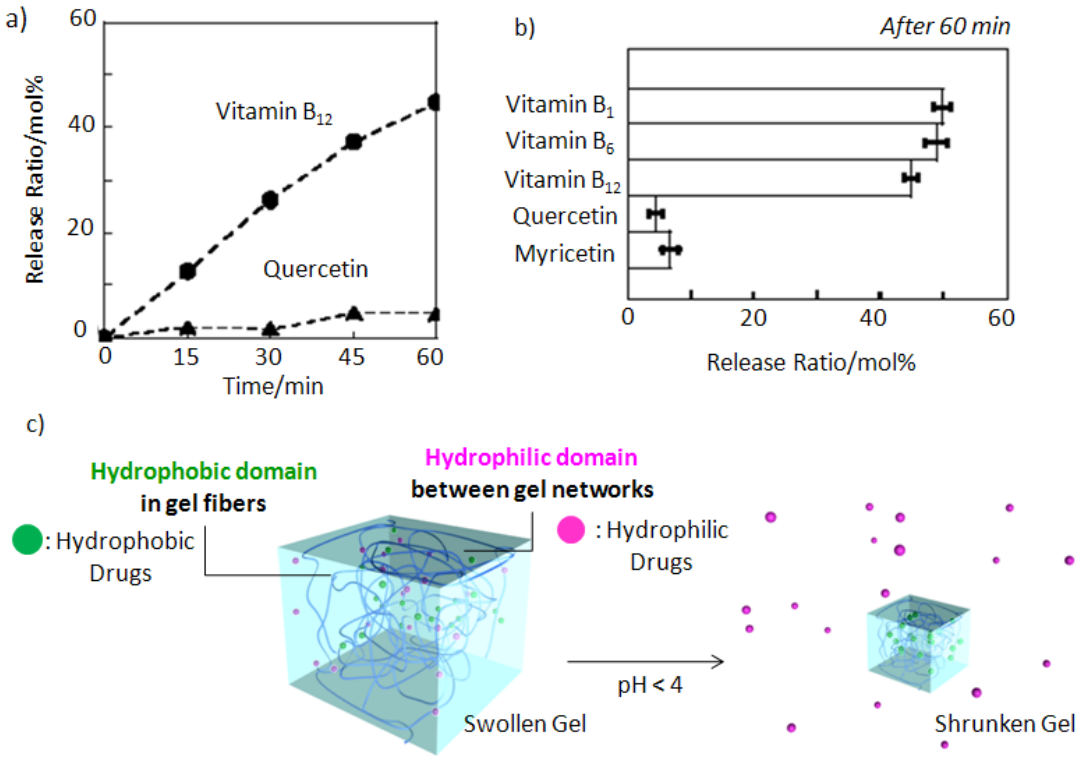


**Figure 15**. a) Time courses of the release of vitamin $B_{12}$ and quercetin substrates from the mixed hydrogel (**1**/**2b** = 10:10), caused by pH triggered gel shrinkage. b) The amount of five distinct substrates released after 60 min for vitamin $B_1$ (thiamine pyrophosphate), vitamin $B_6$ (pyridoxal 5'-phosphate), vitamin $B_{12}$ (cyanocobalamin), quercetin (3,3',4',5,7-pentahydroxyflavone) and myricetin (3,3',4',5,5',7-hexahydroxyflavone). In both a) and b) the average values and experimental errors from three independent experiments were plotted. c) Schematic illustration showing drug releases by pH triggered gel shrinkage.

is because hydrophobic substances localize predominantly in the hydrophobic domain of the supramolecular gel fibers with a lower amount present in the expelled water (Figure 15c). Therefore, controlled release can be performed in this system by employing two controlling factors; pH-induced volume change and the amphiphilic structure of the supramolecular hydrogel.

### 1-2-6. Gel-and-gel communication system using enzymatic reactions triggered by pH change

Our group previously demonstrated that our supramolecular hydrogels could provide a suitable matrix to immobilize native proteins and enzymes without denaturation.[11, 18] A combination of native enzymes, producing the pH change with pH-responsive hydrogels should become an unique semi-wet system as bio-responsive supramolecular matrix.

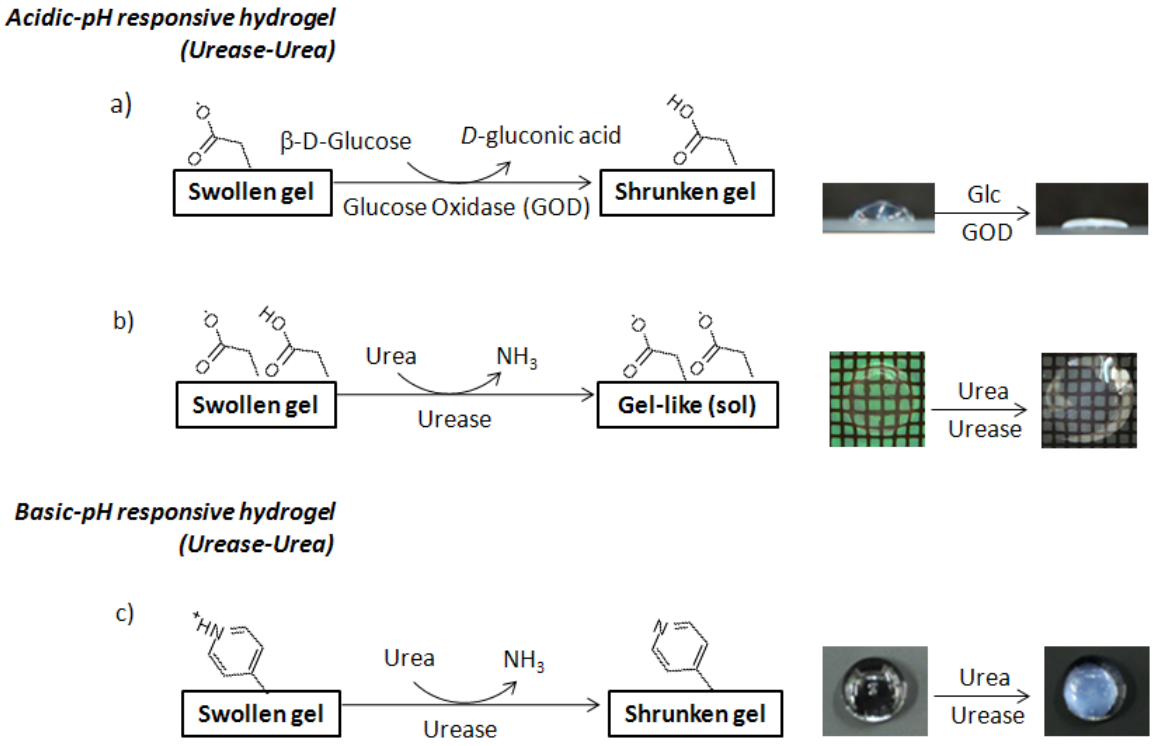


**Figure 16**. pH-responsive hydrogel with enzymatic reactions. a) Swelling/shrinkage transition of acidic-pH responsive hydrogel by GOD/Glc reaction. b) Swelling/collapse (sol) transition of acidic-pH resposnsive hydrogel by urease/urea reaction. c) Swelling/Shrinkage transition of basic-pH responsive hydrogel by urease/urea reaction.

The acidic pH responsive hydrogel immobilizing glucose oxidase (GOD) was prepared under pH 7. When glucose as the substrate was dropped to the gel and gradually osmosed into the gel, GOD oxidized it to gluconic acid, so as to produce an acidic condition in the interior of the hydrogel. Consequently, the swollen gel changed into the shrunken gel (Figure 16a), just like the bulk gel. By rheological measurements, the shrunken gel was $10^2$-fold stiffer than the initial gel (Figure 17a). Interestingly, in the case of acidic pH to $NH_3$, the gel-to-sol transition occurred when urea was added dropwise to the gel (Figure 16b, 17a). By responsive hydrogel containing urease, which hydrolyzed urea contraries, basic pH responsive hydrogel containing urease (pH 4) was changed to the shrunken gel (Figure 16c), which was 30-fold stiffer than the initial gel, by dropping urea (Figure 17b). These macroscopic morphological changes were observed only when the enzymes immobilized in hydrogel could respond to the proper substrates.

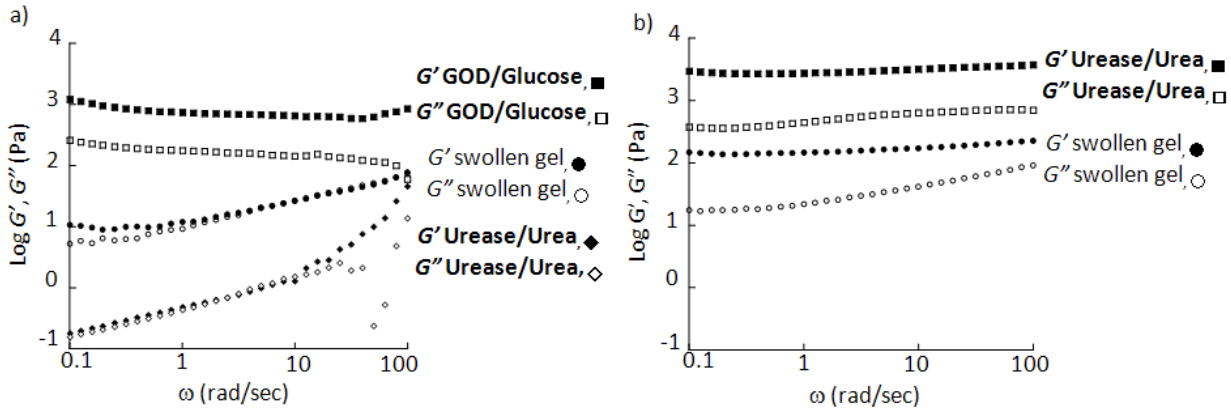


**Figure 17.** Dynamic viscoelastic properties of the mixing hydrogel a) **1**/**2b** and b) **1**/**3** before/after changing pH originated by enzymatic reaction. a) G' (●: before enzymatic reaction (the initial gel sate), ■: after GOD/Glc reaction, ◆: after urease/urea reaction), G" (○: before enzymatic reaction, □: after GOD/Glc reaction, ◇: after urease/urea reaction). b) G' (●: before enzymatic reaction, ■: urease/urea reaction), G" (○: before enzymatic reaction, □: urease/urea reaction).

Owing to the swelling/shrinkage or swelling/sol phenomena, one half of water in volume was expelled from the original swollen hydrogels. Using the combination of two hydrogels that showed the opposite response by hybridizing these enzymatic reactions, we tried to construct a novel "gel-to-gel communication" system. An acidic pH responsive hydrogel (pH 7, swollen state) containing both GOD and urea (as an information molecule) was placed on a glass plate (position GEL 1 in Figure 18), and a basic pH responsive hydrogel (pH 4, swollen state) containing urease was placed at about 1 cm distant from GEL 1 (position GEL 2 in Figure 18). When glucose was dropped to the GEL 1, GOD in the GEL 1 oxidized glucose to gluconic acid, to cause the swelling/shrinkage phase transition. The expelled water containing

urea from GEL 1 consequently flowed out. As soon as the water reached from GEL 1 to GEL 2, GEL 2 became opaque and started to shrink. In the case that GEL 1 didn't contain urea, GEL 2 did not respond at all even if the expelled water reached from GEL 1 to GEL 2. Thus, GEL 2 displayed "shrinkage" as an output of the phenotypic alteration, only when it was able to communicate from GEL 1 to GEL 2 with proper substrates.

We also performed other communication pathway constructed between acidic pH responsive hydrogel (pH 7, swollen state) containing urease as GEL 1 and bacid pH responsive hydrogel (pH 7, swollen state) containing GOD, which could not react with urea, as GEL 2 (Figure 18). Addition of urea to GEL 1 induced the swelling/sol transition in response to the basic pH provided by the urease-catalyzed reaction. The fluidic sol containing urea and conc. $NH_3$ reached the GEL 2. GEL 2 responded the shrinkage by the basic pH but not urea.

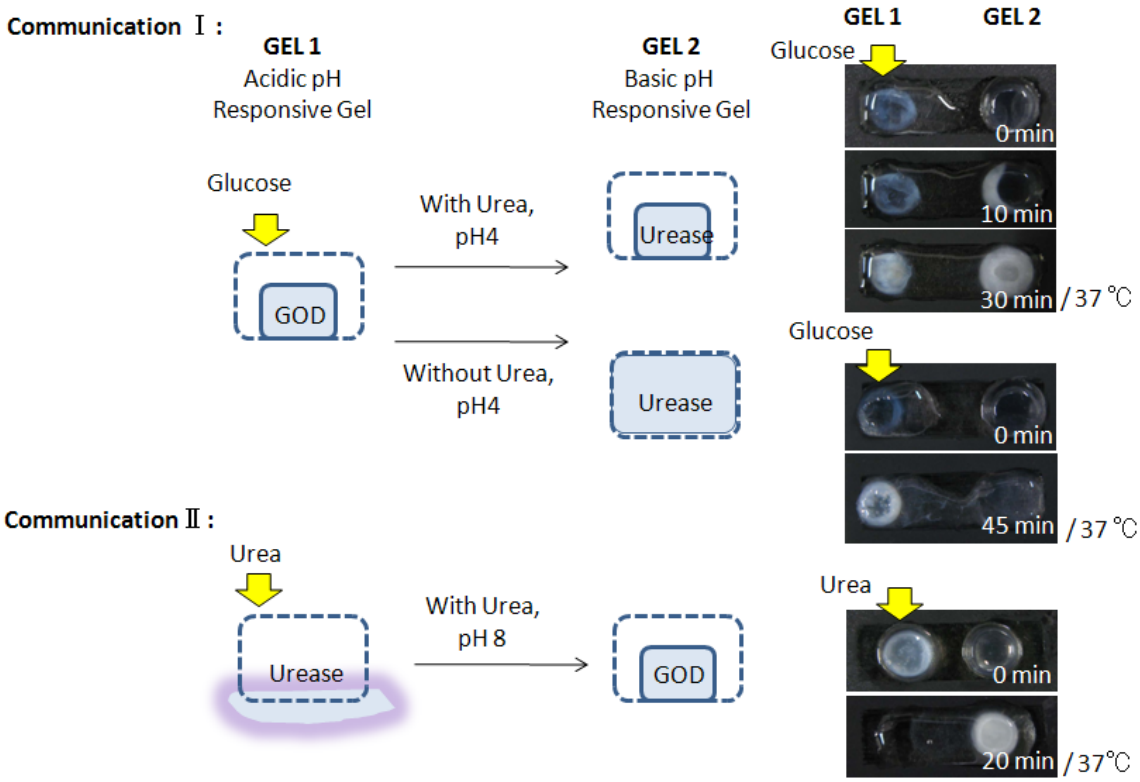


**Figure 18**. Gel-to-gel communication system via transfer of substrates or pH-change using pH-responsive hydrogel combined with enzymatic reactions.

## 1-3. Conclusion

pH-Responsive characteristics were conferred to a supramolecular hydrogel by simple mixing of a hydrogelator with small acidic molecules. Unlike the supramolecular hydrogels reported by others,[9] which exhibited gel–sol transitions, the hydrogel described here displays pH-responsive shrinkage or swelling. The pH-induced shrinkage does not occur in the case of single-component hydrogels **1** or **2b**, that is, **1** forms a stable hydrogel without pH sensitivity and **2b** does not form a supramolecular hydrogel. Therefore, it is conceivable that the hydrogelator **1** provides a superior hydrogel matrix, and that the additive **2b** acts as a commander that is sensitive to environmental pH signals in this supramolecular hydrogel. Using this supramolecular copolymerization strategy, the basic pH responsive hydrogel (**1**/**3**) was also constructed. The pH-induced volume change was successfully applied to not only controlled drug release, but also the construction of a unique gel-to-gel communication system by combination with enzymatic reactions. Such a supramolecular copolymerization strategy (Figure 19) could be applied to other systems,[19] with the aim of designing sophisticated materials that are responsive to various stimuli.

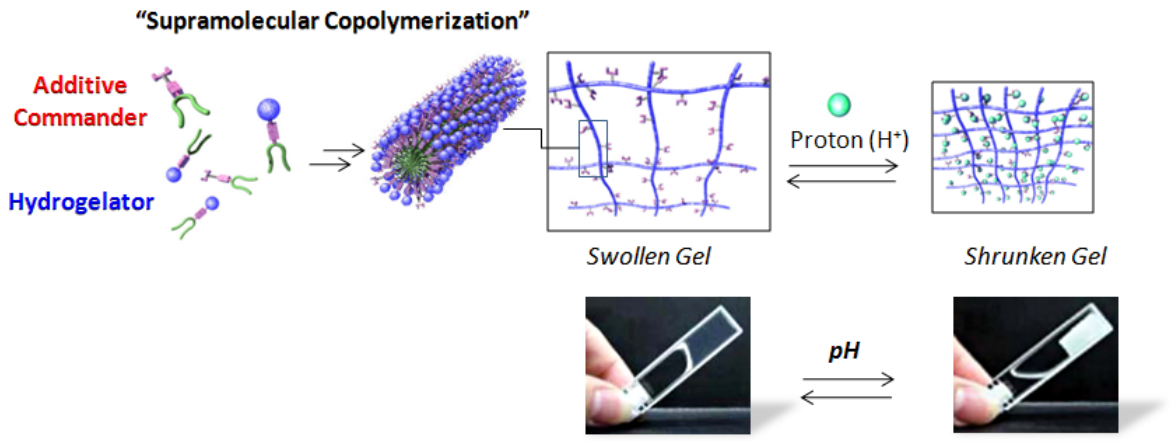


**Figure 19.** Schematic illustration of the supramolecular copolymerization strategy used to design a hydrogel, and the subsequent pH-responsive volume change.

## 1-4. Experimental Section

**Materials and methods** All chemical reagents were obtained from Aldrich, Sigma, TCI, Wako or Watanabe chemical industries. Commercially available reagents were used without further purification. Solvents were dried according to the standard procedure. $^1$H NMR spectra were obtained on JEOL JNM-EX400 (400 MHz). Mass spectra were recorded on MALDI-TOF-Mass spectrometer (PE Voyager DE-RP).

**Synthesis** Compounds **1** and **2** were prepared according to the method reported previously by us.[9n, 13] $^1$H NMR of **2b** (400 MHz, $CDCl_3$, TMS): δ = 6.81 (d, 1H, *J* = 7.6 Hz, COCH(*NH*)$CH_2CH_2CO$), 6.12 (t, 1H, *J* = 5.2 Hz, CHNHCO$CH_2CH_2CO$*NH*$CH_2$), 4.59 (m, 1H, CO*CH*(NH)$CH_2CH_2CO$), 3.95, 3.89 (d, 4H, *J* = 6.4 Hz, 6.4 Hz, COO*CH*$_2C_6H_{11}$), 3.22 (m, 2H, NH*CH*$_2(CH_2)_5CH_2COOH$), 2.60-2.32 (m, 8H, CO*CH*$_2$*CH*$_2$CO, COCH(NH)$CH_2$*CH*$_2$CO, $NHCH_2(CH_2)_5$*CH*$_2$COOH), 2.22, 1.99 (m, 2H, COCH(NH)*CH*$_2CH_2CO$), 1.80-0.91 (m, 32H, $NHCH_2$(*CH*$_2$)$_5CH_2COOH$, $COOCH_2$*C*$_6$*H*$_{11}$); MALDI-TOF-MS: *m*/*z*: calcd for $C_{31}H_{52}N_2O_8$: 580.37; found: 603.80 [*M* + Na]$^+$; elemental analysis of **2b** calcd (%) for $C_{31}H_{52}N_2O_8$: C 64.11, H 9.02, N 4.82; found: C 64.11, H 9.02, N 4.79.

$^1$H NMR of **2a** (400 MHz, $CDCl_3$, TMS): δ = 6.77 (d, 1H, *J* = 7.2 Hz, COCH(*NH*)$CH_2CH_2CO$), 6.41 (m, 1H, CHNHCO$CH_2CH_2CO$*NH*$CH_2$), 4.58 (m, 1H, CO*CH*(NH)$CH_2CH_2CO$), 3.96, 3.89 (d, 4H, *J* = 6.4 Hz, 6.4 Hz, COO*CH*$_2C_6H_{11}$), 3.34 (m, 2H, NH*CH*$_2CH_2CH_2COOH$), 2.61-2.35 (m, 8H, CO*CH*$_2$*CH*$_2$CO, COCH(NH)$CH_2$*CH*$_2$CO, $NHCH_2CH_2$*CH*$_2$COOH), 2.20, 2.00 (m, 2H, COCH(NH)*CH*$_2CH_2CO$), 1.89-0.94 (m, 24H, $NHCH_2$*CH*$_2CH_2COOH$, $COOCH_2$*C*$_6$*H*$_{11}$); FAB-MS: *m*/*z*: calcd for $C_{27}H_{44}N_2O_8$: 524.31; found: 525.40 [*M* + H]$^+$; elemental analysis of **2a** calcd (%) for $C_{27}H_{44}N_2O_8$: C 61.81, H 8.45, N 5.34; found: C 61.72, H 8.43, N 5.28.

$^1$H NMR of **2c** (400 MHz, $CDCl_3$, TMS): δ = 6.71 (m, 1H, COCH(*NH*)$CH_2CH_2CO$), 6.14 (m, 1H, CHNHCO$CH_2CH_2CO$*NH*$CH_2$), 4.58 (m, 1H, CO*CH*(NH)$CH_2CH_2CO$), 3.94, 3.88 (d, 4H, *J* = 6.0 Hz, 6.4 Hz, COO*CH*$_2C_6H_{11}$), 3.21 (m, 2H, NH*CH*$_2(CH_2)_9CH_2COOH$), 2.60-2.25 (m, 8H, CO*CH*$_2$*CH*$_2$CO, COCH(NH)$CH_2$*CH*$_2$CO, $NHCH_2(CH_2)_9$*CH*$_2$COOH), 2.17, 1.97 (m, 2H, COCH(NH)*CH*$_2CH_2CO$), 1.80-0.85 (m, 40H, $NHCH_2$(*CH*$_2$)$_9CH_2COOH$, $COOCH_2$*C*$_6$*H*$_{11}$); FAB-MS: *m*/*z*: calcd for $C_{35}H_{60}N_2O_8$: 636.43; found: 637.50 [*M* + H]$^+$; elemental analysis of **2c** calcd (%) for $C_{35}H_{60}N_2O_8$: C 66.01, H 9.50, N 4.40; found: C 65.89, H 9.47, N 4.37.

**Synthesis of methyl ester of 2b** 8-Aminoctanoic acid methyl ester was used for the condensation step in the synthetic scheme of **2b** to yield the target methyl ester as a colorless solid. $^1$H NMR (400 MHz, $CDCl_3$, TMS): δ = 6.60 (d, *J* = 7.6 Hz, 1H, COCH(*NH*)$CH_2CH_2CO$), 5.88 (m, 1H, CHNHCO$CH_2CH_2CO$*NH*$CH_2$), 4.59 (m, 1H, CO*CH*(NH)$CH_2CH_2CO$), 3.94, 3.88 (d, 4H, *J* = 6.8 Hz, 6.8 Hz, COO*CH*$_2C_6H_{11}$), 3.67 (s, 1H, COO*CH*$_3$), 3.22 (m, 2H, NH*CH*$_2(CH_2)_5CH_2COOCH_3$), 2.58-2.28 (m, 8H, CO*CH*$_2$*CH*$_2$CO, COCH(NH)$CH_2$*CH*$_2$CO, $NHCH_2(CH_2)_5$*CH*$_2$$COOCH_3$), 2.21, 1.99 (m, 2H,

COCH(NH)$CH_2$$CH_2$CO), 1.80-0.94 (m, 32H, NHCH$_2$($CH_2$)$_5$CH$_2$COOCH$_3$, COOCH$_2$$C_6H_{11}$); FAB-MS: *m*/*z*: calcd for $C_{32}H_{54}N_2O_8$: 594.39; found: 595.4 [$M$ + H]$^+$; elemental analysis of methyl ester of **2b** calcd (%) for $C_{32}H_{54}N_2O_8$: C 64.62, H 9.15, N 4.71; found: C 64.66, H 9.08, N 4.65.

**Synthesis of 3** To a solution of **2a** (194 mg, 0.37 mmol) in DMF (10mL) was added 4-pycolylamine (74 μL, 0.74 mmol), WSC-HCl (142 mg, 0.74 mmol), HOBT (113 mg, 0.74 mmol) and DIEA (129 μL, 0.74 mmol). The solution was stirred for 6 h at room temperature under nitrogen atmosphere and the solvent was removed under reduced pressure at ambient temperature. The crude residue was dissolved in chloroform and washed with brine. The residue was dried over anhydrous $Mg_2SO_4$, and the solvent was evaporated in vacuo and then the obtained oil was purified by column chromatography (silica gel, chloroform/methanol = 10/1, v/v) to give **3** 150 mg (66%) as a colorless solid. $^1$H NMR (400 MHz, $CDCl_3$, TMS): δ = 8.55-8.53 (d, d, 2H, Py-2-*CH*, Py-6-*CH*), 7.24-7.22 (d, d, d, 3H, Py-3-*CH*, Py-5-*CH*, PyCH$_2$*NH*CO), 6.63 (d, 1H, J = 7.2, CO*NH*CH(CO)CH$_2$), 6.22 (t, 1H, CH$_2$*NH*COCH$_2$CH$_2$NH), 4.53-4.51 (m, 1H, NH*CH*(CO)CH$_2$CH$_2$), 4.46 (d, 2H, J = 7.2 Hz, Py$CH_2$NHCO), 3.92, 3.90 (d, d, 2H, 2H, J = 1.6 Hz, J = 1.6 Hz, $CH_2$-cyc-hexyl×2), 3.35-3.30 (m, 2H, CH$_2$$CH_2$NHCOCH$_2$CH$_2$CONHCH), 2.60-1.90 (2H, d, PyCH$_2$NHCO$CH_2$, 4H, m, NHCO$CH_2$$CH_2$CONH, 4H, m, NHCH(CO)$CH_2$$CH_2$CO), 1.8-0.9 (22H, m, CH$_2$-cyc-hexyl($C_6H_{11}$)×2, 2H, m, NHCOCH$_2$$CH_2$CH$_2$NHCO); FAB-Mass: m/z: calcd for $C_{33}H_{50}N_4O_7$: 614.37; found: 615.37 [M + H]$^+$; elemental analysis of **3** calcd (%) for $C_{33}H_{50}N_4O_7$: C 64.47, H 8.20, N 9.11; found: C 64.19, H 8.15, N 9.00.

**Gelation test** Hydrogelator **1** and the additive **2a-c** or **3** were mixed various ratios from **1**/**2** or **1**/**3** = 0/10-10/0 mol/mol and were homogenously dispersed with 25 mM Na/K phosphate buffer (pH 7, in the case of **1**/**2a-c**) or 25 mM acetate buffer (pH 4, in the case of **1**/**3**) by heating, and then left at rest for 1 day at room temperature. The content of the total components (**1** + **2**) were fixed to be 0.5 wt% in all cases. Galation abilities for each molecule were checked by up and down invert method and then we classified into four phase states; stable gel, unstable gel, precipitate and homogenous solution.

**Evaluation of the pH-responsive volume change of the mixed hydrogel** The **1**/**2** mixed hydrogels were placed in a box of the acidic atmosphere (a sample tube containing conc-HCl solution was placed in the box for the acidic vapor generation) for 20 min and then the amount of expelled water was weighed for each mixed hydrogel. The pH of the expelled water was determined to pH 1-2 after exposure to HCl vapor. The shrinkage ratio was estimated by dividing the initial weight of the hydrogel by this value. The macroscopic morphology change was also observed and recorded by digital camera. In experiments of shrinkage of the **1**/**3** mixed hydrogel, the gel was exposed to the basic vapor (25%, $NH_3$ aq.) in the box.

**Dynamic viscoelasticity measurement** Dynamic viscoelasticities for the mixed hydrogel (swollen/shrunken gel) were measured with plate-plate rheology equipment (DynAlyser DAR-100, Reologica). The measurement conditions were follows: For 3 mL acidic responsive hydrogel ([**1**/**2b** = 10/10] = 0.5 wt%, swollen state), angular frequency range: 100-0.1 $\omega \cdot sec^{-1}$; strain: 3%; parallel plate: 4 cm in diameter; gap distance: 0.5 mm; measurement temperature; 24 ºC. For 3 mL acidic responsive hydrogel ([**1**/**2b** = 10/10] = 0.5 wt%, shrunken state), angular frequency range: 100-0.1 $\omega \cdot sec^{-1}$; strain: 1%; parallel plate with groove: 4 cm in diameter; gap distance: 0.3 mm; measurement temperature; 24 ºC. For 3 mL basic pH responsive hydrogel ([**1**/**3** = 10/10] = 0.5 wt%, swollen state), angular frequency range: 100-0.1 $\omega \cdot sec^{-1}$; strain: 3%; parallel plate: 4 cm in diameter; gap distance: 0.3 mm; measurement temperature; 24 ºC. For 3 mL basic pH responsive hydrogel ([**1**/**3** = 10/10] = 0.5 wt%, shrunken state), angular frequency range: 100-0.1 $\omega \cdot sec^{-1}$; strain: 1%; parallel plate with groove: 4 cm in diameter; gap distance: 0.3 mm; measurement temperature; 24 ºC.

**X-ray powder diffraction** The xerogel was placed in a glass capillary tube ($\Phi$ = 0.7 mm) and the X-ray diffractogram (MAC Science M18XHF) was recorded on an imaging plate using Cu radiation ($\lambda$ = 1.54 Å) at a distance of 15 cm.

**CLSM observation** The hydrogel sample placed on a glass bottom dish was observed with confocal laser scanning microscopy loaded Ar laser (488 nm, Carl Zeiss: LSM510META). Fluorescence spectra of the focused gel fiber region were also obtained by this microscope.

**TEM and SEM observation** Piece of carbon-coarted copper grid was dipped in each sample. They were dried under reduced pressure for 24 h at room temperature. TEM samples without stain were observed with JEOL-JEM-2010 apparatus under 120 kV accelerating voltage. Whereas, in SEM observation, the samples were coated by platinum vapor deposition (30sec). SEM images were obtained by using a Hitachi S-5000, acceleration voltage 25kV.

**Controlled release of the entrapped substances** After vitamin $B_{12}$ was added to the suspension of **1** and **2b** in phosphate buffer solution (25mM Na/K phosphate buffer, pH 7.0), the mixture was heated to obtain a clear homogeneous solution ([vitamin $B_{12}$] = 0.5 mM, [**1**] = 3.95 mM, [**2b**] = 3.95 mM). After incubation at room temperature for 1 day, the hydrogel containing vitamin $B_{12}$ formed. The obtained hydrogel was exposed to HCl vapor for 15 min and the expelled solution was collected. After neutralization and suitable dilution, the concentration of the released vitamin $B_{12}$ was determined by UV-visible spectrophotometer (Shimadzu UV2550). For other substances, the similar method was employed.

**Preparation of pH-responsive hydrogel containing enzyme** The sol (40 μL/well) of the mixed hydrogel was placed on the 10-wells glass plate. After 15 min at room temperature, enzyme solution was suspended in the sol. After the gelation completed for 12-24 h incubation at 4 ℃, the substrate of enzyme was dropped to the gel and subsequently, we observed the macroscopic changes of the gel at 37 ℃. [Mixed hydrogel] = [**1**/**2b**] = [**1**/**3**] = [10/10 mol/mol] = 0.5 wt%, in 25 mM Na/K phosphate buffer, pH 7.0 for **1**/**2b** gel, in 25 mM acetate buffer, pH 4.0 for **1**/**3** gel. Glucose Oxidase from *Aspergillus niger* (SIGMA; Type Ⅱ-S), 10 units/5 μL. Urease from *Jack Beans* (TCI, U0017), 10 units/5 μL. [Glucose] = 5 mg/10 μL. [Urea] = 0.18 mg/10 μL.

## 1-5. References and Notes


1. a) Furusho, Y.; Kimura, T.; Mizuno, Y.; Aida, T. *J. Am. Chem.Soc.* **1997**, *119*, 5267-5268. b) Yashima, E.; Maeda, K. Okamoto, Y. *Nature* **1999**, *399*, 449-451. c) Sugasaki, A.; Ikeda, M.; Takeuchi, M.; Robertson, A.; Shinkai, S. *J. Chem. Soc., Perkin Trans. 1* **1999**, 3259-3264.
2. As reviews: a) Pease, A. R.; Jeppesen, J. O.; Stoddart, J. F.; Luo, Y.; Collier, C. P.; Heath, J. R.; *Acc. Chem. Res.* **2001**, *34*, 433-444. b) Collin, J.-P.; Dietrich-Buchecker, C.; Gaviña, P.; Jimenez-Molero, M. C.; Sauvage, J.-P. *Acc. Chem. Res.* **2001**, *34*, 477-487.
3. As reviews: a) Ballardini, R.; Balzani, V.; Credi, A.; Gandolfi, M. T.; Venturi, M. *Acc. Chem. Res.* **2001**, *34*, 445-455. b) Schalley, C. A.; Beizai, K.; Vögtle, F. *Acc. Chem. Res.* **2001**, *34*, 465-476. c) Feringa, B. L. *Acc. Chem. Res.* **2001**, *34*, 504-513.
4. Collier, C. P.; Mattersteig, G.; Wong, E. W.; Luo, Y.; Beverly, K.; Sampaio, J.; Raymo, F. M.; Stoddart, J. F.; Heath, J. P.; *Science* **2000**, *289*, 1172-1175.
5. As reviews: a) Osada, Y.; Gong, J.-P. *Adv. Mater.* **1998**, *10*, 827-837. b) Jeong, B.; Gutowska, A. *TREND Biotechnol.* **2002**, *20*, 305-305. c) Lendlein, A.; Kelch, S. *Angew. Chem.* **2002**, *114*, 2138-2162; *Angew. Chem. Int. Ed.* **2002**, *41*, 2034-2057.
6. a) Fouquey, C.; Lehn, J.-M.; Levelut, A.-M. *Adv. Mater.* **1990**, *2*, 254-257. b) Sijbesma, R. P.; Beijer, F. H.; Brunsveld, L.; Folmer, B. J. B.; Ky Hirschberg, J. H. K.; Lange, R. F. M.; Lowe, J. K. L.; Meijer, E. W. *Science* **1997**, *278*, 1601-1604. c) Castellano, R. K.; Rudkevich, D. M.; Rebek Jr., J. *Proc. Natl. Acad. Sci. USA* **1997**, *94*, 7132-7137.
7. a) Kiyonaka, S.; Sugiyasu, K.; Shinkai, S.; Hamachi, I. *J. Am. Chem. Soc*. **2002**, *124*, 10954-10955. After our report, another example was newly added: b) Zhang, Y.; Gu, H.; Yang, Z.; Xu, B. *J. Am. Chem. Soc.* **2003**, *125*, 13680-13681.
8. a) Tanaka, T. *Phys. Rev. Lett.* **1978**, *40*, 820-823. b) Tanaka, T. *Sci. Am.* **1981**, *244*, 124-136. c) Suzuki, A.; Tanaka, T. *Nature* **1990**, *346*, 345-347. d) Annaka, M.; Tanaka, T. *Nature* **1992**, *355*, 430-432. e) Oya, T.; Enoki, T.; Grosberg, A. Y.; Masamune, S.; Sakiyama, T.; Takeoka, Y.; Tanaka, K.; Wamg, G.; Yilmaz, Y.; Feld, M. S.; Dasari, R.; Tanaka, T. *Science* **1999**, *286*, 1543-1545. f) Enoki, T.; Tanaka, K.; Watanabe, T.; Oya, T.; Sakiyama, T.; Takeoka, Y.; Ito, K.; Wang, G.; Annaka, M.; Hara, K.; Du, R.; Chuang, J.; Wasserman, K.; Grosberg, A. Y.; Masamune, S.; Tanaka, T. *Phys. Rev. Lett.* **2000**, *85*, 5000-5003.
9. a) Aggeli, A.; Bell, M.; Boden, N. Keen, J. N.; Knowles, P. F.; McLeish, T. C. B.; Pitkeathly, M.; Radford, S. E. *Nature* **1997**, *386*, 259-262. b) Petka, W. A.; Harden, J. L.; McGrath, K. P.; Wirtz, D.; Tirrell, D. A. *Science* **1998**, *281*, 389-392. c) Estroff, L. A.; Hamilton, A. D. *Angew. Chem.* **2000**, *112*, 3589-3592; *Angew. Chem. Int. Ed.* **2000**, *39*, 3447-3450. d) Collier, J. H.; Hu, B.-H.; Ruberti, J. W.; Zhang, J.; Shum, P.; Thompson, D. H.; Messersmith, P. B. *J. Am. Chem. Soc.* **2001**, *123*, 9463-9464. e) Maitra, U.; Mukhopadhyay, S.; Sarkar, A.; Rao, P.; Indi, S. S. *Angew. Chem.* **2001**, *113*, 2341-2343; *Angew. Chem. Int. Ed.* **2001**, *40*, 2281-2283. f) Nowak, A. P.; Breedveld, V.; Pakstis, L.; Ozbas, B.; Pine, D. J.; Pochan, D.; Deming, T. J. *Nature* **2002**, *417*, 424-428. g) Schneider, J. P.; Pochan, D. J.; Ozbas, B.; Rajagopal, K.;

Pakstis, L.; Kretsinger, J. *J. Am. Chem. Soc.* **2002**, *124*, 15030-15037. h) Iwaura, R.; Yoshida, K.; Masuda, M.; Yase, K.; Shimizu, T. *Chem. Mater.* **2002**, *14*, 3047-3053. i) Haines, S. R.; Harrison, R. G. *Chem. Commun.* **2002**, 2846-2847. j) Kobayashi, H.; Friggeri, A.; Koumoto, K.; Amaike, M.; Shinkai, S.; Reinhoudt, D. N. *Org. Lett.* **2002**, *4*, 1423-1426. k) Pochan, D. J.; Schneider, J. P.; Kretsinger, J.; Ozbas, B.; Rajagopal, K.; Haines, L. *J. Am. Chem. Soc.* **2003**, *125*, 11802-11803. l) Suzuki, M.; Yumoto, M.; Kimura, M.; Shirai, H.; Hanabusa, K. *Chem. Eur. J.* **2003**, *9*, 348-354. m) Park, S. M.; Lee, Y. S.; Kim, B. H. *Chem. Commun.* **2003**, 2912-2913. n) Kiyonaka, S.; Zhou, S-L.; Hamachi, I. *Supramol. Chem.* **2003**, 15, 521-528. o) van Bommel, K. J. C.; van der Pol, C.; Muizebelt, I.; Friggeri, A.; Heeres, A.; Meetsma, A.; Feringa, B. L.; van Esch, J. *Angew. Chem.* **2004**, *116*, 1695-1699; *Angew. Chem. Int. Ed.* **2004**, *43*, 1663-1667. p) As an excellent review on a low molecular weight hydrogelator: Estroff, L. A.; Hamilton, A. D. *Chem. Rev.* **2004**, *104*, 1201-1217.

10. For supramolecular organogels: a) Hanabusa, K.; Miki, T.; Taguchi, Y.; Koyama, T.; Shirai, H. *J. Chem. Soc. Chem. Commun.* **1993**, 1382-1384. b) Murata, K.; Aoki, M.; Suzuki, T.; Harada, T.; Kawabata, H.; Komori, T.; Ohseto, F.; Ueda, K.; Shinkai, S. *J. Am. Chem. Soc.* **1994**, *116*, 6664-6676. c) Terech, P.; Weiss, P. *Chem. Rev.* **1997**, *97*, 3133-3159. d) van Esch, J. H.; Feringa, B. L. *Angew. Chem.* 2000, *112*, 2351-2354; *Angew. Chem. Int. Ed.* **2000**, *39*, 2263-2266.
11. Kiyonaka, S.; Sada, K.; Yoshimura, I.; Shinkai, S.; Kato, N.; Hamachi, I. *Nature Mater.* **2004**, *3*, 58-64.
12. For two-component supramolecular gels: a) Mieden-Gundert, G.; Klein, L.; Fischer, M.; Vogtle, F.; Heuze, K.; Pozzo, J.-L.; Vallier, M.; Fages, F. *Angew. Chem.* **2001**, *113*, 3266-3267; *Angew. Chem. Int. Ed.* **2001**, *40*, 3164-3166. b) Yang, Z.; Gu, H.; Zhang, Y.; Wang, L.; Xu, B. *Chem. Commun.* **2004**, 208-209.
13. a) Hamachi, I.; Kiyonaka, S.; Shinkai, S. *Chem. Commun.* **2000**, 1281-1282. b) Hamachi, I.; Kiyonaka, S.; Shinkai, S. *Tetrahedron Lett.* **2001**, *42*, 6141-6145. c) Kiyonaka, S.; Shinkai, S.; Hamachi, I. *Chem. Eur. J.* **2003**, 9, 976-983.
14. Molecular modeling was performed on the basis of the X-ray crystallographic data of **1** with assumption that all methylene chains form into trans conformation.
15. This may suggest good miscibility of these two components in the mixed hydrogel (**1**/**2** = 10/10), which is supported by the following evidence that the molecular ratio (**1**/**2**) did not practically change before and after shrinkage when we analyze the mixture ratio of these hydrogel by $^{1}$H NMR (Figure 7b).
16. Gershevitz, O.; Sukenik, C. N. *J. Am. Chem. Soc.* **2004**, *126*, 482-483.
17. a) Tiller, J. C. *Angew. Chem.* **2003**, *115*, 3180-3183; *Angew. Chem. Int. Ed.* **2003**, *42*, 3072-3075. b) Friggeria, A.; Feringab, B. L.; van Esch, J. *J. Controlled Release* **2004**, *97*, 241. c) van Bommel, K.J. C.; Stuart, M. A. C.; Feringa, B. L.; van Esch, J. *Org. Biomol. Chem.* **2005**, *3*, 2917. d) Yang, Z.; Xu, K.; Wang, L.; Gu, H.; Wei, H.; Zhang, M.; Xu, B. *Chem. Commun.* **2005**, 4414. e) Yang, Z.; Liang, G.; Ma, M.; Abbah, A. S.; Luc, W. W.; Xu, B. *Chem. Commun.* **2007**, 843.
18. a) Yamaguchi, S.; Yoshimura, I.; Kohira, T.; Tamaru, S.-I.; Hamachi, I. *J. Am. Chem. Soc.* **2005**, *127*,

11835. b) Tamaru, S.-I.; Kiyonaka, S.; Hamachi, I. *Chem. Eur. J.* **2005**, *11*, 7294. c) Koshi, Y.; Nakata, E.; Yamane, H.; Hamachi, I. *J. Am. Chem. Soc.* **2006**, *128*, 10413.

19. a) Zhang, S. *Nature Biotechnol.* **2003**, *21*, 1171-1178. b) Zhang, S. *Nature Mater.* **2004**, *3*, 7-8.

# Chapter 2

## Photo-responsive Gel Droplet as a Nano- or Pico-Liter Container Comprising a Designer Supramolecular Hydrogel

**Abstract**

**Although photo-responsive hydrogels are desired as one of the intriguing biomaterials applicable to biological and medical research and engineering, examples for hydrogels having a talented photo-responsive property have been very limited. Here we designed a new photo-responsive hydrogel composed of self-assembled small molecules (gelators). This supramolecular hydrogel showed a light-induced gel-to-sol phase transition, resulting in a drastic change of mechanical toughness and aggregation morphology due to the trans/cis photo-isomerization of the double bond unit of the gelator. As well as the bulk gel formation, photo-responsive gel droplets having nano- or pico-L volume that showed photo-induced gel/sol transition were successfully developed, in which the inter-droplet mass transport and the subsequent enzymatic reactions in the interior of the gel droplets were photo-triggered. Focused laser light irradiation allows one to spatially and temporarily regulate the stepwise fusion of the gel droplets mediating a precisely controlled inter-droplet reaction. A novel supramolecular container with such photo-responsiveness might be promising as one of the attractive semi-wet biomaterials.**

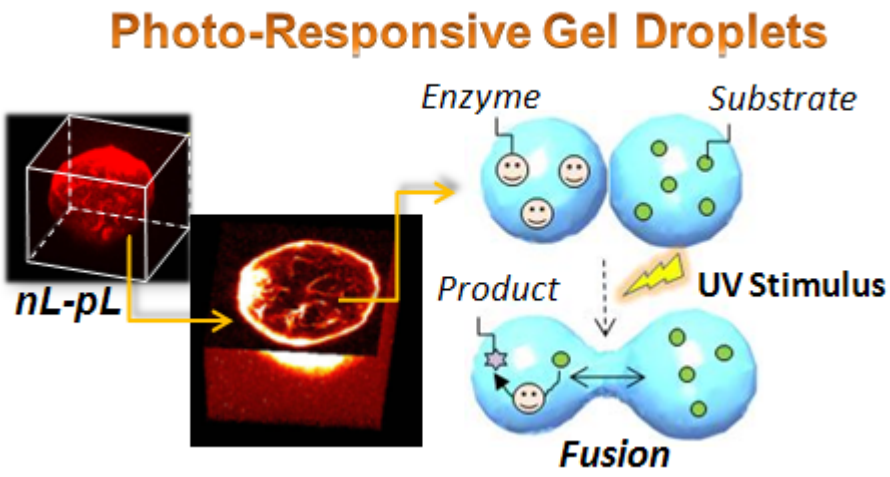

## 2-1. Introduction

Light is one of the ideal stimuli for fabricating and manipulating various properties of materials because of its clean, fast, and spatio-and-temporarily controllable features. Coupling of such features of light to appropriately designed substances is anticipated to produce sophisticated functional materials. Therefore, many kinds of photo-responsive soft-materials such as photo-memory, switches, sensors, actuators and other devices have attracted much attention ranging from fundamental science to practical application.[1] Among them, photo-responsive hydrogels are regarded as one of the intriguing biomaterials applicable to biological and medical fields. However, hydrogels having an efficient photo-responsive property have not been sufficiently developed,[2] compared to other types of hydrogels responsive to physical stimuli such as pH or heat. This is partially due to the difficulty of design and synthesis of photo-responsive hydrogels, especially in compatibly balancing between the stable gel formation and the effective photo-response. It is now crucial to explore the capability and the limitation of photo-responsive hydrogels as potential biomaterials,[3,4] along with creating novel hydrogels.

Supramolecular hydrogels consisting of self-assembled small molecules have recently emerged and are expected to be useful, novel and soft materials with a benefit that elaborate design of their component small molecules may directly influence their macroscopic hydrogel properties.[5] Such a straightforward and flexible design principle is believed to afford various stimuli-responsive materials. We describe herein a new supramolecular hydrogel which shows a photo-induced gel-to-sol phase transition not only in bulk scale, but also in a gel droplet of nano- or pico-L volume. The inter-droplet mass transport and the subsequent enzymatic reactions confined in the interior of the gel droplets were effectively photo-controlled.

## 2-2. Results and Discussion

### 2-2-1. Molecular design and synthesis

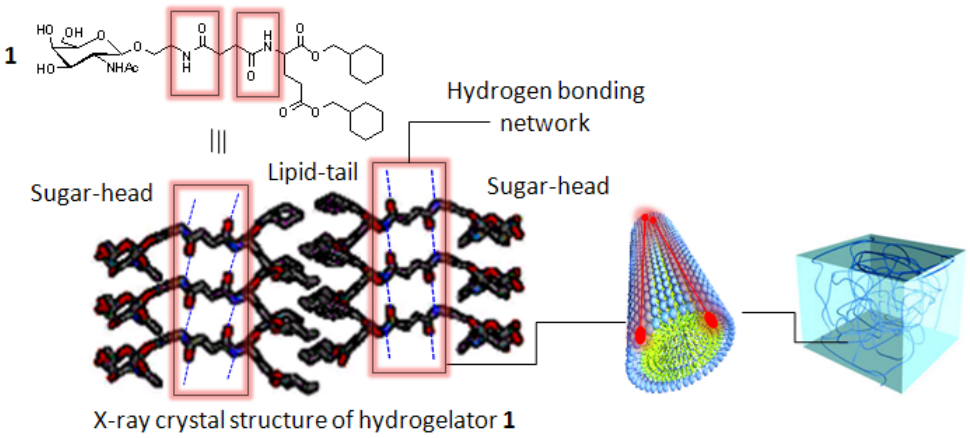


**Figure 1.** Chemical structure of hydrogelator **1** and schematic illustration showing supramolecular gel fiber network of **1**.

Our previously reported detailed structural analysis of a glycolipid-based supramolecular hydrogel **1** (Figure 1),[6] suggested that well-developed hydrogen bonding (H-B) networks in the spacer region cooperatively contribute to the stabilization of self-assembled gel fibers, together with van-der Waals packing at the tail modules and water-mediated H-B linkages with intermolecular saccharide heads. On the basis of these structural features, a potential candidate for photo-responsive hydrogelators was designed by incorporating a photo-responsive double bond into the spacer unit of the gelator. We expected that the photo-induced trans/cis conformational change would produce the destruction and/or construction of the central H-B networks, so that the macroscopic gel-to-sol transition would take place. A new gelator **2** having fumaric amide as the trans double bond was found to form a transparent hydrogel at low concentration (0.05 wt% of the critical gelation concentration) (Figure 2 a, b).

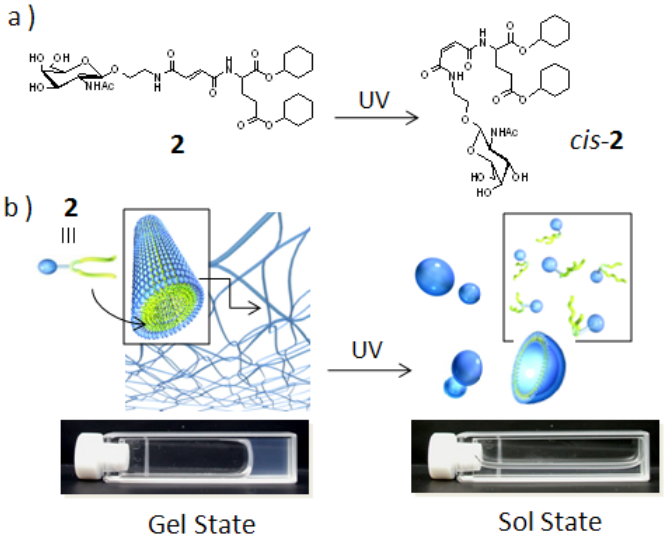


**Figure 2.** Design of photo-responsive hydrogelator **2**. a) Structures of photo-responsive hydrogelator **2** before and after UV irradiation. b) Schematic illustration and photographs showing photo-induced gel-to-sol transition of hydrogelator **2**.

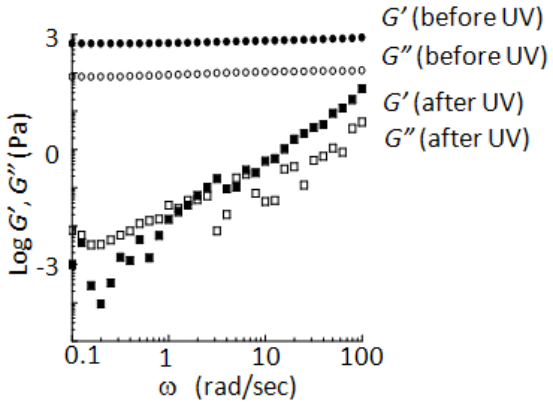


**Figure 3.** Dynamic viscoelastic properties of hydrogel **2** before and after UV irradiation with xenon lamp for 1h. *G'* (●: before UV, ■: after UV), *G''* (○: before UV, □: after UV).

It was observed by naked eye that UV light irradiation of the hydrogel **2** yielded the fluidic sol state as shown in Figure 2b. Figure 3 shows the dependence of storage (*G'*) and loss (*G"*) moduli of the hydrogel **2** on the angular frequency ω (rad $sec^{-1}$) before and after photoirradiation. A plateau appeared for both *G'* and *G"* in the frequency range of 100-0.1 rad $sec^{-1}$, clearly indicating that hydrogelator **2** was formed in a rheologically stable gel before photo-irradiation. On photo-irradiation, the values of both *G'* and *G"* dramatically decreased to almost the same values, to become $10^5$-fold smaller than those of the initial gel state at 0.1 rad $sec^{-1}$. It is clear that a typical gel-to-sol phase transition occurred upon UV irradiation. The $^1$H NMR study of the sol state indicated that 89% of the fumaric (trans) form turned into the maleic (cis) form (Figure 4). TEM (transmission electron micrograph) and SEM (scanning electron micrograph) gave an insight into the morphology of the self-assembled gel fibers (Figure 5). In the gel state, many fibers having a length longer than 10 μm and a width less than 20 nm are entangled similarly to other supramolecular hydrogels, whereas in the photo-induced sol state only spherical aggregates like vesicles (ca. 30-100 nm in diameter) were observed. It is reasonable that such spherical aggregates are not capable of entangling each other so that loss of the cross-linking points essential for gel formation resulted in the destruction of the macroscopic hydrogel.

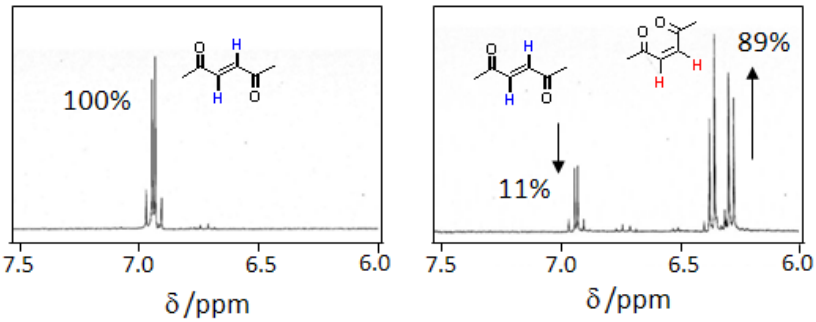


**Figure 4.** $^1$H NMR spectra for the gel state of **2** (left) and the sol state sample after UV irradiation with xenon lamp for 30 min (right).

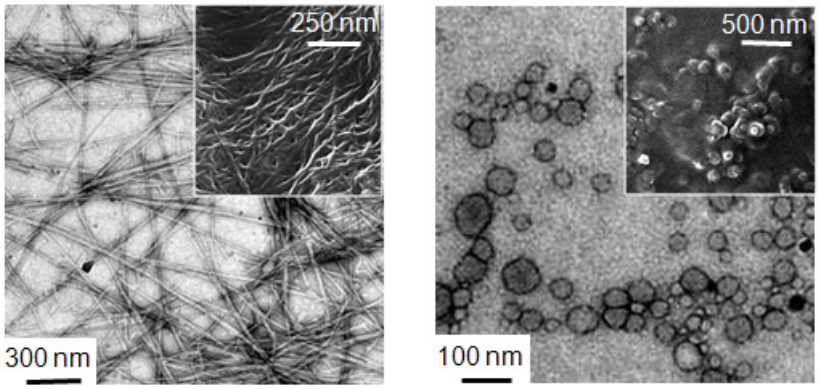


**Figure 5.** TEM and SEM (inset) images of the gel state of **2** before UV irradiation (left) and the sol state after UV irradiation to the gel with xenon lamp for 30 min (right).

### 2-2-2. Nano- and pico-liter supramolecular hydrogel droplets

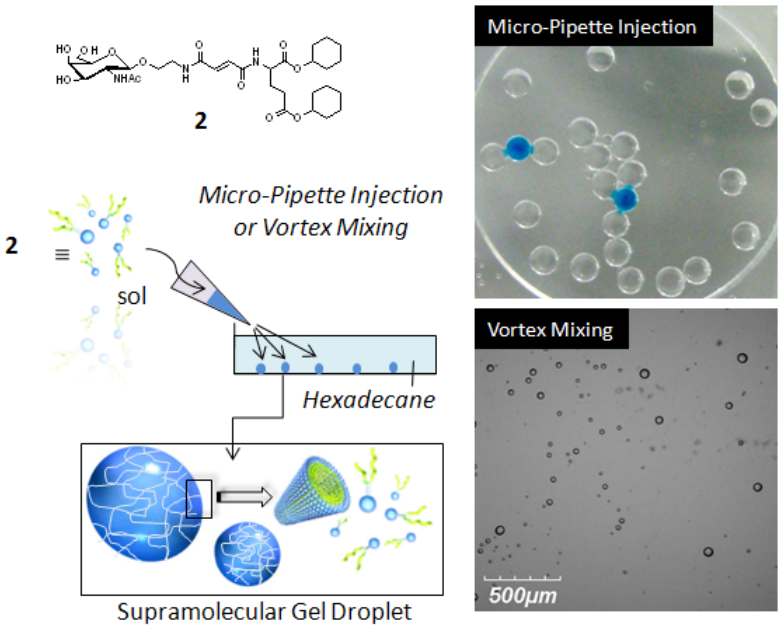


**Figure 6.** Schematic illustration of preparation of supramolecular gel droplets (left). Bright-field image of nL-pL volume gel droplets in hexadecane (right).

In addition to the bulk hydrogel, one can prepare supramolecular microgels of hydrogelator **2** by using the water-in-oil type of emulsion. By injecting 2 μL of the sol of **2** to hexadecane solution followed by Vortex mixing, spherical sol droplets are formed which gradually turn into gel droplets (ca. 50-100 μm in diameter, that is 60 pL-0.5 nL in volume) by self-assembly manner (Figure 6, 7). Unlike the limp droplets of the sol or water, the gel droplets seem relatively stiff. The surface morphology of the gel droplet was uneven, in contrast to the smooth surface of the sol droplet. The 3D-mapping of a supramolecular gel droplet stained with octadecyl-rhodamine ($C_{18}$-Rh) or fluorescein bearing synthetic lipid (Fl-$C_6$) by confocal laser scanning microscopy (CLSM) revealed well-developed fibrous networks of the self-assembled gelator **2** within the droplet sphere as shown in Figure 7, 8. UV irradiation to the gel droplet changed the rough surface of the droplet into the smooth spherical surface, with concurrent disappearance of the network of inner fibers, corresponding to the photo-induced gel-to-sol transition in droplets (Figure 9). The gel state of the interior space of the droplet was probed by the Brownian motion of nano-beads. As shown in Figure 10, we observed by CLSM that the Brownian motion of all beads (250 nm) embedded in the gel droplet stopped, indicating that the formation of the gel fiber network entrapped the nano-beads in the inner space. The Brownian motion of the nano-beads re-started when the sol droplet was photo-produced.

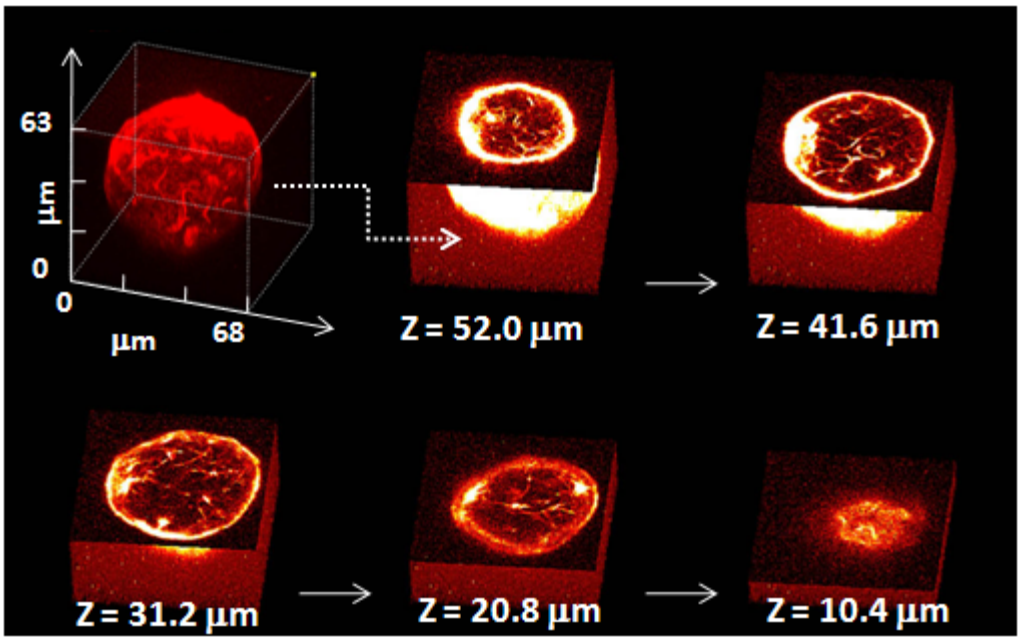


**Figure 7.** CLSM images of the supramolecular gel (**2**) droplet in hexadecane. 3D-fluorescence image of hydrogel **2** droplet (ca. 60 pL) stained with a hydrophobic rhodamine ([$C_{18}$-Rho] = 100 μM, excitation wavelength at 543 nm) and the Z-axial profiles of the gel droplet.

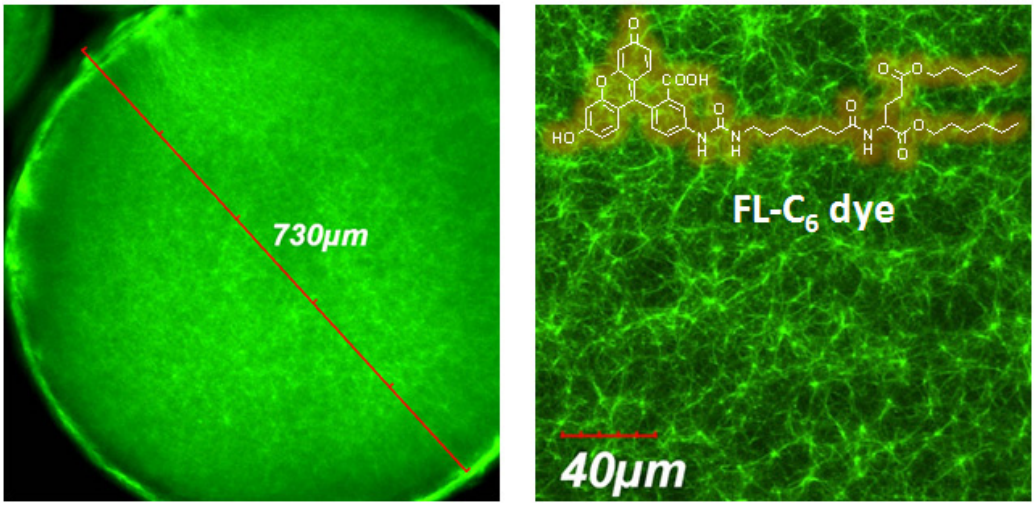


**Figure 8.** CLSM images of the supramolecular gel (**2**) droplet in hexadecane. 3D-fluorescence image of hydrogel **2** droplet stained with a hydrophobic fluorescein ([Fl-$C_6$] = 25 μM (2.5% DMSO), excitation wavelength at 488 nm).

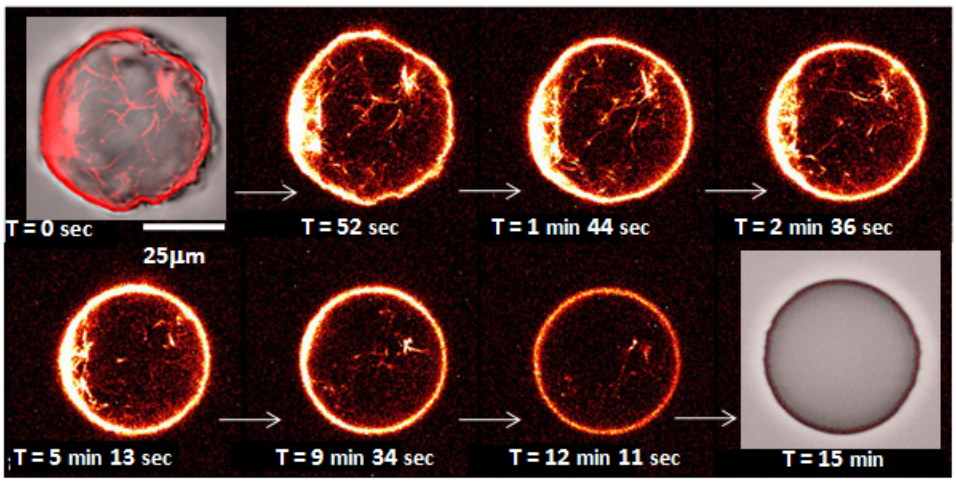


**Figure 9.** CLSM images of the supramolecular gel droplet (**2**) in hexadecane. The inner space fluorescence images of the gel (**2**, ca. 60 pL) droplet during UV irradiation with a low-pressure mercury vapor lamp. Droplet (**2**) was stained with a hydrophobic rhodamine ([$C_{18}$-Rho] = 100 µM, excitation wavelength at 543 nm)

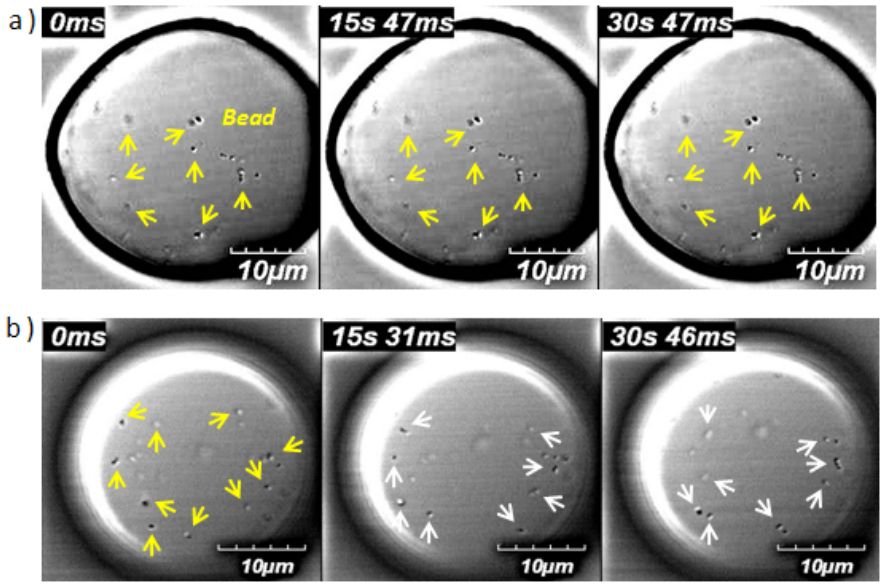


**Figure 10.** CLSM Time-dependent confocal laser scanning micrographs for the analysis of Brownian motion of hydrophilic 250 nm-beads a) in gel (**2**) droplet and b) in the sol droplet after UV irradiation with a low-pressure mercury vapor lamp for about 10 min.

### 2-2-3. Photo-induced partial fusion between two gel droplets

Because of their stiffness, two gel droplets brought into contact with each other retain their shape, whereas two sol or water droplets readily fuse into one larger droplet. Interestingly, two gel droplets can be partially fused into a dumbbell shape by the light stimulus (UV irradiation) as shown in Figure 11. We observed by CLSM that short-time (2-3 min) UV irradiation caused closer contact and subsequent partial fusion of two gel droplets. The trans/cis photoisomerization ratios of **2** in the gel droplets for varied UV-irradiation times were estimated by HPLC analysis (Figure 12). After UV irradiation for 2-3 min, at the time point of which the partial fusion occurred, the trans/cis ratios were in the range of 34-53%, which were still greater than 11% for the perfect sol state. This suggested that the partial fusion took place in the intermediate state between gel and sol state.

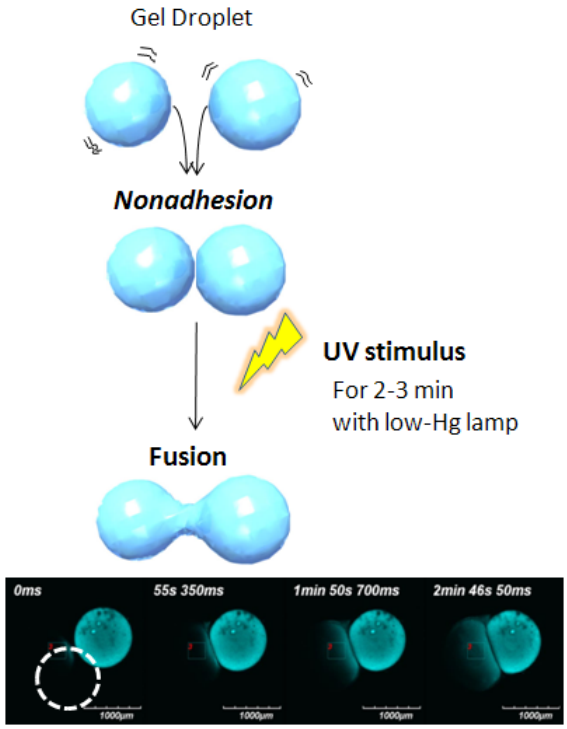


**Figure 11.** Schematic illustration of photo-induced fusion between gel droplets.

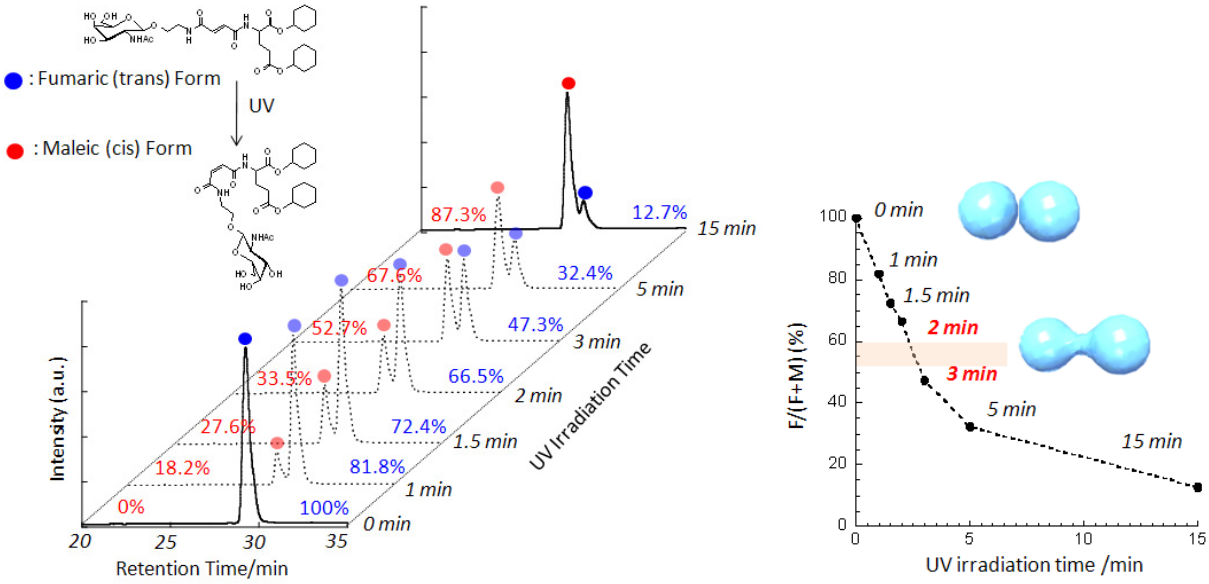


**Figure 12.** HPLC analysis for photo-isomerization ratio of hydrogelator **2** in gel droplets ([**2**] = 0.125 wt%) by UV irradiation with a low-pressure mercury vapor lamp (0, 1, 1.5, 2, 3, 5 or 15 min).

The mass transport between two gel droplets in contact was examined using fluorescent probes such as water-soluble fluorescein (Fl) and Cy-5. When a gel droplet that did not contain Fl was placed into contact with another gel droplet containing Fl, no transport of Fl occurred within 4 h as shown in Figure 13, indicating entrapment of the dye in the gel droplet. In contrast, when two gel droplets were partially fused by UV irradiation into the dumbbell shaped droplet, Fl rapidly diffused into the other space until equilibration (within 20 min). This implies that the mass transport between two distinct gel spaces was successfully photo-regulated.

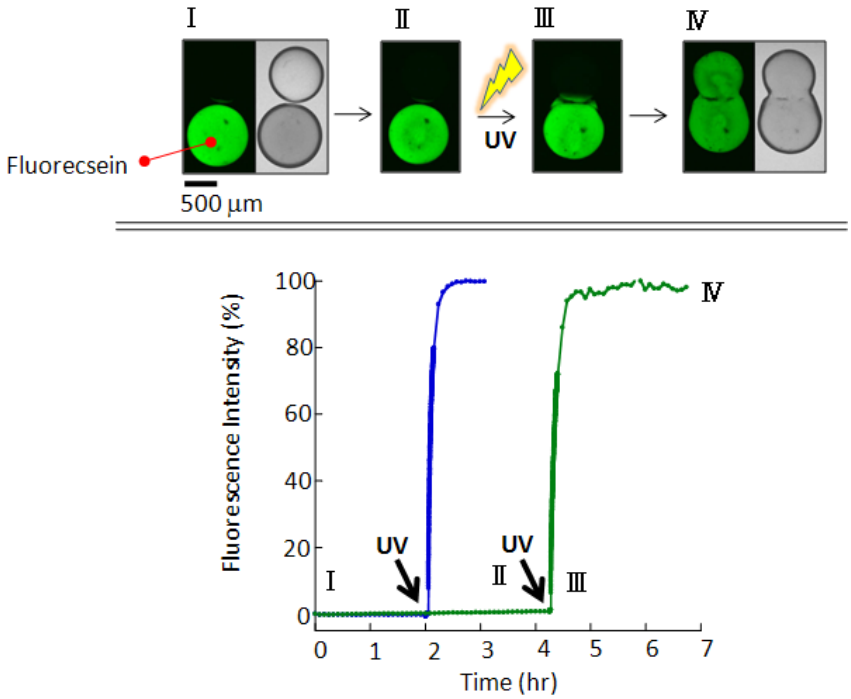


**Figure 13.** Photo-triggered fusion of two gel droplets. Time courses of the transport (fluorescence intensity) (%) of Cy-5 (blue) and Fluorescein (green) from the dye containing gel droplet to the blank one. Black arrows indicate the initial time of UV light (ca. 2-3 min) irradiation with a low-pressure mercury vapor lamp. Inset: fluorescence and DIC images (dash line) of the gel droplets at I, II, III and IV stage in the left panel.

### 2-2-4. Regulation of enzymatic reactions using the photo-induced partial fusion between gel droplets

Besides simple diffusion, enzymatic reactions in the gel droplet could be photo-regulated. We previously demonstrated that our supramolecular hydrogels can provide a suitable matrix to immobilize native proteins and enzymes without denaturation.[6c, 7] Even though two distinct gel droplets containing Alkaline Phosphatase (AP, a hydrolytic enzyme) or the corresponding fluorogenic substrate, were placed in contact, the enzymatic reaction did not take place (Figure 14). Upon the photo-induced partial fusion of the two droplets, the strong fluorescence emission of the AP-catalyzed reaction product rapidly appeared at the

interface, indicating that the reaction had been initiated. A similar photo-triggered reaction was also carried out for glucosidase enzyme (Figure 15). Careful observation showed that the enzymatic reaction occurred predominantly in the gel droplet containing AP at the initial stage (inset of Figure 14), presumably because the small substrate (ca. 500 in MW) diffused much more rapidly through the gel network, than the enzyme AP (140,000 in MW). A mass filter effect was achieved with the supramolecular gel network in the fused droplet.

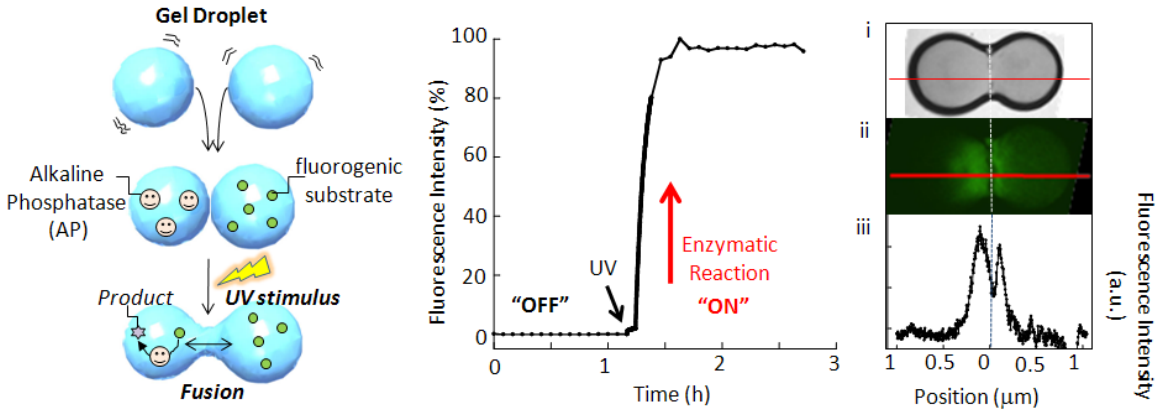


**Figure 14.** Enzymatic reaction triggered by the photo-fused gel droplets containing enzyme (AP, the left droplet) and the substrate (the right droplet). Time course of the fluorescence intensity of a region in the AP-containing droplet. Inset: i) Bright-field image, ii) fluorescence image and iii) the cross-section profile of integrated fluorescence intensity of the gel droplet (red line in panel (i) and (ii)) for ca. 30 sec immediately after the light-induced partial fusion between the gel droplets, which was prepared by subtracting the background fluorescence intensity before the fusion.

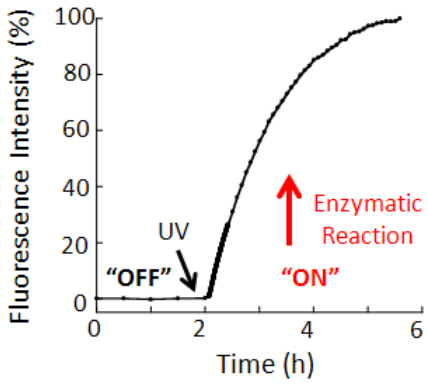


**Figure 15.** Off/on controlling of enzymatic reaction for glucosidase (GD) to 4-methylumbelliferyl b-D-glucopyranoside (MUG, substrate of GD) with photo-fused hydrogel droplets (**2**). Time course of fluorescence intensity of the reacted fluorescent substrate in the GD containing droplet was monitored with CLSM at excitation wavelength of 351 nm. Red arrow showed the UV irradiation time for approximately 4 min with a low-pressure mercury vapor lamp.

Using focused laser light, more precise photo-fusion between gel droplets was carried out. Figure 16 shows three distinct gel droplets in contact, with different contents, that is AP in droplet 1, none in droplet 2, and the substrate in droplet 3. When the interface between droplet 2 and 3 was irradiated (for 2-3 sec) with laser light (266 nm), 4 min after mechanical contact between droplets, very weak fluorescence was diffused from droplet 3 to droplet 2, but not droplet 1. This indicates that the photo-fusion area was strictly limited into the interface between droplet 2 and 3. Subsequently, more than 4 min later, the interface between droplet 1 and 2 was photo-irradiated by the laser to fuse the two droplets. Immediately after the fusion, strong emission appeared at droplet 2, suggesting that the AP-catalyzed hydrolysis took place mainly in the central droplet 2.

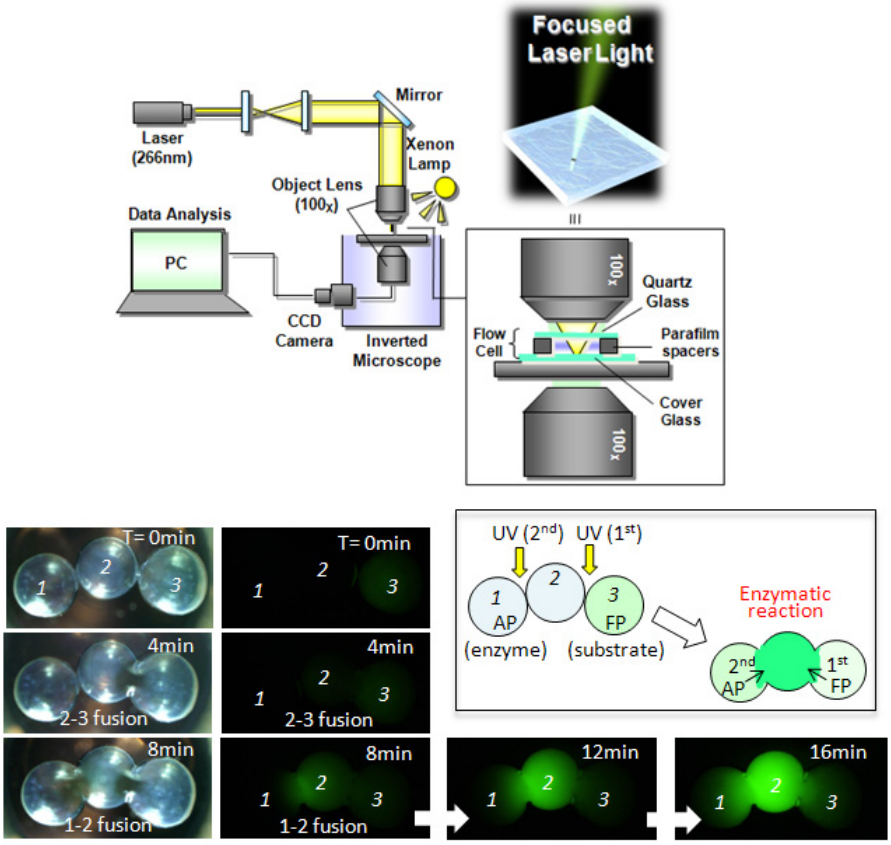


**Figure 16.** The photo-induced stepwise fusion between three gel droplets using focused laser light (266 nm) for ca. 2 sec. i) Bright-field images and ii) fluorescence images of the three distinct gel droplets in contact containing the different interior, that is AP in droplet 1, none in droplet 2, and the substrate in droplet 3. The focused laser light was irradiated step-by-step to the interface between droplet 2 and 3, and subsequently between droplet 1 and 2.

This can be extended to a gel droplet array consisted of more than 10 droplets having a variety droplet-pathways. As shown in Figure 17a, a droplet-array composed of thirteen gel droplets (droplet *2*-*12*, *14*, *15*), one containing AP-enzyme (droplet *1*) and another containing the fluorogenic sbstrate (droplet *13*), was successfully prepared in hexadecane. Using the focused laser light at the distinct interfaces, the stepwise partial fusion of the gel droplets were performed, so as to fabricate a droplet-pathway "*1-2-3-4-5-13*" (Figure 17a). After 20-30 min, the enzymatic reaction occurred predominantly in the gel droplet *4* which was placed close to the droplet *13* containing AP, and not in the droplet *11* and *12* (Figure 17b). These results indicated that spatial and temporal control of the mass transport and the consequent chemical reactions in the confined space in the gel droplet is accomplished by use of photo-responsive gel droplets.[8]

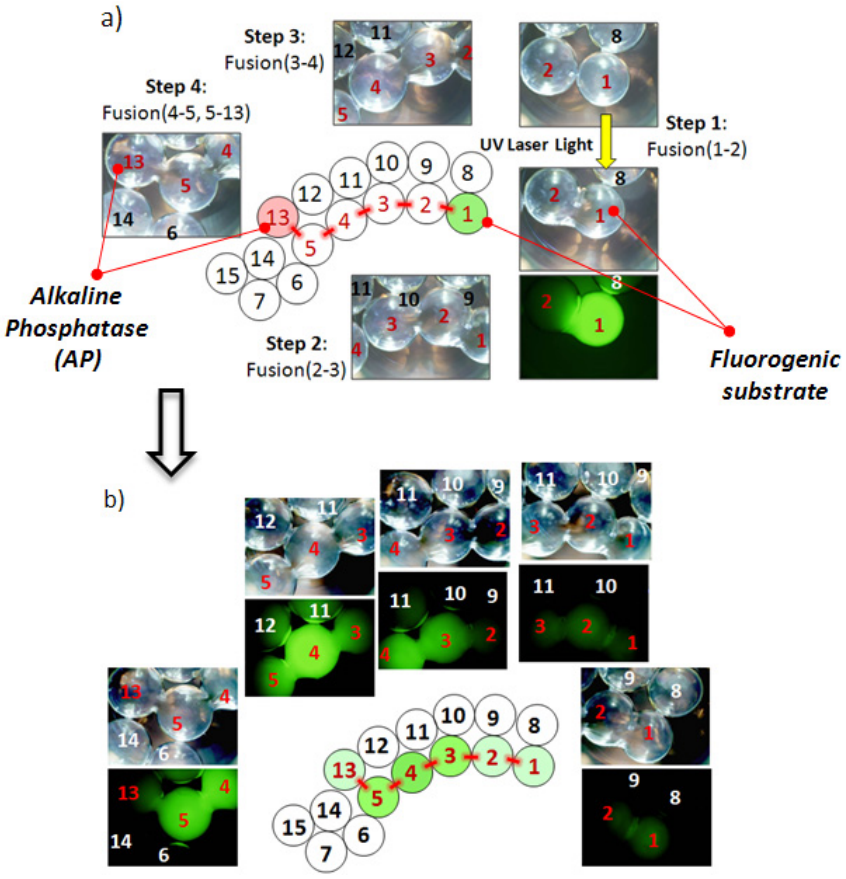


**Figure 17.** The gel droplets path fabricated between multi-gel droplets. a) Before connecting between the gel droplets.b) At 20-30 min later after fabricating the gel droplets path by photo-induced partial fusion with focused UV laser light. Gel droplet 13 was containing AP and gel droplet 1 was containing the fluorogenic substrate.

## 2-3. Conclusion

In conclusion, a photo-responsive gel droplet having nano- or pico-L volume was successfully developed using a newly designed supramolecular hydrogelator that induced the gel-to-sol phase transition by UV light. Recently, thermal- or pH-responsive polymer-based microgels (gel droplets) are actively developed by several researchers,[9] but photo responsive gel droplets have been rarely reported.[2d, 10] Using the present system, mass transport between gel droplets was controlled at will by light, and this may be applicable to the spatial control of various reactions, or intelligent delivery systems of various substrates nano-micrometer range such as nanoparticles or cells as a nano- or pico-L volume container.

## 2-4. Experimental Section

**Synthesis of photo-responsive hydrogelator 2** The synthetic scheme of the photo-responsive hydrogelator **2** is shown as above. The compound **3** and sugar-derivative (GalNAc-$NH_2$) were synthesized according to the method reported previously.[22] The syntheses and characterizations of compound **4**, **5** and the hydrogelator **2** were described as follows.

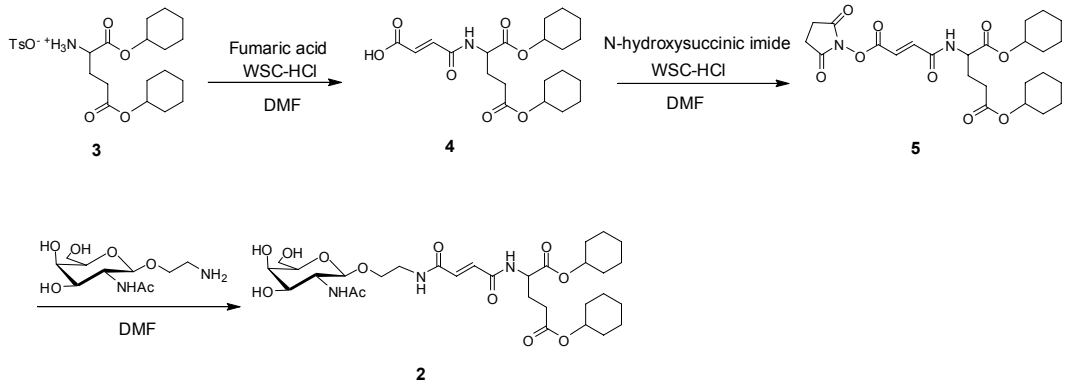


**Synthesis of Fum-glu(O-cyc-hexyl)$_2$ (4)** Under nitrogen atmosphere, a solution of WSC-HCl (7.7 g, 40 mmol) in DMF (50 mL) was added dropwise to a stirring solution of fumaric acid (18.6 g, 161 mmol) and **3** (12.5 g, 40 mmol) in anhydrous DMF (150 mL) at room temperature. After 12 h, the solvent was removed under reduced pressure at 50 ˚C. The residue was dissolved in ethyl acetate and the solution was washed 3 times with 5% critic acid solution. The organic layer was collected and dried over anhydrous $Mg_2SO_4$ and the solvent was evaporated to dryness. To remove excess amount of fumaric acid, the obtained oil was extracted with chloroform, and the filtrate was evaporated to yield crude **4** (13.1 g) as a brown oil, which was used without further purification.

**Synthesis of N-suc-fum-glu(O-cyc-hexyl)$_2$ (5)** To a solution of crude compound **4** (13 g) in DMF (150 mL) was added *N*-hydroxysuccinic imide (7.3 g, 63.5 mmol) and WSC-HCl (12.2 g, 63.5 mmol). The solution was stirred for 12 h at room temperature under nitrogen atmosphere and the solvent was removed under reduced pressure at ambient temperature. The crude residue was dissolved in ethyl acetate and washed with brine. The residue was dried over anhydrous $Mg_2SO_4$, and the solvent was evaporated in vacuo and then the obtained oil was purified by column chromatography (silica gel, ethyl acetate/hexane = 2/1, v/v) to give **5** 10.1 g (63% / 2 steps) as a colorless oil. $^1$H NMR (400 MHz, $CDCl_3$, TMS, ppm): $\delta$ 1.26-1.68 (m, 12H), 1.68-1.93 (m, 8H), 2.05-2.15 (m, 1H), 2.20-2.30 (m, 1H), 2.30-2.50 (m, 2H), 2.88 (s, 1H), 4.63-4.72 (m, 1H), 4.72-4.80 (m, 1H), 4.80-4.95 (m, 1H), 6.91 (d, $J$ = 7.2 Hz, 1H), 7.04-7.19 (m, 2H); FAB-HRMS: *m/z*: calcd for $C_{25}H_{34}O_9N_2$ ($M$): 506.2264; found: 506.2257.

**Synthesis of GalNAc-fum-glu(*O-cyc*-hexyl)$_2$ (2)** GalNAc-$NH_2$ [22] (3.7 g, 14 mmol) was added to a stirring solution of **5** (7.4 g, 14.7 mmol) in DMF 200 ml at 35 ˚C for 12 h. The solvent was removed by evaporation at 50 ˚C, and the crude compound was washed with methanol several times and ion-exchanged water three times and dried for 12 h at 40 ˚C to give **2** as a colorless solid (4.8 g, 52%). $^1$H NMR (400 MHz, $CDCl_3$/$CD_3OD$, TMS, ppm): $\delta$ 1.29-1.56 (m, 20H), 2.01 (s, 1H), 1.70-1.90, 1.98-2.09, 2.17-2.26 (m, 2H), 2.36-2.46 (m, 2H), 3.47-3.77 (m, 4H), 3.80-3.89 (m, 6H), 4.41 (d, $J$ = 8.4 Hz, 1H), 4.56-4.58 (m, 1H), 4.74-4.82 (m, 2H), 6.87-6.93 (m, 2H); FAB-MS: *m/z*: calcd for $C_{31}H_{49}N_3O_{12}$: 655.33; found: 656.38 $[M+H]^+$, 678.34 $[M+Na]^+$; Elemental analysis calcd (%) for $C_{31}H_{49}N_3O_{12}$: C 56.78, H 7.53, N 6.41; found: C 56.51, H 7.52, N 6.14.

**Photo-induced (bulk) gel-to-sol transition** UV light irradiated to the hydrogel **2** (0.1 wt%, ion-exchanged water) prepared in a quartz cell (light path length; 2 mm) with a xenon lamp (USHIO, Optical Modulex, SX-UI500XQ, Figure S1) for at least 10 min at 15 ºC.

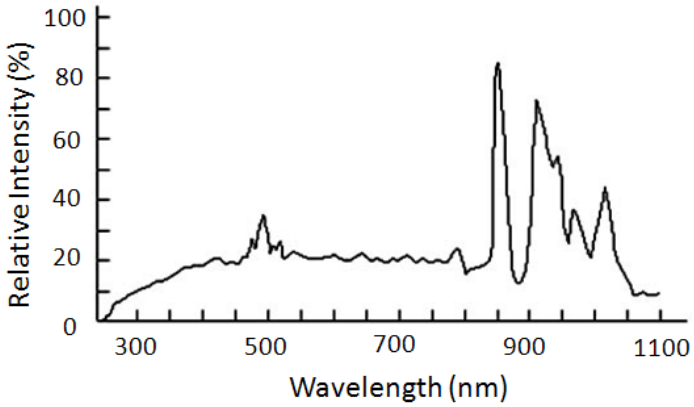


**Figure S1.** Spectral distribution of xenon shrot-arc lamp excerpted by USHIO website.

**Dynamic viscoelasticity measurement** Dynamic viscoelasticities of the hydrogel **2** (0.2 wt%) before and after UV irradiation with a xenon lamp for 1 h were measured with a plate-plate rheology equipment (DynAlyser DAR-100, Reologica). The measurement conditions were as follows: angular frequency range: 100-0.1 rad·sec$^{-1}$; strain: 2% for the gel sample and 0.5% for the sol sample (after UV irradiation to the gel **2**); parallel plate: 4 cm in diameter; gap distance: 1.2 mm; measurement temperature; 24 ºC.

**$^1$H NMR measurement** [hydrogel **2**] = 0.2 wt%, $D_2O$. Photo-isomerization ratios of fumaric (trans) to maleic (cis) amide form were estimated from these *H*-integrals by $^1$H NMR measurement (JEOL-JNM-EX400 apparatus, 400 MHz) of each sample, to which $CD_3OD$ added ($CD_3OD/D_2O$ = 1/1 v/v) for preparing the homogenous dispersed solution of gel/sol. These ratios showed as (fumaric)/(fumaric + maleic amide form) × 100. In addition, remarkable by-products were not observed in NMR measurement.

**TEM and SEM observation** Carbon-coated copper grids were dipped in the hydrogel **2** or the sol after UV irradiation to gel with a xenon lamp for 30 min. They were dried under reduced pressure for 24 h at room temperature. TEM samples were stained with 2 wt% aqueous solution of uranyl acetate. TEM observations were carried out with a JEOL JEM-2010 apparatus under 120 kV accelerating voltage. For SEM observation, the samples were coated by platinum vapor deposition (30 sec). SEM images were obtained by using a Hitachi S-5000, acceleration voltage 25 kV. [Hydrogelator **2**] = 0.2 wt% (ion-exchanged water).

**Preparation of gel droplets** 1.0-0.1 μL of gel droplets were prepared by adding heat-dispersed sol of **2** to hexadecane via micro-pipette injection. For the preparation of less than 0.1 μL of gel droplets, immediately after 2 μL of the heat-dispersed sol of **2** was added dropwised to 2 mL hexadecane solution, the solution was agitated via Vortex mixing. This solution was transferred to a glass-bottom dish and then we observed gel droplets thus prepared with a confocal laser scanning microscope (CLSM, OLYMPUS, FV1000). [Hydrogelator **2**] = 0.1 wt% (ion-exchanged-water).

**Observation for Brownian motions of micro-beads in gel droplet** The heat-dispersed sol of **2** in ion-exchanged water containing 250 nm-fluorescent beads (micromer®-red F, POL) were dropped to hexadecane solution on a glass-bottom dish and left for 30 min at room temperature. These samples were monitored with a confocal laser scanning microscope (CLSM, OLYMPUS; FV1000) in real time. [Hydrogel **2**] = 0.1 wt% (ion-exchanged water).

**HPLC analysis** HPLC conditions are as follows: column, YMC-pack ODS-A, 4.6 Φ×250 mm; mobile phase, $CH_3CN$ (0.1% TFA)/$H_2O$ (0.1% TFA) = 20/80-70/30 (linear gradient over 60 min); flow rate, 1.0 mL/min; detection, UV (204 nm, at isosbestic point before and after UV irradiation to **2**).

**Regulations for dye transfers and enzymatic reactions by photo-responsive fusion-capable gel droplets** 0.5 μL of heat-dispersed sol of **2** (0.125 wt%, 50 mM Tris-HCl buffer, pH 8.0) containing 50 mM Cy-5 (50 mM Tris-HCl buffer, pH 8.0) or 50 mM Fluorescein (50 mM Tris-HCl buffer, pH 8.0) was dropped into 1.5 mL hexadecane solution on a glass-bottom dish. In the same way, gel droplets without dye were prepared. These droplets were placed in contact with each other by lightly shaking the dish. In the experiment of UV irradiation, a low-pressure mercury vapor lamp (Ushio; UL0-6DQ, Figure S2) was located approximately 1 cm above the dish and UV-irradiation was conducted for less than 3 min. In enzymatic reactions, alkaline phosphatase (TOYOBO) and 3-*O*-Methylfluorescein phosphate cyclohexyl ammonium salt (SIGMA) as the substrate, or glucosidase (SIGMA) and 4-Methylumbelliferyl β-*D*-Glucopyranoside (Wako) as the substrate were separately entrapped in gel droplets in the same manner. [Alkaline phosphatase] = 0.21 x $10^{-3}$ units/droplet (0.5 μL), [3-*O*-Methylfluorescein phosphate cyclohexyl

ammonium salt] = 0.11 mM, [Glucosidase] = 4.0 x $10^{-3}$ units/droplet (0.5 μL), [4-Methylumbelliferyl β-*D*-Glucopyranoside] = 0.60 mM, 50 mM Tris-HCl buffer (pH 8.0).

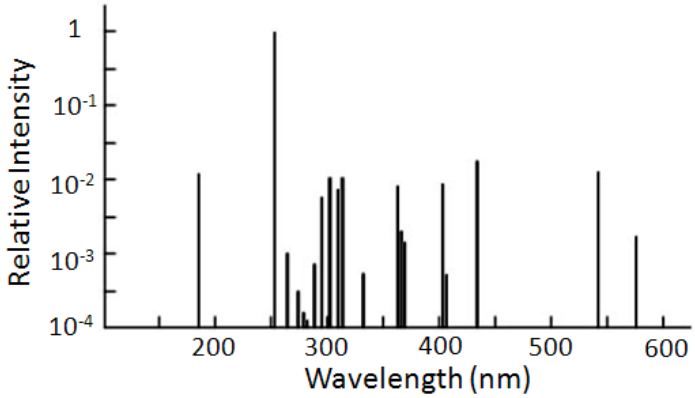


**Figure S2.** Spectral distribution of low-pressure UV lamp excerpted by USHIO website.

## 2-5. References and Notes


1. a) Irie, M. *Chem. Rev.* **2000**, *100*, 1685. b) Yu, Y.; Nakano, M.; Ikeda, T. *Nature* **2003**, *425*, 145. c) Browne, W. R.; Feringa, B. L. *Nat. Nanotechnol.* **2006**, *1*, 25. d) Jiang, H.; Kelch, S.; Lendlein, A. *Adv. Mater.* **2006**, *18*, 1471. e) Kobatake, S.; Takami, S.; Muto, H.; Ishikawa, T.; Irie, M. *Nature* **2007**, *446*, 778. f) Kay, E. R.; Leigh, D. A.; Zerbetto, F. *Angew Chem. Int. Ed.* **2007**, *46*, 72.
2. a) Irie, M.; Kunwatchakun, D. *Macromolecules* **1986**, *19*, 2476. b) Mamada, A.; Tanaka, T.; Kungwatchakun, D.; Irie, M. *Macromolecules* **1990**, *23*, 1517. c) Frkanec, L.; Jokic, M.; Makarevic, J.; Wolsperger, K.; Zinic, M. *J. Am. Chem. Soc.* **2002**, *124*, 9716. d) Hirakura, T.; Nomura, Y.; Aoyama, Y.; Akiyoshi, K. *Biomacromolecules* **2004**, *5*, 1804. e) Haines, L. A.; Rajagopal, K.; Ozbas, B.; Salick, D. A.; Pochan, D. J.; Schneider, J. P. *J. Am. Chem. Soc.* **2005**, *127*, 17025. f) Tomatsu, I.; Hashidzume, A.; Harada, A. *Macromolecules* **2005**, *38*, 5223. For photoresponsive organogels: g) Murata, K.; Aoki, M.; Suzuki, T.; Harada, T., Kawabata, H.; Komori, T.; Ohseto, F.; Ueda, K.; Shinkai,S. *J. Am. Chem. Soc.* **1994**, *116*, 6664. h) de Jong, J. J. D.; Hania, P. R.; Pugzlys, A.; Lucas, L. N.; de Loos, M.; Kellogg, R. M.; Feringa, B. L.; Duppen, K.; van Esch, J. H. *Angew Chem. Int. Ed.* **2005**, *44*, 2373.
3. Silva, G. A.; Czeisler, C.; Niece, K. L.; Beniash, E.; Harrington, D. A.; Kessler, J. A.; Stupp, S. I. *Science* **2004**, *303*, 1352.
4. Zhang, S. *Nat. Biotechnol.* **2003**, *21*, 1171.
5. a) Estroff, L. A.; Hamilton, A. D. *Chem. Rev.* **2004**, *104*, 1201. b) Sangeetha, N. M.; Maitra, U. *Chem. Soc. Rev.* **2005**, *34*, 821. c) De Loos, M.; Feringa, B. L.; van Esch, J. H. *Eur. J. Org. Chem.* **2005**, *17*, 3615.
6. a) Kiyonaka, S.; Sugiyasu, K.; Shinkai, S.; Hamachi, I. *J. Am. Chem. Soc.* **2002**, *124*, 10954. b) Kiyonaka, S.; Zhou, S. L.; Hamachi, I. *Supramol. Chem.* **2003**, *15*, 521. c) Kiyonaka S.; Sada, K.; Yoshimura, I.; Shinkai, S.; Kato, N.; Hamachi, I. *Nat. Mater.* **2004**, *3*, 58. d) Zhou, S. L.; Matsumoto, S.; Tian, H.-D.; Yamane, H.; Ojida, A.; Kiyonaka, S.; Hamachi, I. *Chem. Eur. J.* **2005**, *11*, 1130.
7. a) Kiyonaka, S.; Shinkai, S.; Hamachi, I. *Chem. Eur. J.* **2003**, *9*, 976. b) Tamaru, S.-I.; Kiyonaka, S.; Hamachi, I. *Chem. Eur. J.* **2005**, *11*, 7294. c) Koshi, Y.; Nakata, E.; Yamane, H.; Hamachi, I. *J. Am. Chem. Soc.* **2006**, *128*, 10413.
8. We confirmed that the photo-triggered fusion did not occur for non-photoresponsive gel doroplets composed of agarose hydrogel (Figure S3).



**Figure S3.** Gel droplets composed of agarose hydrogel (2 wt%, 0.5 μL/droplet). a) Before, b) during and c) after UV irradiation for 20 sec with 266 nm focused laser light.


9. For reviews, see: Saunders, B. R.; Vincent, B. *Adv. Colloid Interface Sci.* **1999**, *80*, 1-25; Pelton, R. *Adv.*

*Colloid Interface Sci.* **2000**, *85*, 1-33; As examples for microgels, see: Xu, S.; Nie, Z.; Seo, M.; Lewis, P.; Kumacheva, E.; Stone, H. A.; Garstecki, P.; Weibel, D. B.; Gitlin, I.; Whitesides, G. M. *Angew. Chem. Int. Ed.* **2005**, *44*, 724-728; Suzuki, D.; Tsuji, S.; Kawaguchi, H. *J. Am. Chem. Soc.* **2007**, *129*, 8088-8089; Tan, W.-H.; Takeuchi, S. *Adv. Mater.* **2007**, *19*, 2696-2701.

10. Garcia, A.; Marquez, M.; Cai, T.; Rosario, R.; Hu, Z.; Gust, D.; Hayes, M.; Vail, S. A.; Park, C.-D. *Langmuir* **2007**, *23*, 224-229.

# Chapter 3

## Photo Gel-Sol/Sol-Gel Transition and Its Patterning of a Supramolecular Hydrogel as Stimuli-Responsive Biomaterials

**Abstract**

**In a focused library of glycolipid-based hydrogelators bearing fumaric amide as a trans-cis photo-switching module, a few of the photo-responsive supramolecular hydrogelators were newly discovered, the gel-sol and sol-gel transition of which was pseudo-reversibly induced by light. NMR and various microscopy studies of the optimal hydrogel demonstrated that the trans-cis photo-isomerization of the double bond of the fumaric amide unit effectively caused the formation or deformation of the self-assembled supramolecular fibers, so as to yield the macroscopic hydrogel or the corresponding sol, respectively. The entanglement of the supramolecular fibers produced the nano-meshes, the void space of which was roughly evaluated to be 250 nm by the confocal laser scanning microscopy observation for the size dependent Brownian motion of the nano-beads embedded in the supramolecular hydrogel. It is clearly shown that such nano-meshes become a physical obstacle to capture the sub-micro to micro meter sized substrates such as the beads, or *E-coli* bacteria. On the benefit of the photo-responsive property of the supramolecular nano-meshes, we succeeded in the off-on switching of the bacteria movement and the rotary motion of the beads-tethered ATPase, a biomolecular motor protein, in the supramolecular hydrogel. Furthermore, by the photolithographic technique or the focused laser light, "photo gel-sol patterning" was successfully conducted to produce the sol spots within the gel matrix. Using the fabricated sol/gel pattern, not only the regulation of the bacteria motility in the limited area, but also the off/on switching of the bead tethered $F_1$-ATPase rotary motion at a single molecular level were accomplished. These reults demonstrated that the photo-responsive supramolecular hydrogel and the consequent nano-meshes may provide a unique biomaterials for the spatiotemporal manipulation of various biomolecules and live bacteria.**

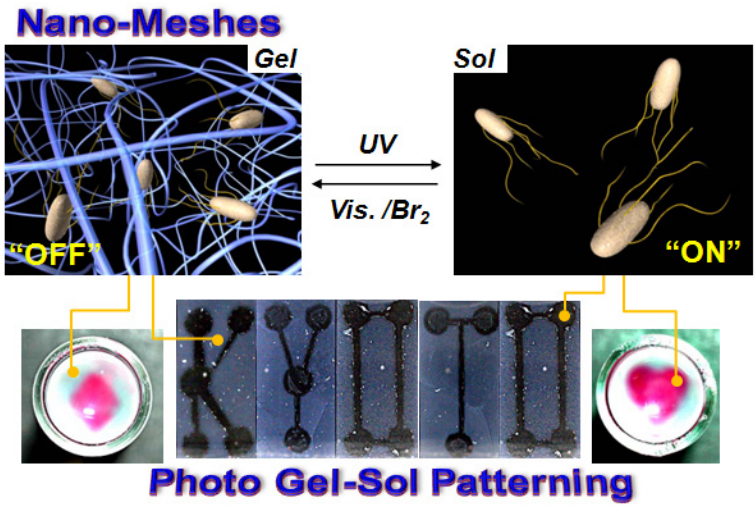

## 3-1. Introduction

For the advancement of nano-biotechnology and nao-medicine, sophisticated devices[1] and materials[2] capable of manipulating the function, the activity or the mobility of biomacromolecules such as DNA, proteins, organellas and cells is crucial. In order to develop such intelligent bio-devices, the bottom-up approach is now considered to be complimentary to the top-down approach, so that the rational combination of them should be promising. Among the bottom-up approaches for well-organized structures and functions, a supramolecular strategy seems promising in which the molecular self-assembly based on the weak non-covalent interactions is elegantly utilized. Supramolecular hydrogel,[3] for example, is one of the attractive biomaterials not only because it can entrap various biomolecules without denaturation, but also the hierarchal molecular assemblies are built-up from the flexible nano-fibers with the high aspect ratio to 3D-fiber networks with sub-micro to hundred micro scales, and finally to the macroscopic hydrogel with the millimeter size.[4,5] The hierarchy gave us a valuable characteristic that the subtle structural change in the constitute element level can directly influence the macroscopic properties of the supramolecular materials. Due to such a benefit, in fact, growing numbers of intelligent supramolecular hydrogels that respond to thermal, [3] pH,[6] enzyme[7] and other stimuli[8] recently emerged. In these examples, a stimuli-responsive module was built-in the small molecule, an element of the corresponding supramolecule, in order to induce a macroscopic change of the self-assembled hydrogel.

Among these stimuli, light is unique in the point that the remote input with temporally and spatially controlled manner is readily accomplished. Thus, photo-stimuli is expected to be highly useful especially for the fabrication of supramolecular materials.[9] However, photo-responsive supramolecular hydrogels[10] have been poorly developed in contrast to rich examples for photo-driven molecular machine or molecular switching.[11] We describe herein a strategy on the basis of coupling of the partially rational design with the focused combinatorial library, which becomes powerful for the discovery of novel photo-responsive supramolecular hydrogels. In addition to the conventional structural analysis, the meshes size formed of the supramolecular fibers was examined by experiments of the substrates release and the direct observation of Brownian motion of the embedded nano-beads in the hydrogel, both of which were found to be photo-regulated. Using the photo-induced gel-to-sol phase transition of the supramolecular hydrogel, the photo-sol/gel patterning was also successful, so that the rotational movement of micro-bead tethering $F_1$-ATPase, a biological motor protein, and the bacteria motility were spatially controlled.

## 3-2. Results and discussion

### 3-2-1. Molecular design and synthesis

A photo-switchable module was incorporated into the spacer unit of a glycolipid-based gelator, on the basis of our structural data of a supramolecular hydrogel **1** (Figure 1 in Chapter 2) which possesses well-developed hydrogen bonding (H-B) networks in the spacer region cooperatively contributing to the stabilization of self-assembled gel fibers, as well as van-der Waals packing at the tail modules and the

water-mediated H-B linked with the intermolecular saccharide heads.[4a] The subtle change by the trans/cis isomerization of the module of the component molecule was expected to produce the destruction and/or construction of the central H-B network, and as a result, the macroscopic gel-sol and/or sol-gel transition in the supramolecular hydrogel may be induced. In practice, with restoring other structural modules, the succinic amide spacer of the gelator **1** was replaced with the fumaric amide as a photo-responsive module which can undergo the photo-isomerization to maleic amide. It seemed reasonable to assume that the H-B network is retained in the trans conformation (fumaric amide) because of the structural similarity to the succinic amide without any strain, whereas it may be partially disrupted in the cis conformation (maleic amide). Unfortunately, however, the simple replacement of succinic amide with fumaric amide caused the loss of the gelation capability. Thus, we prepared a small combinatorial library of the relevant derivatives by changing other modules such as the sugar head and the hydrophobic tail, from which several low molecular weight hydrogelators were discovered (Figure 1a). The molecules consisting of the GalNAc head and cyc-hexyl tail or the Gal head and methyl-cyc-pentyl tail formed stable and transparent hydrogels. In

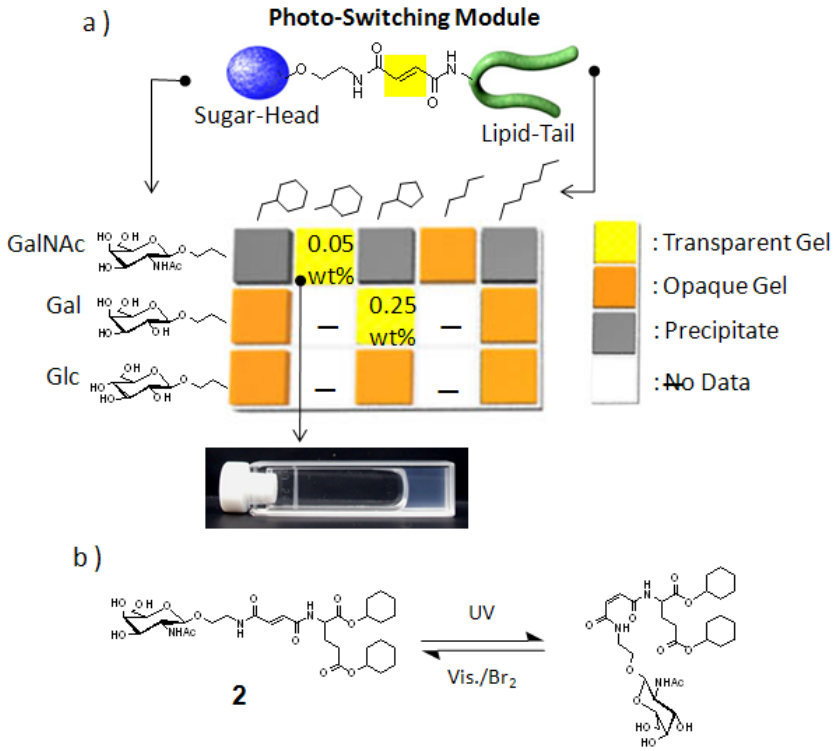


**Figure 1.** Structure of glyco-lipid based supramolecular hydrogelator. a) A small combinatorial library for screening photo-responsive hydrogelators. Hydrophilic sugar-head (in column) and hydrophobic lipid-tail (in row) modules were altered. The gelation test results were classified into transparent gel, opaque gel, precipitate and homogenous solution as shown in the table. For transparent gel, the critical gelation concentration was also written into the table. b) The scheme of trans/cis photo-isomerization of **2** induced by UV/Vis irradiation.

particular, the gelator **2** (Figure 1b) displayed a superior hydrogelation property, that is a transparent hydrogel formed at low concentration (0.05 wt% of the critical gelation concentration). The reological study showed that a plateau appeared in both the *G'* (the storage moduli) and *G"* (and loss moduli) at 100-0.1 (rad $sec^{-1}$) of hydrogel **2** in the wide range of the angular frequency (ω), clearly indicating that the hydrogelator **2** formed in a rheologically stable gel (Figure 3 in Chapter 2).

The usual thermal gel-sol transition occurred at about 60 ˚C, estimated by the changing of the light scattering of the gel **2** at 400 nm depending on the incubation temperature. In Figure 2a, among 24 and 50 ˚C, the light scattering of gel **2** gradually increased, indicating the formation of gel fiber networks. On the other hand, at 60-65 ˚C, the slope of the transmittance change became flat or decreasing during the incubation, suggesting that the gel fiber network melted and did not reform around this temperature. This thermal gel-sol transition could be reversibly repeated by cooling/heating cycle operation (Figure 2b).

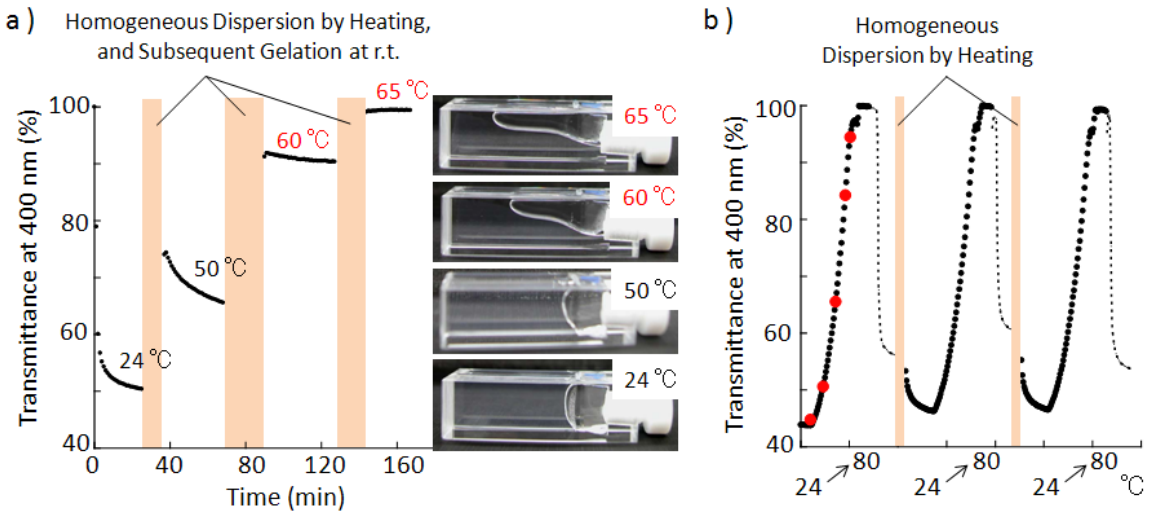


**Figure 2.** Thermal gel-sol transition of hydrogel **2** (0.1 wt%). a) The light scattering of the gel **2** at each constant temperature (24, 50, 60 and 65 ˚C). b) Heat-induced reversible change of the light scattering of the hydrogel **2** monitored at 400 nm.

### 3-2-2. Photo-induced gel/sol and sol/gel transition

As shown in Figure 3a, the resultant hydrogel consisting of **2** was turned into the sol state by the UV light irradiation and the sol state was returned back to the gel state by visible light in the presence of small amount of $Br_2$. By the dynamic viscoelasticity measurement of the fluidic sol (Figure 3b), we found that *G'* at 0.1 (rad $sec^{-1}$) became $10^5$-fold smaller than initial gel state and both *G'* and *G"* drastically decreased depending on the angular frequency, whereas these values almost recovered to the original ones after the gel was reformed by the visible light/$Br_2$ (Figure 3b). This rheological behavior showed that a typical gel-sol and sol-gel phase transition occurred upon photo-irradiation. The $^1H$ NMR study of the sol

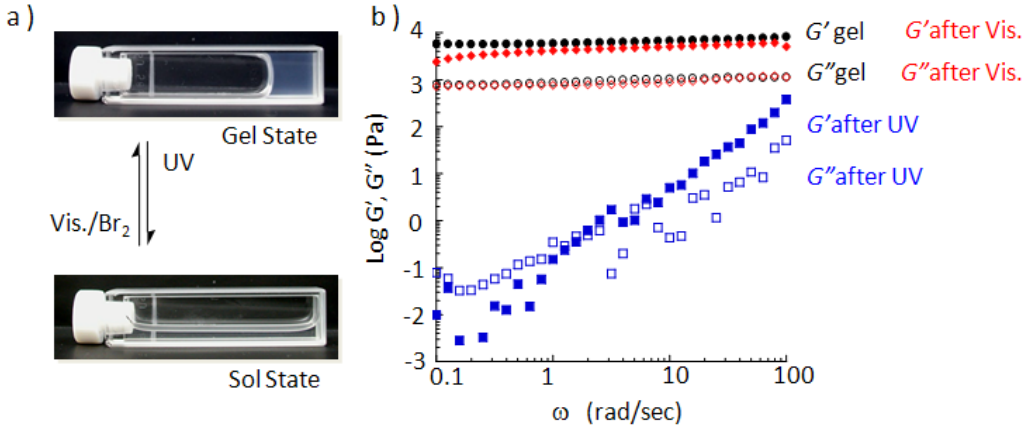


**Figure 3.** Pseudo-reversible photo gel-sol transition of hydrogel **2**. a) Photographs of hydrogel **2** before and after UV or Vis ($Br_2$) irradiation. b) Dynamic viscoelasticitc properties of hydrogel **2**, the sol after UV irradiation to the gel **2**, and the reconstructed gel **2** after Vis ($Br_2$) irradiation to the sol. *G'* (●: before UV, ■: after UV, ◆: after Vis), *G"* (○: before UV, □: after UV, ◇: after Vis).

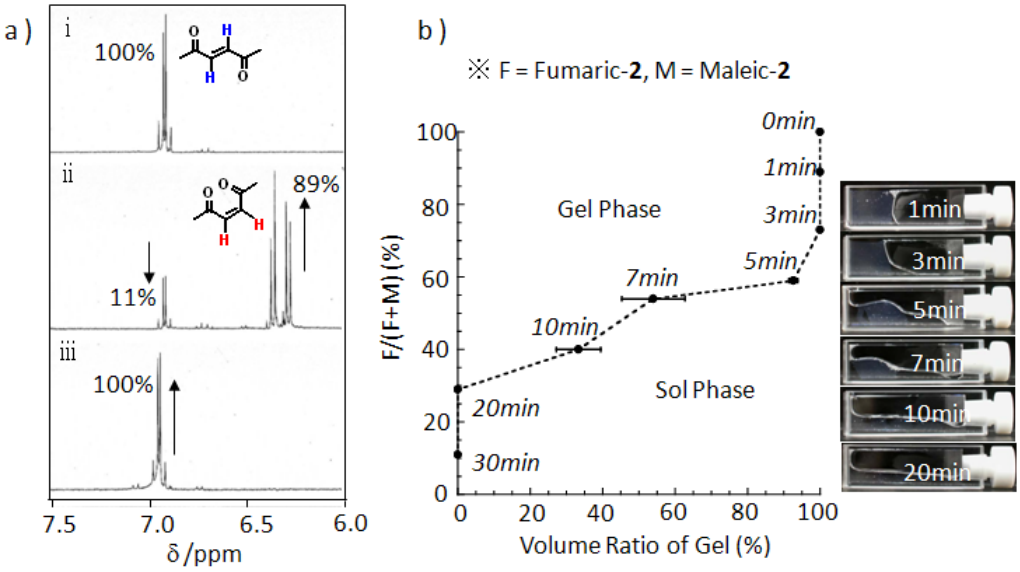


**Figure 4.** a) Enlarged $^1$H NMR spectra of (i) the gel state of **2**, (ii) the sol state sample after UV irradiation for 30 min and (iii) the re-gelated sample after Vis ($Br_2$) irradiation for 10 min. b) Phase diagram for gel volume against the composition of fumaric-**2** (%) (F/(F+M); F = fumaric-**2**, M = maleic-**2**) at each UV irradiation time (0, 1, 3, 5, 7, 10, 20 and 30 min). Inset images: photographs of photo responsive gel-sol transition in panel b.

state indicated that 89% of the fumaric (trans) form turned into the maleic (cis) form by UV irradiation and the cis rich sol state changed again into the gel state including 100% of the trans isomer (Figure 4a). By the careful analysis, it is clear that the gel/sol transition is dependent on the trans/cis isomerization ratio, showing a threshold content with which at least 50% of the cis form is needed for the gel-sol transition (Figure 4b). A Quantum yield for the photo-isomerization ($\Phi_f$) of hydrogelator **2** for the gel-sol transition induced by light (254 nm) was determined to be 0.039. It was slightly lower than the value of fumaric acid in water ($\Phi_f$ = 0.063).[12] This may be due to the steric-hindrance for the photo-isomerization in the self-assembled fiber, relative to in the homogeneous solution.

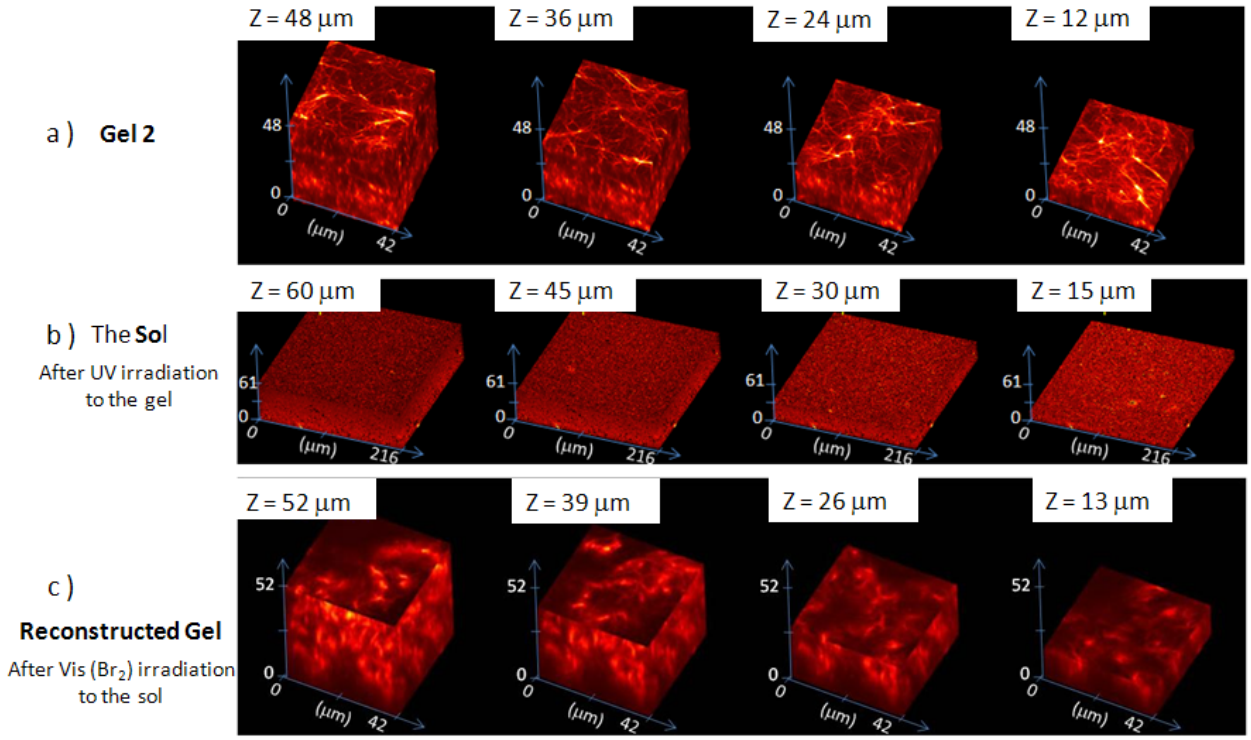


**Figure 5.** 3D-CLSM fluorescence images of the hydrogel **2** stained with a hydrophobic fluorescent rhodamine ([$C_{18}$-Rho] = 25 µM, excitation wavelength at 543 nm) Hydrogel **2** a) before, b) after UV irradiation, and c) after Vis irradiation.

The confocal laser scanning microscopy observation directly gave the 3D image of the hydrogel as shown in Figure 5. In this method, we did not need drying the gel sample, but instead the gel fiber domain was stained by the fluorescent and hydrophobic rhodamine probe (Octadecyl rhodamine B chloride) in the wet gel state. By the depth profiling, we clearly observed the well-entangled 3D-network (so-called supramolecular meshes) of the fibers in the gel state, whereas the fibrous network disappeared after the photo-irradiation. TEM (transmission electron micrograph) and SEM (scanning electron micrograph) gave us the insight for the morphology of the self-assembled gel fibers in the dry state. In the gel state, many

fibers having the length longer than 10 μm and the width less than 20 nm are entangled similar to other supramolecular hydrogels (Figure 6a), whereas only spherical aggregates like vesicles, instead of the entangled fibers, were observed in the sol state (Figure 5 in Chapter 2). It is reasonably considered that such spherical aggregates are not capable of entangling each other so that loss of the cross-linking points essential for the gel formation resulted in the destruction of the macroscopic hydrogel. The morphological observations of the reconstructed gel, which was prepared by the visible light irradiation to the sol in the presence of a small amount of bromine, by TEM, SEM and CLSM demonstrated the regeneration of the well-developed fibrous networks that are indistinguishable from the original gel state, as shown in Figure

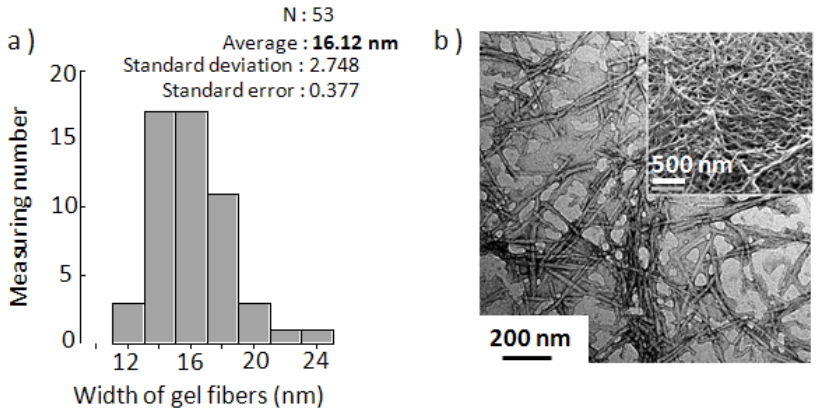


**Figure 6.** a) Distribution of the width of the supramolecular fibers consisting of hydrogelator **2**. The fiber width was determined by TEM observation (Figure 5 in Chapter 2). Average width = 16 nm. b) TEM and SEM (inset) images of reconstructed hydrogel **2** after Vis.($Br_2$) light irradiation to the sol. [Hydrogel **2**] = 0.2 wt%.

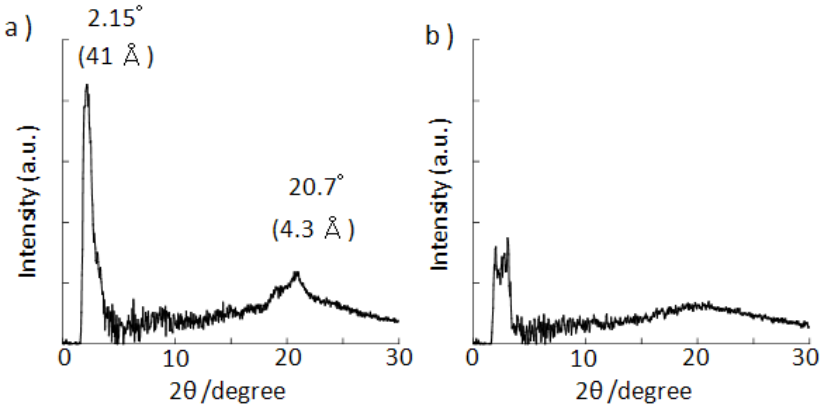


**Figure 7.** X-ray powder diffractions of a) the xero-gel **2** and b) the xero-sol after UV irradiation for 30 min with a xenon lamp.

5c and Figure 6b. In Figure 7a, the powder x-ray diffraction (XRD) measurement of the gel showed two main peaks at 2.15˚ (41 Å) and 20.7˚ (4.3 Å), the pattern of which is almost identical with the case of the succinic amide type of the gelator **1** (Figure 8b in Chapter 1).[4a] Based on the previous examination, it is clear that the small angle peak is assigned to the tilted bimolecular length of **2** and the peak of the wide angle corresponds to the packed thickness of the cyclohexyl ring. On the other hand, these two peaks were greatly broadened in the sample prepared from the sol state, suggesting that the regular packing structure was greatly disturbed by the photo-induced trans-to-cis conformational change (Figure 7b).

It should be noted that the photo-induced gel-to-sol and sol-to gel cycle can be repeated several times. This implies that the trans-to-cis isomerization disrupted the regular structure of the self-assembled fiber **2** and the subsequent cis-to-trans photo-isomerization repaired the tight packing, so that the regenerated long fibers facilitated the formation of the hydrogel. Thus, it is concluded that the macroscopic gel-sol and sol-gel transition was pseudo-reversibly photo-controlled by the molecular level conformational alternation in the present supramolecular hydrogel (Figure 8).

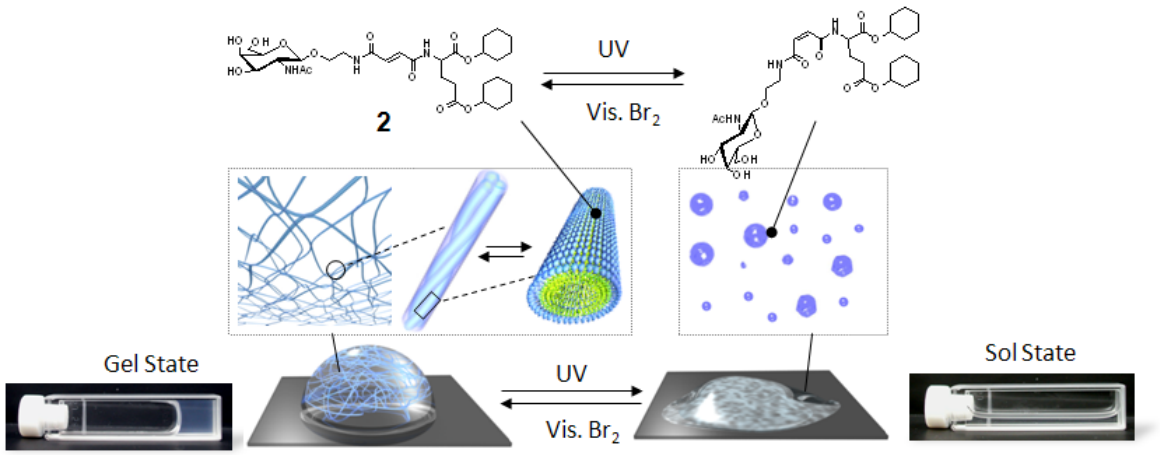


**Figure 8.** Schematic illustration of pseudo reversible gel-sol transition of hydrogel **2** induced by UV/Vis ($Br_2$) irradiation.

### 3-2-3. Photo-controlled substrate release using photo-responsive hydrogel

It was well-established that the supramolecular fibrous network of the gel is capable of immobilizing various substrates. Using the photo-responsive gel-sol transition of the hydrogel **2**, we next attempted the photo-control of the substrate release. When vitamin $B_{12}$ ($B_{12}$), a water-soluble vitamin, was entrapped in the supramolecular hydrogel **2**, $B_{12}$ was slowly released from the gel into the bulk aqueous solution over a period longer than 10 hours (7.8% of the embedded $B_{12}$ was released in the initial 3 hours, Figure 9). On the other hand, the rapid release of $B_{12}$ was carried out upon the photo-induced gel-to-sol, that is, almost 100% of the $B_{12}$ was released within 10 min due to the UV light irradiation. Similarly, Con A, a glucose-binding protein, and nano-beads with a 100 or 250 nm diameter, which were entrapped in the gel

**2**, were released by the photo-induced gel-to-sol transition with almost the same efficiency as the photo-release of $B_{12}$ (Table 1).

Interestingly, the substrate release rate without UV light was dependent on the substrate size. For vitamin $B_{12}$, the size of which is about 2.5 nm in diameter, 7.8% of the embedded $B_{12}$ was released in the initial 3 hours, whereas both Con A (10.5 nm diameter) and the 100-nm beads showed only about a 2.6% release in 3 hours. The release was almost completely suppressed (about 0% in 3 hours) in the case of the 250-nm beads. These results indicated that the present supramolecular hydrogel can act as a barrier against the releases of various sizes of substrates with various efficiencies depending on the substrate size, and the barrier capability was photo-modulated regardless of the substrate size.

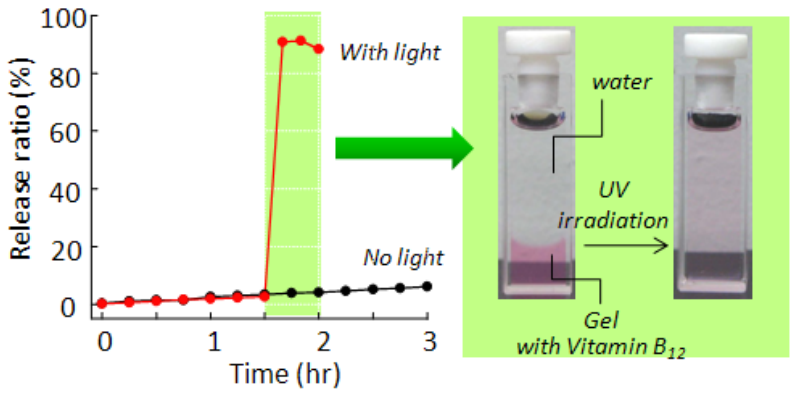


**Figure 9.** Photo-responsive release of biomolecules and microbeads using photo-responsive gel-sol transition. a) Photo-controlled release of vitamin $B_{12}$ from hydrogel **2**. Time courses of release ratio (%) of vitamin $B_{12}$ from gel to bulk solution without or with UV irradiation (filled black circle: spontaneous release; filled red circle: photo-triggered release (irradiation at 1.5 h)).

**Table 1.** The release ratio (%) of vitamin $B_{12}$, FITC-ConA, 100-nm and 250-nm fluorescent beads from hydrogel **2** without or with UV irradiation.

| | **Vitamin $B_{12}$** (2.5 nm) | **ConA** (tetramer) (10.5 nm) | **100 nm beads** | **250 nm beads** |
|---|---|---|---|---|
| Release ratio *without light* [1)] | : 7.8% (±1.5) | 2.6% (±1.9) | 2.7% (±2.0) | 0.3% (±0.4) |
| Release ratio *with light* [2)] | : 88% | 99% | 97% | 99% |

*1) Data at 3 h.*

*2) Data at 2 h containing UV irradiation time (0.5 h), between 1.5 and 2 h.*

### 3-2-4. Evaluation of size of the meshes composed of the photo-responsive hydrogel

The CLSM study of the Brownian motion of fluorescent nano-beads in the gel matrix gave more insights into understanding how the supramolecular hydrogel can entrap these substrates in the inner space.[13] We can directly observe the motion of the fluorescent beads by CLSM. In the case of the 100-nm diameter beads, the smooth diffusion occurred inside the hydrogel **2** (0.10 wt%), so that the static image is difficult to obtain as shown in Figure 10a. In contrast, all the beads with a 250-nm diameter stopped in the gel matrix (Figure 10b). A perfect stopping was also observed for the 500-nm and 1000-nm beads (Figure 10c, d). Thus, we obtained the 3D spatial fixation of these beads in the CLSM image. It should be emphasized that the moving or stopping of the Brownian motion of the nano-beads showed a critical threshold in the bead size. This suggests that the present supramolecular hydrogel formed into the nano-meshes with relatively homogeneous void spaces between 100 and 250 nm, which are strong enough to function as a physical obstacle to trap the beads. As shown in Table 2, by increasing the gelator concentration to 0.30 wt%, the motion of even the 100-nm beads perfectly stopped. At lower than the cgc. (critical gelation concentration) (0.035 wt%; sol state), on the other hand, no beads of any size did not stop, probably due to the insufficient development or the entanglement of the fibers for the well-developed meshes. Between 0.05 wt% (cgc) and 0.20 wt%, the threshold (100-250 nm) was not substantially affected. These results imply that the mesh-size of the supramolecular hydrogel was dependent on the gelator concentration. It is also noteworthy that the present method is much simpler and more general for directly evaluating the mesh size of intact hydrogels without drying, compared to a method using a nano-bead tethered ATPase that was recently reported by us.[14]

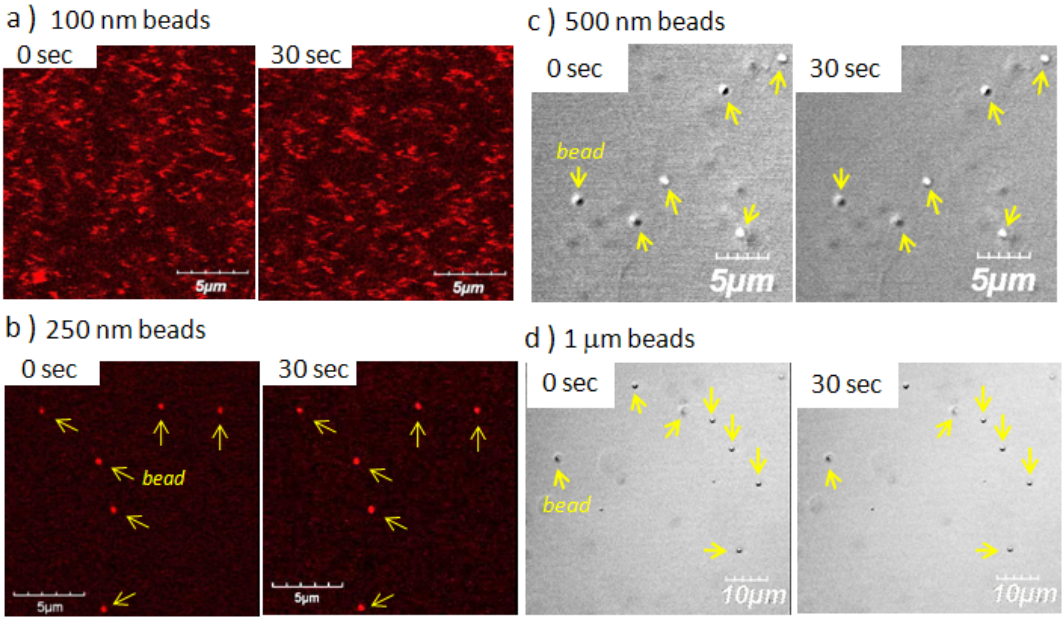


**Figure 10.** Time-dependent CLSM images for the analysis of Brownian motion of hydrophilic microbeads in hydrogel **2** (0.10 wt%, ion-exchanged water). a) 100-nm and b)-250 nm beads stained by rhodamine dye. c) 500 nm and d) 1000 nm beads.

**Table 2.** Summary for the Brownian motions of 100-1000 nm beads in hydrogel **2**. "ON" and "OFF" mean move and stop of Brownian motions of micro-beads, respectively.

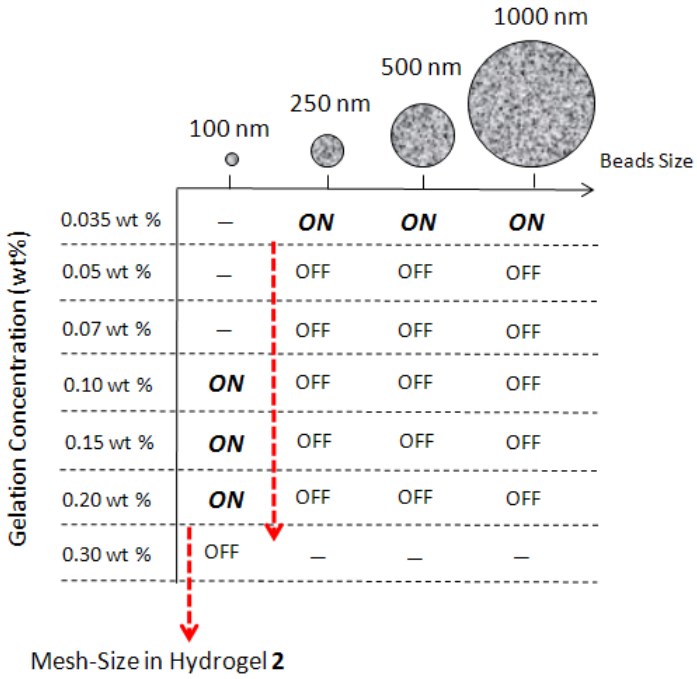


### 3-2-5. Off/on switching of bacteria movement and the rotation of $F_1$-ATPase motor using the photo-responsive supramolecular nano-meshes

Like the nano-beads, the movement of living *E. Coli.* bacteria (EGFP-BL21) may be photo-controlled by the supramolecualr meshes, because the size of the objects is within the micrometer range, slightly larger than the 250-nm beads. For the direct detection of both the bacteria and the gel fibers, the green fluorescent bacteria over-expressing EGFP and the red fluorescent fiber stained by $C_{18}$-Rho were used. We observed the free movement of the bacteria in the sol state of **2** in a flow cell chamber and stopping of the movement by the gel formation using the CLSM method similar to the nano-beads (Figures 10a, b, c). On the other hand, bacteria restarted the movement together with the disappearance of the gel meshes when the UV light irradiated the gel matrix for 30 sec. The careful CLSM observation of the bacteria embedded in the hydrogel **2** gave us images that many bacteria were entangled within the supramolecular meshes (Figure 10a), suggesting that the meshes consisting of the gel-fibers could become an efficient physical obstacle against bacteria movement (Figure 13).

In addition to bacteria, the photo-induced on/off switching of an enzymatic motion was successfully conducted when the nano-beads were attached to the enzyme. In a proof-of–concept experiment, we examined the motion of $F_1$-ATPase, an enzyme-based molecular motor, by microscopy. After tethering submicro-beads (normally 0.73 μm in diameter) to $F_1$-ATPase, we observed the rotary motion of the microbead-appended $F_1$-ATPase by following the motion of the beads at the single molecule level.[14, 15] It is

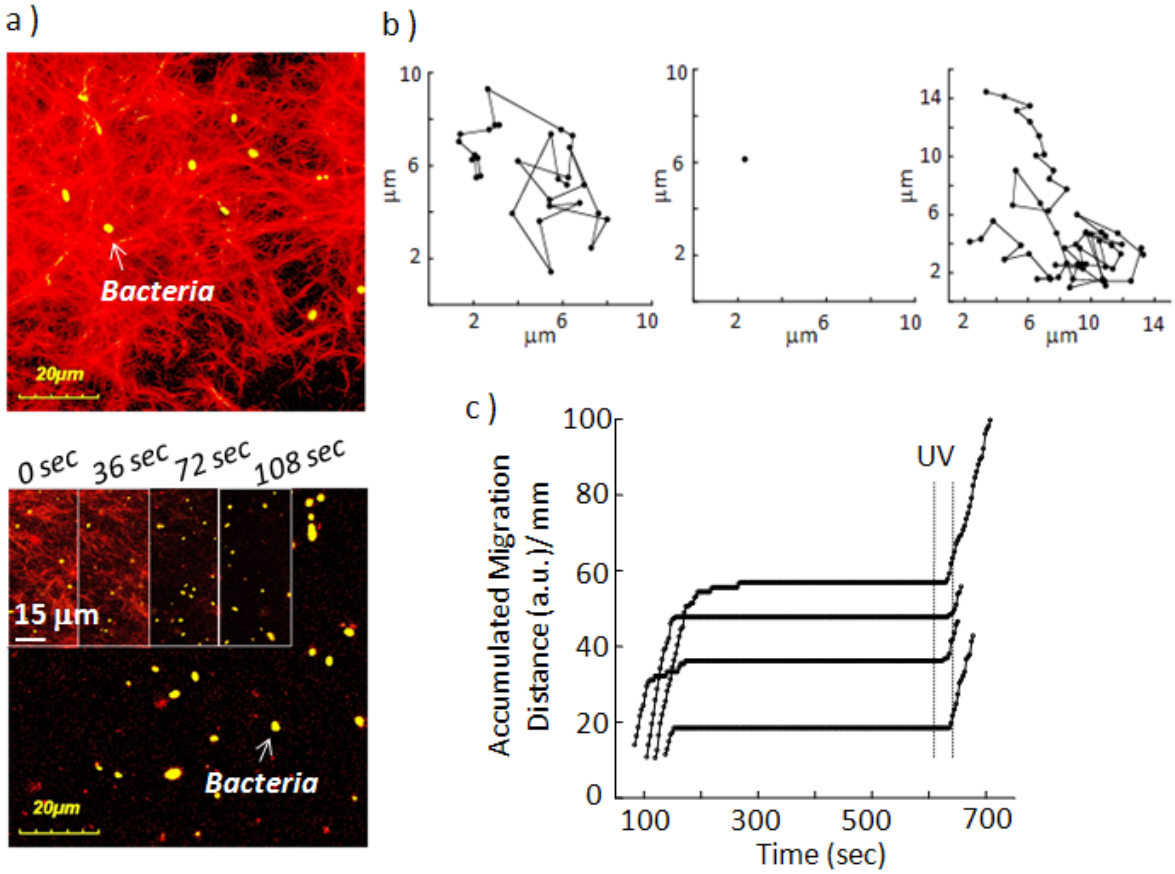


**Figure 11.** On/off switching of *E.Coli.* bacteria movement, which was controlled using the photo-responsive supramolecular meshes comprised of **2**. a) CLSM observation of *E. Coli.* (BL21) overexpressed EGFP in hydrogel **2** stained with $C_{18}$-Rho before (upper) and after (below) UV irradiation. Inset in the below panel show images during UV irradiation. b) The movement locus of the bacteria for 126 sec before galation completed (left), after the gelation (middle) and for 177 sec after UV irradiation (right). c) Time course of the accumulated migration distance of four representative bacteria in photo-switching experiments. UV light irradiation for 30 sec showed the two dotted lines in the Figure. [Hydrogelator **2**] = 0.15 wt%.

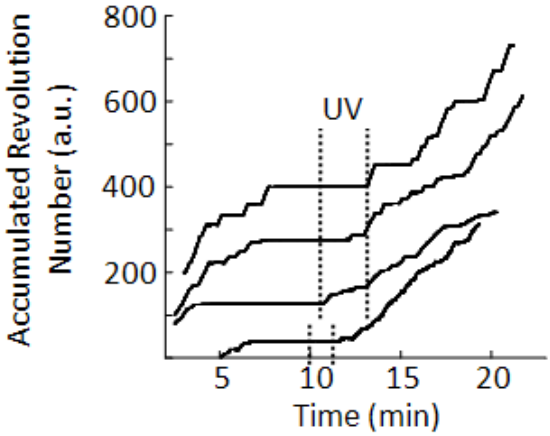


**Figure 12.** Time courses of the accumulated rotation numbers of four distinct $F_1$-ATPase molecules under photo-switching experiments was plotted every 0.033 sec. The microbeads rotation stopped by gelation for more than 5 min without UV light and then restarted by UV light irradiation for 1.5-3.5 min (between two dotted lines in the Figure). [gelator **2**] = 0.15 wt%.

shown that the rotary motion of the microbead-tethering $F_1$-ATPase stopped concurrently with the gel formation in the cell chamber after the infusion of the sol state of **2** (Figure 12). Interestingly, for 1.5-3.5 min of UV irradiation by a low-pressure Hg lamp, the $F_1$-ATPase rotation restarted along with the photo-induced gel-to-sol transition of **2** as shown in Figure 12.

We confirmed that photo-regulated off/on switching of the $F_1$-ATPase rotation did not occur in the case of usage of non-photoresponsive supramolecular hydorgel mixed with fumaric acid. The pause and subsequent restart of the $F_1$-ATPase rotation by UV irradiation implies that the stopping process was neither due to the denaturation of the $F_1$-ATPase nor the detachment of the microbead from the γ-subunit by the denaturation of the connecting avidin. In addition, the gel fiber-meshes of 100-250 nm size in diameter may be too large to tightly fix ATP, a substrate of ATPase, in the meshes and the ATP flux change by the gelation if any, was not a significant factor affecting the ATPase rotation. This indicates that the light-stimulus responsive supramolecular hydrogel can confer the off/on switching of the motor protein (Figure 13).

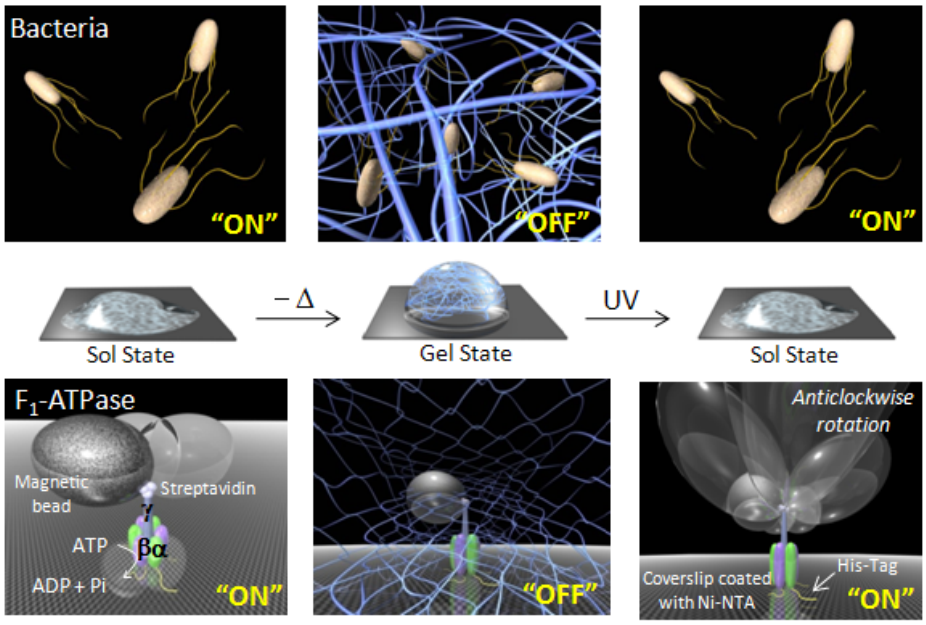


**Figure 13.** Schematic illustration of the on/off switching of bacteria motions and micro-beads tethered $F_1$-ATPase rotation by entanglement in the photo-responsive supramolecular hydrogel fibers (nano-meshes)..

### 3-2-6. Photo gel/sol patterning of the supramolecular hydrogel

The present photo-triggered gel-sol transition provided us with a unique method for photo-patterning the hydrogel. Using an appropriate photo-mask, the photo-irradiation in a limited area of the supramolecular hydrogel prepared in a quartz cell was conducted. Typical examples are shown in Figure 14a. The photo-irradiated area of the gel gradually turned into the transparent sol due to the

gel-to-sol phase transition. The sol areas produced by a 10-min UV light irradiation were more fluidic and less viscous than the original gel, so that the sol area was replaced with an aqueous solution containing vitamin $B_{12}$ (Figure 14a). The sol-gel patterning could be also fabricated by the visible light irradiation to the sol in the presence of a small amount of bromine (Figure 14b).

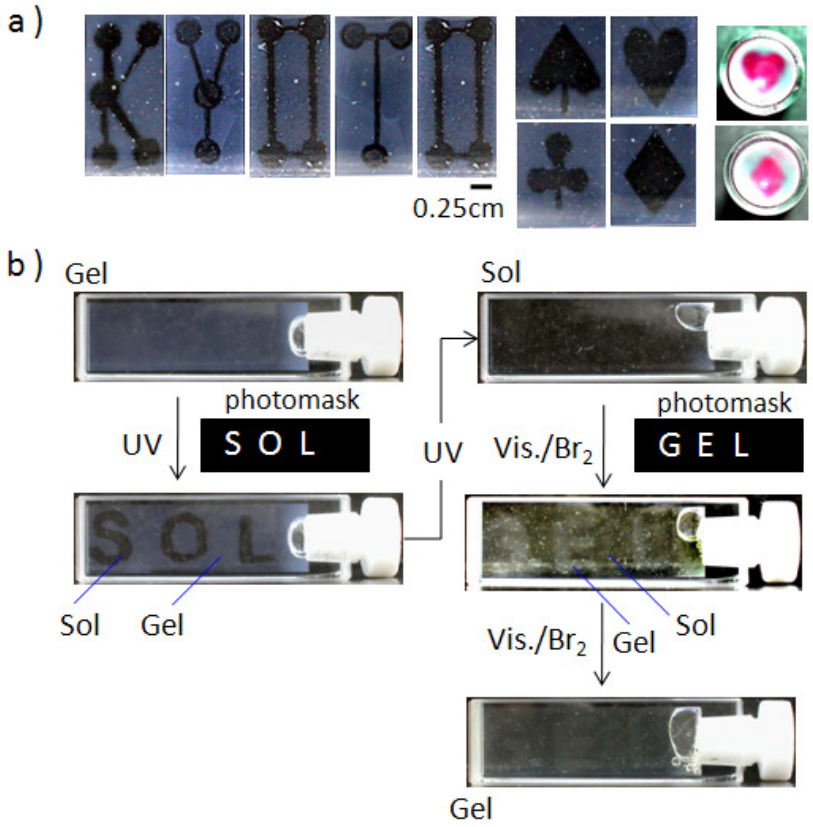


**Figure 14.** Photo gel-sol-gel patterning of hydrogel **2**. a) Photographs of gel-sol patterning in milli-scale with man-made photo-masks. The gel in which the photo-generated sol domains were replaced with vitamin $B_{12}$ solution. b) Photographs of photo gel-sol-gel patterning. [Hydrogel **2**] = 0.20 wt% (prepared in a quartz cell (light path length: 2 mm), ion-exchanged water).

The down-sizing of the photo gel-sol patterns was conducted by the direct irradiation of the focal laser light (266 nm, Figure 15a). The sol spot surrounded by the gel was produced by the spot irradiation of the laser light (< 50 mm diameter) in the flow cell chamber (Figure 15b). The fluidity of the photo-generated sol in the small space (40-50 μm diameter) was evaluated by the Brownian motion of the fluorescent microbeads. The Brownian motion of the microbeads in the solution phase and the sol phase of **2** stopped concurrently with the gel formation. After the laser irradiation for 1/8-1/4 sec, the motion of 7 microbeads at the focused spot re-started, whereas other beads not in the area of the laser beam never re-started moving. The motional velocity for the re-started beads was almost identical to that for the beads

in an aqueous solution (Figure 15c), demonstrating that the area in the laser spot turned into the sol state. By laterally shifting the laser spot, we prepared various sol-gel patterns such as a dot pattern, continuous flow pathway, or characters as shown in Figure 16. In the photo-prepared dot pattern, we confirmed that a sufficient distance to maintain two independent sol spots was less than 10 μm (Figure 15b), implying that the supramolecular gel wall having a 10 μm width became a barrier among the sol areas.

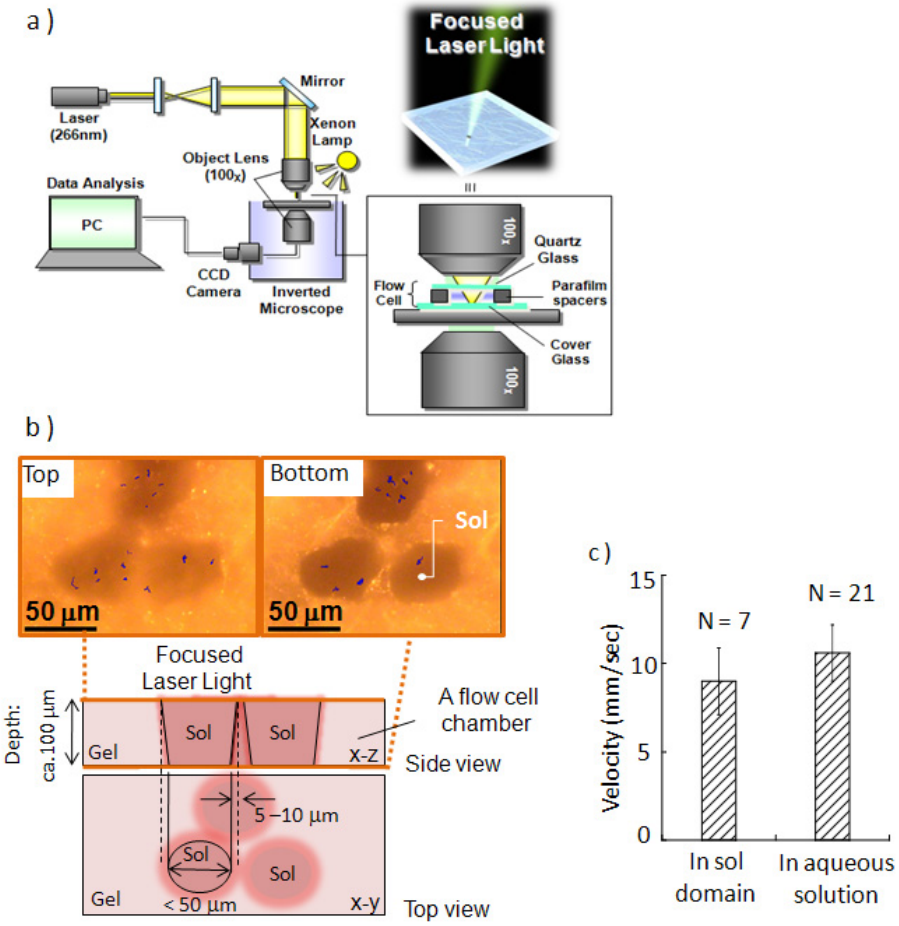


**Figure 15.** The photo gel-sol patterning in a micrometer-size. a) The schematic illustration of the focused laser irradiation equipment in this study. The focused laser light (266 nm) irradiated to the flow cell fixed on the stage of inverted microscope and the image monitored with CCD camera in real time. b) The dotted sol domains in hydrogel **2** which immobilized 250-nm fluorescent beads were fabricated with the focused laser light (266 nm). The blue lines show Brownian motions of micro-beads in the fabricated sol area at the bottom (z = 0 μm) and upper (z = ca. 100 μm) surface. c) Comparison of the mean velocities of the Brownian motions of the beads in the sol domain and in the aqueous solution.

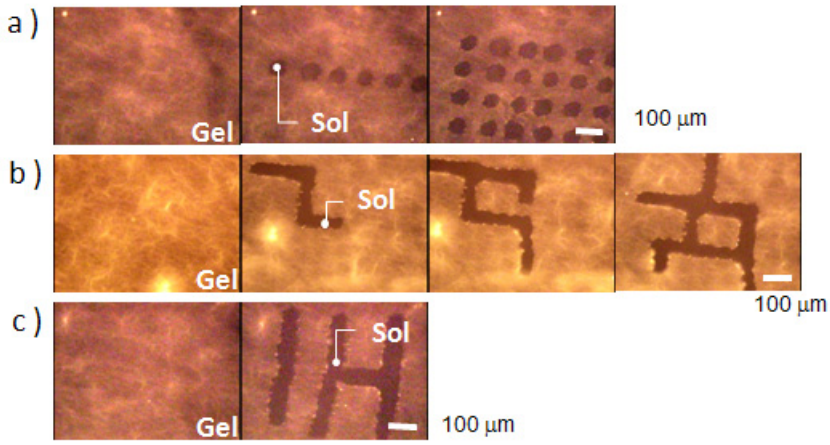


**Figure 16.** Various photo gel-sol patterning using the focused laser. a) Dots, b) lines and c) character patterns "IH" were fabricated in hydrogel **2** with the focused 266 nm laser light.

### 3-2-7. Off/on switching of biomolecules movement using photo-responsive nano-meshes at a restricted small area

Using the above-mentioned gel-sol patterning in a flow cell chamber, the bacterial motion was spatially restricted in the sol spot produced by light. After all the bacteria were entrapped in the supramolecular hydrogel **2**, the focused laser spot was irradiated for 1/4 sec to yield the sol with a 40-μm diameter. As shown in Figure 17a, the bacteria in the sol spot started moving, again, whereas bacteria in the gel area that is not in the laser spot did not move. When the continuous sol pathway was fabricated within the gel matrix by the photo gel-sol patterning, we found that all the bacteria moved within the continuous path (Figure 17b). Importantly, no bacteria moved across the gel matrix, clearly

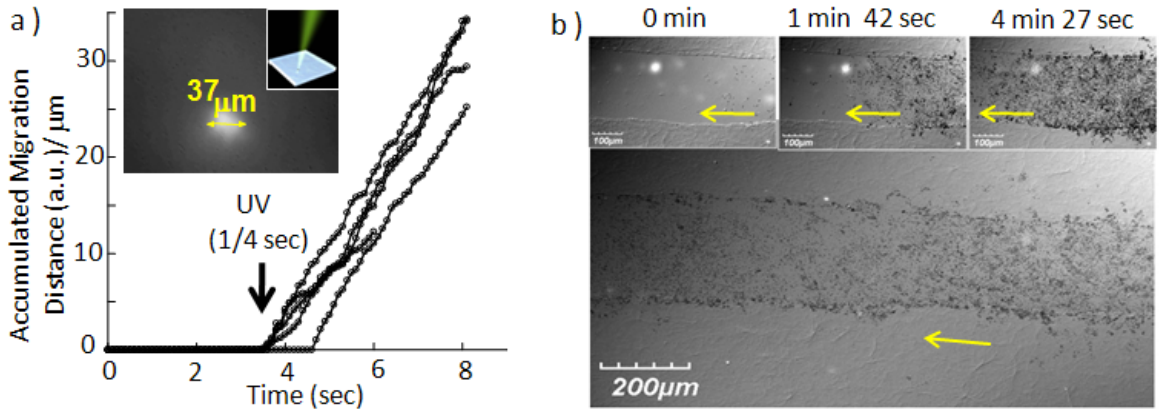


**Figure 17.** The off-on switching of the bacteria (BL21) movement at the spatially limited area. a) Time courses of the accumulated migration distance of five distinct bacteria before and after UV irradiation with focused 266 nm laser light (the diameter of ca. 40 μm, see inset panel). b) The bacteria movement within the flow sol path fabricated using the focused laser light (266 nm).

indicating that the gel wall consisting of the entangled gel meshes acted as a barrier against bacteria movement.

In a similar manner, we carried out switching the $F_1$-ATPase rotary motion in a small restricted area of the photo-responsive hydrogel meshes **2** using the focused laser light. After stopping of the $F_1$-ATPase motion for more than 5 min in the hydrogel matrix, the laser light was irradiated for 2 sec (1sec/shot×2 times) in a focused area (10-20 μm diameter). Within two seconds, the $F_1$-ATPase located in the photo-irradiated spot started rotating again, whereas the other $F_1$-ATPases out of the laser spot remained stopped (Figure 18a).[16] Analysis of the trace of the center of the re-rotating bead clearly indicates that the restarted motion is almost identical with the motion of ATPase in the original sol state (Figure 18b).

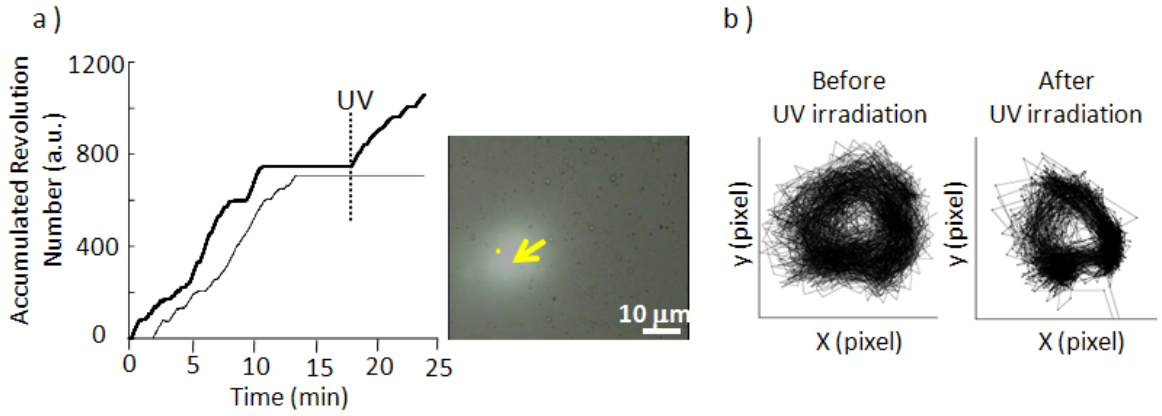


**Figure 18.** The off-on switching of a $F_1$-ATPase rotation at a single molecular level. a) The courses of the accumulated rotation numbers of $F_1$-ATPase molecules inside (thick line) and outside (thin line) of the laser irradiated area (the diameter of 10-20 μm, see a inset image). The micro-bead rotation stopped by gelation for more than 5 min and then restarted by focused laser light irradiation within two seconds. b) Traces of the centroid of a micro-bead image for 120 sec at 8 min after the injection of the sol **2** (left panel), and for 120 sec immediately after focused laser light irradiated to identical micro-bead for a few sec (right panel).

### 3-3. Conclusion

We successfully prepared biocompatible and photo-responsive supramolecular hydrogels based on the partial rational design coupled with a combinatorial library method. It is interesting that the sol state was produced within the gel matrix using the focused UV light with a 1 mm to 10 μm spatial resolution. We also found that the hydrogel is comprised of supramolecular meshes with a void space between 100 nm and 250 nm, which can entrap not only nano-beads, but also microbead-tethering $F_1$-ATPase and bacteria along with the suppression of their movement through physical blocking by the gel meshes. The photo-gel-to-sol phase transition induced the deformation of the supramolecular nano-meshes, so that the microbead-tethering $F_1$-ATPase rotation and the bacterial motion were re-started in a spatially and

temporally regulated manner. In this system, it is conceivable that the microbead tethered to the $F_1$-ATPase motor acts as a knob which can transduce the physical restriction/relaxation given by the nano-meshes to the enzyme active center. On the other hand, the supramolecular nano-meshes operate as an intelligent hand of a nano/micro-size that can appear or disappear in order to grip or release the knob, respectively, in response to the external photo-stimuli. There are several reports of switching enzyme motion, based on the direct incorporation of a switching unit such as metal binding site, magnetic bead or photochromic artificial molecules into the protein framework via a covalent bond for response to a chemical stimulus, magnetic field or visible light.[17-19] Recently, Ionov et al. successfully switched kinesin motion on a thermoresponsive polymer-grafted surface by hindering the binding of microtubules with the thermo-induced extension of polymer chains.[20] The present strategy is unique in that soft materials entrapping the enzyme can be used as an active operator. The supramolecular nanomeshes can selectively regulate the movement of microscale objects without disturbing the diffusion and the activity of nanoscale biomolecules, and thereby are promising matrices for versatile application in the manipulation of micro-biomachine powered by biological motors such as kinesin- or myosin-based molecular shuttles and living bacteria (Figure 19). The elaborate combination of bio-active molecules (e.g. engineered enzymes with nanofabricated hard substrates, live bacteria and so on) through intelligent soft materials such as the present photo responsive supramolecular nano-meshes, should not only actively operate functions of bio-molecules, but also facilitate the development of novel protein-based molecular devices.

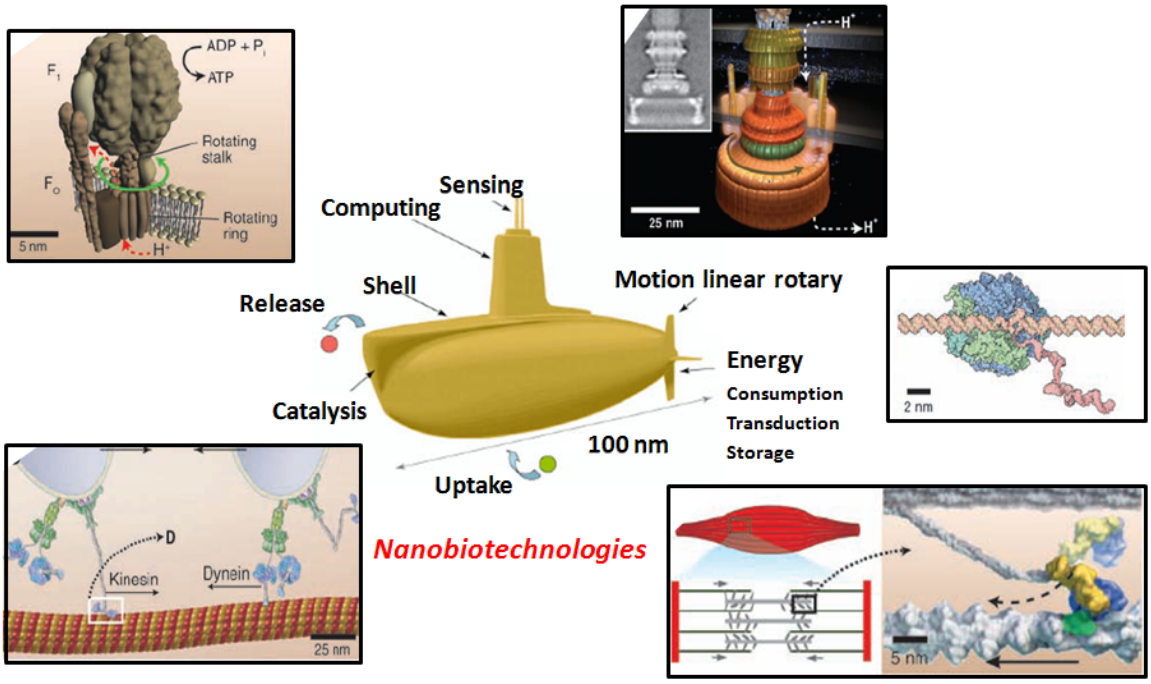


**Figure 19.** Motor Proteins at work for nanotechnology

## 3-4. Experimental Section

**Generals** All gelators in this paper were synthesized according to Scheme 1, our synthetic method reported previously.[21] Reagents for the synthesis of gelator were obtained from Kishida Chemical, Watanabe Chemical Industries, Wako, or TCI (Japan). A mutant $\alpha_3\beta_3\gamma$subcomplex ($\alpha$-C193S, $\beta$-His-10 at N-terminus, $\gamma$-S107C/I210C) from a thermophilic Bacillus PS3 (referred to as $F_1$-ATPase) was expressed and purified as described elsewhere.[22] Streptavidin-coatead magnetic beads (Seradyn; normally 0.73 μm) were sonicated to disperse in a suspension and lightly centrifuged as described.[23]

### Synthesis and characterization

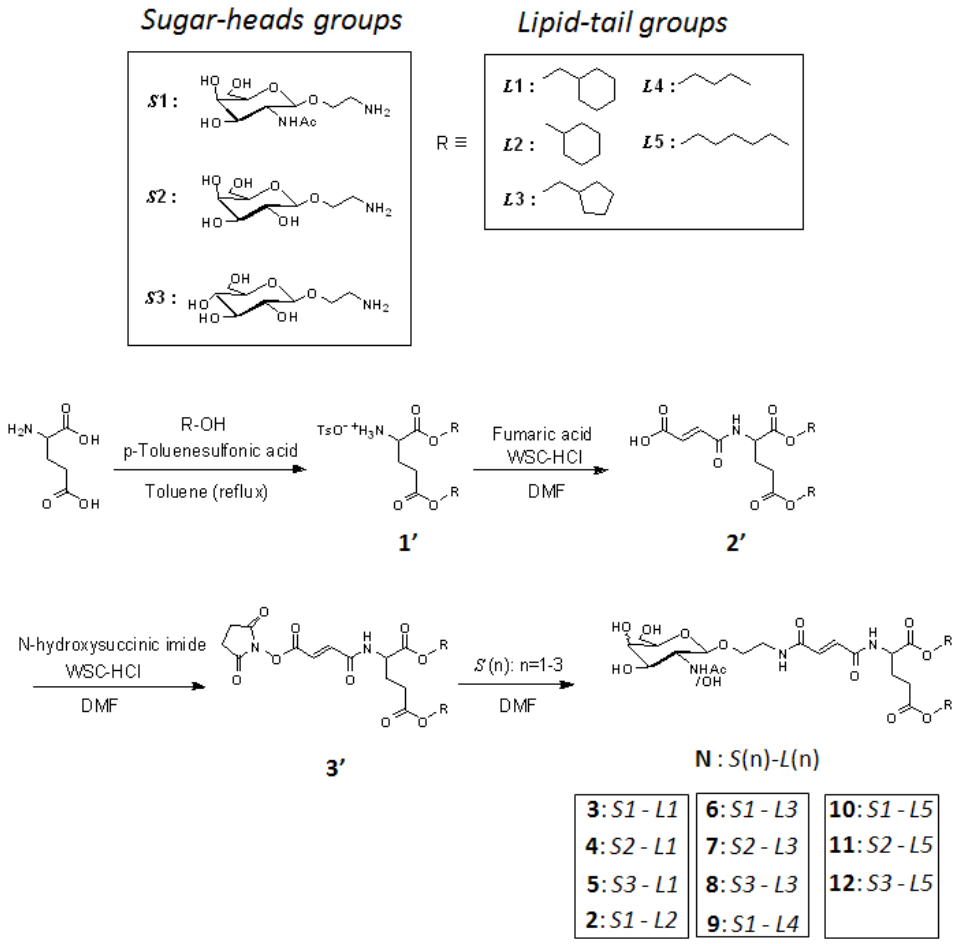


**Scheme 1.** The general synthetic schemes of the candidate molecules for the photo responsive hydrogelator. .

**GalNAc-fum-glu(*O* -*cyc*-hexyl)$_2$ (2)** See Experimental section in Chapter 2.

**GalNAc-fum-glu(*O*-methyl-*cyc*-hexyl)$_2$ (3)** $^1$H NMR (400 MHz, $CDCl_3/CD_3OD$, TMS, ppm): δ 0.90-0.98, 1.15-1.30, 1.67-1.74 (m, 22H), 2.01 (s, 1H), 199-2.08, 2.21-2.26 (m, 2H), 2.41-2.46 (m, 2H),

3.36-3.90 (m, 14H), 4.49 (d, $J$ = 8.4 Hz, 1H), 4.55-4.65 (m, 1H), 6.87-6.89 (m, 2H); FAB-HRMS: *m/z*: calcd (%) for $C_{33}H_{54}O_{12}N_3$ ($M$+$H^+$): 684.3707; found: 684.3711.

**Gal-fum-glu(*O*-methyl-*cyc*-hexyl)$_2$ (4)** $^1$H NMR (400 MHz, $CDCl_3$/$CD_3OD$, TMS, ppm): δ 0.90-0.99, 1.15-1.27, 1.67-1.75 (m, 22H), 2.01-2.06, 2.21-2.26 (m, 2H), 2.42-2.47 (m, 2H), 3.50-3.98 (m, 14H), 4.24 (d, $J$ = 7.2 Hz, 1H), 4.59-4.63 (m, 1H), 6.89-6.91 (m, 2H); FAB-HRMS: *m/z*: calcd (%) for $C_{31}H_{50}O_{12}N_2$ ($M$): 642.3364; found: 642.3368.

**Glc-fum-glu(*O*-methyl-*cyc*-hexyl)$_2$ (5)** $^1$H NMR (400 MHz, $CDCl_3$/$CD_3OD$, TMS, ppm): δ 0.90-0.98, 1.15-1.30, 1.63-1.74 (m, 22H); 2.01-2.06, 2.21-2.26 (m, 2H), 2.41-2.46 (m, 2H), 3.28-3.98 (m, 14H), 4.29 (d, $J$ = 7.2 Hz, 1H), 4.60-4.63 (m, 1H), 6.88-6.89 (m, 2H); FAB-HRMS: *m/z*: calcd (%) for $C_{31}H_{50}O_{12}N_2$ ($M$): 642.3364; found: 642.3351.

**GalNAc-fum-glu(*O*-methyl-*cyc*-pentyl)$_2$ (6)** $^1$H NMR (400 MHz, $CDCl_3$/$CD_3OD$, TMS, ppm): δ1.10-1.30, 1.50-1.70, 1.70-1.80 (m, 18H), 1.99 (s, 1H), 1.95-2.10, 2.17-2.24 (m, 2H), 2.40-2.50 (m, 2H), 3.37-3.90 (m, 14H), 4.40 (d, $J$ = 8.0 Hz, 1H), 4.55-4.65 (m, 1H), 6.87-6.89 (m, 2H); FAB-HRMS: *m/z*: calcd (%) for $C_{31}H_{50}O_{12}N_3$ ($M$+$H^+$): 656.3394; found: 656.3393.

**Gal-fum-glu(*O*-methyl-*cyc*-pentyl)$_2$ (7)** $^1$H NMR (400 MHz, $CDCl_3$/$CD_3OD$, TMS, ppm): δ 1.18-1.30, 1.50-1.68, 1.68-1.74 (m, 18H), 1.98-2.06, 2.17-2.26 (m, 2H), 2.41-2.46 (m, 2H), 3.48-4.06 (m, 14H), 4.24 (d, $J$ = 7.2 Hz, 1H), 4.58-4.65 (m, 1H), 6.87-6.89 (m, 2H); FAB-HRMS: *m/z*: calcd (%) for $C_{29}H_{47}O_{12}N_2$ ($M$+$H^+$): 615.3129; found: 615.3126.

**Glc-fum-glu(*O*-methyl-*cyc*-pentyl)$_2$ (8)** $^1$H NMR (400 MHz, $CDCl_3$/$CD_3OD$, TMS, ppm): δ 1.18-1.30, 1.50-1.68, 1.68-1.80 (m, 18H), 1.98-2.10, 2.10-2.30 (m, 2H), 2.35-2.50 (m, 2H), 3.36-4.05 (m, 14H), 4.29 (d, $J$ = 7.2 Hz, 1H), 4.58-4.64 (m, 1H), 6.87-6.89 (m, 2H); FAB-HRMS: *m/z*: calcd (%) for $C_{29}H_{47}O_{12}N_2$ ($M$+$H^+$): 615.3129; found: 615.3145.

**GalNAc-fum-glu(*O*-*n*-butyl)$_2$ (9)** $^1$H NMR (400 MHz, $CDCl_3$/$CD_3OD$, TMS, ppm): δ 0.94 (t, $J$ = 7.2 Hz, 6H), 1.35-1.45, 1.60-1.67 (m, 8H), 2.01 (s, 1H), 1.98-2.10, 2.19-2.30 (m, 2H), 2.41-2.46 (m, 2H), 3.50-3.61, 3.79-3.88 (m, 10H), 4.09 (t, $J$ = 7.2 Hz, 2H), 4.16 (t, $J$ = 7.2 Hz, 2H), 4.40 (d, $J$ = 8.4 Hz, 1H), 4.58-4.61 (m, 1H), 6.89-6.90 (m, 2H); FAB-HRMS: *m/z*: calcd (%) for $C_{27}H_{45}O_{12}N_3$ ($M$): 603.3003; found: 603.2993.

**GalNAc-fum-glu(*O*-*n*-hexyl)$_2$ (10)** $^1$H NMR (400 MHz, $CDCl_3$/$CD_3OD$, TMS, ppm): δ 0.89 (t, $J$ = 7.2 Hz, 6H), 1.20-1.40, 1.55-1.70 (m, 16H), 2.01 (s, 1H), 1.98-2.10, 2.19-2.30 (m, 2H), 2.39-2.43 (m, 2H),

3.50-3.95 (m, 10H), 4.07 (t, $J$ = 7.2 Hz, 2H), 4.14 (t, $J$ = 7.2 Hz, 2H), 4.40 (d, $J$ = 8.0 Hz, 1H), 4.58-4.65 (m, 1H), 6.89-6.90 (m, 2H); FAB-MS: *m/z*: calcd (%) for $C_{31}H_{53}N_3O_{12}$: 659.36; found: 682.20 $[M+Na]^+$, 698.27 $[M+K]^+$.

**Gal-fum-glu(*O*-*n*-hexyl)$_2$ (11)** $^1$H NMR (400 MHz, $CDCl_3/CD_3OD$, TMS, ppm): δ 0.89 (t, $J$ = 7.2 Hz, 6H), 1.23-1.40, 1.60-1.67 (m, 16H), 2.01-2.06, 2.20-2.24 (m, 2H), 2.39-2.45 (m, 2H), 3.38-4.00 (m, 10H), 4.07 (t, $J$ = 7.2 Hz, 2H), 4.14 (t, $J$ = 7.2 Hz, 2H), 4.23 (d, $J$ = 7.2 Hz, 1H), 4.59-4.62 (m, 1H), 6.87-6.88 (m, 2H); FAB-HRMS: *m/z*: calcd (%) for $C_{29}H_{50}O_{12}N_2$ ($M$): 618.3364; found: 618.3362.

**Glc-fum-glu(*O*-*n*-hexyl)$_2$ (12)** $^1$H NMR (400 MHz, $CDCl_3/CD_3OD$, TMS, ppm): δ 0.89 (t, $J$ = 7.2 Hz, 6H), 1.23-1.40, 1.60-1.67 (m, 16H), 2.01-2.06, 2.20-2.24 (m, 2H), 2.39-2.45 (m, 2H), 3.38-4.00 (m, 10H), 4.07 (t, $J$ = 7.2 Hz, 2H), 4.14 (t, $J$ = 7.2 Hz, 2H), 4.30 (d, $J$ = 7.2 Hz, 1H), 4.59-4.62 (m, 1H), 6.89-6.90 (m, 2H); FAB-HRMS: *m/z*: calcd (%) for $C_{29}H_{51}O_{12}N_2$ ($M+H^+$): 619.3442; found: 619.3455.

**Gelation test** Synthesized glyco-lipid based molecules were homogenously dispersed with ion-exchanged water (0.05-2.0 wt%) by heating, and then left at rest over 12 h at room temperature. Gelation abilities for each molecule were checked visually by vial inversion method and then we classified into four phase states; transparent gel, opaque gel, precipitate and homogenous solution.

**The light transmittance measurement** The light transmittances were measured using Shimadzu UV-Visible spectrophotometer UV-2550. A 0.1 wt% hydrogelator **2** was prepared in a quartz cell, and the change in the light transmittance of the solution was monitored at 400 nm at 24 ºC. After the equilibrium, the temperature of the cell holder was raised to 80 ºC. After reached at 80 ºC, the gelator solution was homogeneously dispersed by more heating, and subsequently incubated at 24 ºC. This procedure was repeated several times.

**Photo-irradiation conditions for bulk gel-sol/sol-gel transition** UV light was irradiated to the hydrogel **2** (0.10-0.25 wt%, ion-exchanged water) prepared in a quartz cell (light path length; 2 mm) with a xenon lamp (USHIO, Optical Modulex, SX-UI500XQ) for at least 10 min under 15 ºC. In the sol-gel transition of **2**, visible light was irradiated to the above prepared sol containing a small amount of bromine with a xenon lamp attached with two filters, which cut less than 290 nm and 350 nm wavelength, for at least 10 min under 15 ºC. This pseudo photo-reversible phenomenon could repeat for several times.

**Dynamic viscoelasticity measurement** Dynamic viscoelasticities of the hydrogel **2** (0.20 wt%) before and after UV irradiation with a xenon lamp for 1 h, and the reconstructed hydrogel after visible light irradiation to the sol for 30 min with slight amount of bromine, were measured with a plate-plate rheology

equipment (DynAlyser DAR-100, Reologica). The measurement conditions were as follows: angular frequency range: 100-0.1 rad·sec$^{-1}$; strain: 2% for the gel and the reconstructed gel sample and 0.5% for the sol sample (after UV irradiation to the gel **2**); parallel plate: 4 cm in diameter; gap distance: 1.2 mm; measurement temperature; 24 ºC.

**Phase diagram for photo-responsive gel-sol transition** UV light was irradiated to hydrogel **2** (0.2 wt%, $D_2O$) with a xenon lamp every 5 min (for 0 to 30 min) at 15 ºC. The gel and sol volume ratios of each sample were estimated by measuring the sol volume with a syringe and shown as (gel/(gel + sol) volume) × 100 (%) (horizontal axis)). Photo-isomerization ratios of fumaric (*trans*) to maleic (*cis*) amide form were estimated from the integrals of these peaks by $^1$H-NMR measurements (JEOL-JNM-EX400 apparatus, 400 MHz) of each sample, to which $CD_3OD$ added ($CD_3OD/D_2O$ = 1/1 v/v) for preparing the homogenous dispersed solutions. These ratios were shown as (fumaric)/(fumaric + maleic-amide form) × 100 (%) (vertical axis). From three times of the same experiments, the average and error bar were calculated and plotted. In addition, by-products were not observed in the $^1$H NMR spectra.

**TEM and SEM observation** Carbon-coated copper grids were dipped in the hydrogel **2**, the sol after UV irradiation to gel with a xenon lamp for 30 min, or the re-constructed hydrogel **2**, which was prepared by Vis. light irradiation to the sol in the presence of a small amount of bromine for 10 min with xenon lamp attached with UV cut filters. They were dried under reduced pressure for 24 h at room temperature. TEM samples were stained with 2 wt% aqueous solution of uranyl acetate. TEM observations were carried out with a JEOL JEM-2010 apparatus under 120 kV accelerating voltage. For SEM observation, the samples were coated by platinum vapor deposition (30 sec). SEM images were obtained by using a Hitachi S-5000, acceleration voltage 25 kV. [Hydrogelator **2**] = 0.20 wt% (ion-exchanged water).

**CLSM observation** Hydrogel **2** and the sol after UV irradiation with low-pressure Hg lamp for 1.5 to 3.5 min, which were staining with hydrophobic fluorescent dye (15 mM, Octadecyl rhodamine B chloride, Molecular probe), were observed with a CLSM (Confocal laser scanning microscopy, OLYMPUS: FV1000, IX81). [Hydrogelator **2**] = 0.10 wt%, ion-exchanged water). The excitation wavelength was 543 nm.

**X-ray powder diffraction** The xero-gel **2** and the xero-sol , which was prepared by UV irradiation to the gel **2**, were placed in a glass capillary tube ($\phi$ = 2 mm), respectively. The X-ray diffractogram (MAC Science M18XHF) was recorded on an imaging plate by using CuK$\gamma$ radiation ($\lambda$ = 1.54 Å) at a distance of 15 cm.

**Observation of Brownian motions of micro-beads in hydrogel 2** The heat-dispersed gelator **2** in ion-exchanged water containing 100-nm-, 250-nm fluorescent beads, 500-nm and 1000-nm beads

(micromer®-red F, POL) were dropped to petri dish and left at rest for 3 h at room temperature. These samples were monitored with confocal laser scanning microscope (CLSM, OLYMPUS; FV1000) at excitation laser wavelength of 543 nm in real time. Objective lens: × 100. [Hydrogel **2**] = 0.10 wt% (ion-exchanged water).

**Biomolecules and micro-beads releasing from hydrogel 2** Ion-exchanged water (400 μL) was added to hydrogel **2** (150 μL, 0.1 wt%, ion-exchanged water) containing vitamin $B_{12}$, FITC-ConA (tetramaer), 100 nm- and 250 nm-fluorescent beads solution in quartz cell. The part of superior solution was monitored with a UV-Vis absorption spectrometer (SHIMADZU, UV-2550) in real-time for 0 to 3 h. Time course of vitamin $B_{12}$ (0.20 mM) releasing was monitored by the absorption at 550 nm before UV irradiation, and 410 nm after UV irradiation (410 nm was an isosbestic point of vitamin $B_{12}$ in aqueous solution before and after UV irradiation). Time course of FITC-ConA (0.14-0.27 mg/mL) releasing was monitored by the absorption at 492.5 nm before UV irradiation, and 421 nm after UV irradiation (421 nm was an isosbestic point of FITC-ConA in aqueous solution before and after UV irradiation). Time courses of monodispersed 100 nm- or 250 nm fluorescent beads (micromer®-red F, POL) releasing were traced by the transmittance at 400 nm. In addition, we checked that the solubility of hydrogelator **2** to balk solution was less than 1% volume of gel in 5 h. From three times of the same experiments, the average and error bar were calculated and plotted.

**Observation of bacteria entrapped in hydrogel** A flow cell chamber for observing the bacteria movement was constructed from two uncoated glass plates (Matsunami; a top cover glass was 18 mm × 18 mm, and a bottom one was 24 mm × 32 mm) sandwiching two parallel strips of greasy paper as spacers.[15e] Bacteria, *Escherichia coli* BL21 (DE3) (Novagen), was suspended in the sol state of the gelator **2** (0.15 wt% in ion-exchanged water) and immediately put into a flow chamber. After the gelation completed for 30 minutes incubation at room temperature, we observed the movement of bacteria with a microscope by using DIC (differential interference contrast) method and analyzed the locus and the accumulated distances of bacteria movement every 3 sec with software (Move-tr/2D 7.0, Library). To induce the photo gel-sol transition, a low-pressure mercury vapor lamp (Ushio; UL0-6DQ) was located approximately 5 mm above the flow chamber and used to irradiate for 30 sec. For the experiments of UV irradiation at the limited area, the 266 nm laser light focused with objective lens (100 ×) was used for a few seconds.

**Observation of $F_1$-ATPase rotation regulated in hydrogel** Two parallel strips of greasy paper were placed on the Ni-patterned glass plate, and a quartz plate (10 mm × 10 mm, 1 mm thick) was put on the strips to form a flow chamber.[15e] $F_1$-ATPase were immobilized on the glass plates in a flow chamber and modified with magnetic beads according to the method reported previously (see Scheme S2).[15e] All rotating assays were started by infusion of a heat-dispersed gelator **2** (0.06-0.15 wt%) in MOPS buffer (50 mM

3-(*N*-morpholino)propanesulphonic acid-KOH (pH 7.1), 50 mM KCl) supplemented with 2 mM Mg-ATP, and the rotating beads were observed as bright-field images in the single molecular level. The images were videotaped and analyzed with a custom software and the accumulated revolution numbers were plotted every 0.033 sec.[15e] In the experiment of UV irradiation, a low-pressure mercury vapor lamp (Ushio; UL0-6DQ) was located approximately 5 mm above the flow chamber and used to irradiate for less than 3 min. For the experiments of UV irradiation at the limited area, the 266 nm laser light focused with objective lens (100 ×) was used for a few seconds.

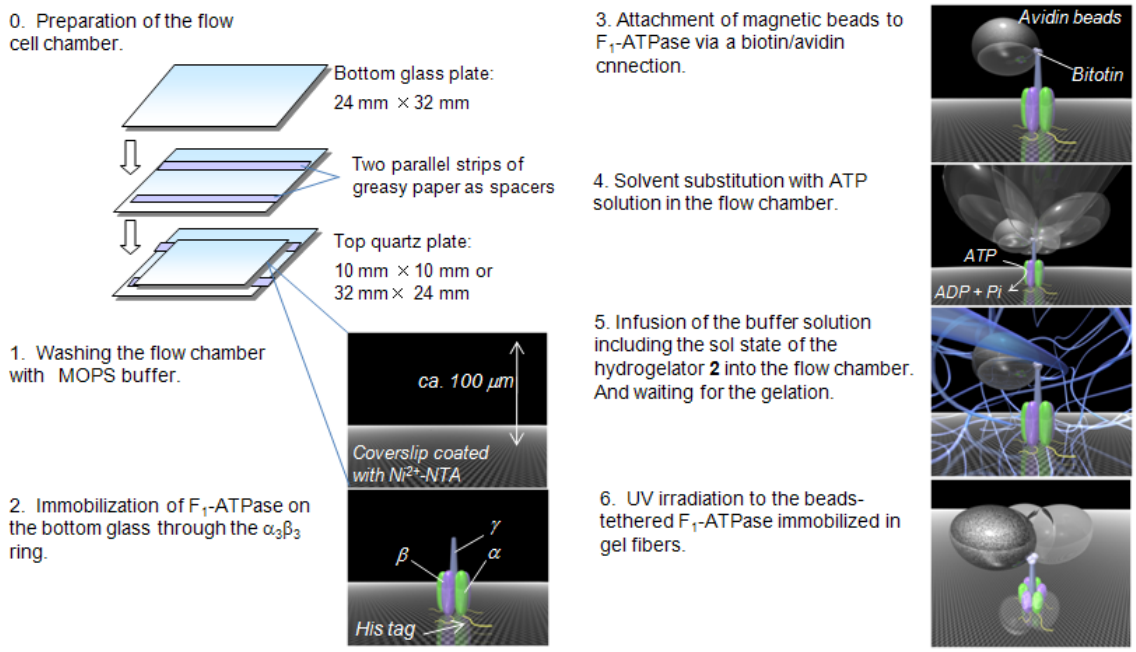


**Scheme S2.** Preparation procedure of $F_1$-ATPase rotation assay in flow cell chamber.

**Photo gel-sol patterning in micro scale** Hydrogel **2** (0.10 wt%, ion-exchanged water) containing 250 nm fluorescent beads to visualize the gel-sol pattern was prepared in flow-cell. By using focused laser equipment (266 nm, 1/8-1/4 sec/shot), various line- and character-patterns were fabricated by connecting dots pattern. In the bottom surface area of flow-cell, sol domain of < 50 μm in diameter was formed. Whereas, in the upper surface area of flow-cell, sol domain of < 50 ± (5-10) μm in diameter was confirmed by the Brownian motion of micro-beads. The accumulated movement distances of the Brownian motion of micro-beads in sol domain were analyzed with a software (Move-tr/2D 7.0, Library).

### 3-5. References and Notes


1. a) Weibel, D. B.; Whitesides, G. M. *Curr. Opin. Chem. Biol.* **2006**, 10, 584-591. b) Whitesides, G. M. *Nature* **2006**, *442*, 368-373 c) Weibel, D. B.; DiLuzio, W. R.; Whitesides, G. M. *Nat. Rev. Microbiol.* **2007**, *5*, 209-218.
2. a) Soong, R. K.; Bachand, G. D.; Neves, H. P.; Olkhovets, A. G.; Craighead, H. G.; Montemagno, C. D. *Science* **2000**, *290*, 1555-1558. b) Yeates, T. O.; Padilla, J. E. *Curr. Opin. Struct. Biol.* **2002**, *12*, 464-270. c) Zhang, S. G.; Marini, D. M.; Hwang, W.; Santoso, S. *Curr. Opin. Chem. Biol.* **2002**, *6*, 865-871. d) Sarikaya, M.; Tamerler, C.; Jen, A. K. Y.; Schulten, K.; Baneyx, F. *Nat. Mater.* **2003**, *2*, 577-585. e) Seeman, N. C. *Biochemistry* **2003**, *42*, 7259-7269. f) Hess, H.; Bachand, G. D.; Vogel, V. *Chem. Eur. J.* **2004**, *10*, 2110-2116. g) MacPhee, C. E.; Woolfson, D. N. *Curr. Opin. Solid State Mat. Sci.* **2004**, *8*, 141-149. h) Rajagopal, K.; Schneider, J. P. *Curr. Opin. Struct. Biol.* **2004**, *14*, 480-486. i) Weibel, D. B.; Garstecki, P.; Ryan, D.; DiLuzio, W. R.; Mayer, M.; Seto, J. E.; Whitesides, G. M. *Proc. Natl. Acad. Sci. USA.* **2005**, *102*, 11963-11967. j) Xi, J.; Schmidt, J. J.; Montemagno, C. D. *Nat. Mater.* **2005**, *4*, 180-184. k) Astier, Y.; Bayley, H.; Howorka, S. *Curr. Opin. Chem. Biol.* **2005**, *9*, 576-584. l) Hiratsuka, Y.; Miyata, M.; Tada, T.; Uyeda, T. Q. P. *Proc. Natl. Acad. Sci. USA.* **2006**, *103*, 13618-13623. m) Woolfson, D. N.; Ryadnov, M. G. *Curr. Opin. Chem. Biol.* **2006**, *10*, 559-567. n) Jaeger, L.; Chworos, A. *Curr. Opin. Struct. Biol.* **2006**, *16*, 531-543.
3. For reviews, see: a) Estroff, L. A.; Hamilton, A. D. *Chem. Rev.* **2004**, *104*, 1201-1218. b) Sangeetha, N. M.; Maitra, U. *Chem. Soc. Rev.* **2005**, *34*, 821-836. c) De Loos, M.; Feringa, B. L.; van Esch, J. H. *Eur. J. Org. Chem.* **2005**, *17*, 3615-3631.
4. a) Kiyonaka, S.; Sada, K.; Yoshimura, I.; Shinkai, S.; Kato, N.; Hamachi, I. *Nat. Mater.* **2004**, *3*, 58-64. b) Lutolf, M. P.; Hubbell, J. A. *Nat. Biotechnol.* **2005**, *23*, 47-55. c) Ulijn, R. V. *J. Mater. Chem.* **2006**, *16*, 2217-2225. d) Ulijn, R. V.; Bibi, N.; Jayawarna, V.; Thornton, P. D.; Todd, S. J.; Mart, R. J.; Smith, A. M.; Gough, J. E. *Materials Today* **2007**, *10*, 40-48.
5. a) Zhang, S. *Nat. Biotechnol.* **2003**, *21*, 1171-1178. b) Silva, G. A.; Czeisler, C.; Niece, K. L.; Beniash, E.; Harrington, D. A.; Kessler, J. A.; Stupp, S. I. *Science* **2004**, *303*, 1352-1355.
6. As examples for pH-responsive supramolecular hydrogels: a) Haines, S. R.; Harrison, R. G. *Chem. Commun.* **2002**, 2846-2847. b) Kiyonaka, S.; Zhou, S. L.; Hamachi, I. *Supramol. Chem.* **2003**, *15*, 521-528. c) Zhou, S. L.; Matsumoto, S.; Tian, H. D.; Yamane, H.; Ojida, A.; Kiyonaka, S.; Hamachi, I. *Chem. Eur. J.* **2005**, *11*, 1130-1136. d) Khatua, D.; Maitib, R.; Dey, J. *Chem. Commun.* **2006**, 4903-4905.
7. a) Yang, Z. M.; Gu, H. W.;. Fu, D. G.; Gao, P.; Lam, J. K.; Xu, B. *Adv. Mater.* **2004**, *16*, 1440-1444. b) Yang, Z.; Liang, G.; Wang, L.; Xu, B. *J. Am. Chem. Soc.* **2006**, *128*, 3038-3043. c) Yang, Z.; Xu, B. *Adv. Mater.* **2006**, *18*, 3043-3046. d) Vemula, P. K.; Li, J.; John, G. *J. Am. Chem. Soc.* **2006**, *128*, 8932-8938. e) Toledano, S.; Williams, R. J.; Jayawarna, V.; Ulijn, R. V. *J. Am. Chem. Soc.* **2006**, *128*, 1070-1071. f) Yang, Z.; Liang, G.; Xu, B. *Soft Matter* **2007**, *3*, 515-520. g) Yang, Z.; Liang, G.; Ma, M.; Gao, Y.; Xu, B. *Small* **2007**, *3*, 558-562. h) Yang, Z.; Ho, P.-L.; Liang, G.; Chow, K. H.; Wang, Q.; Cao, Y.; Guo, Z.; Xu,

B. *J. Am. Chem. Soc.* **2007**, *129*, 266-267.

8. a) Zhang, Y.; Gu, H.; Yang, Z.; Xu, B. *J. Am. Chem. Soc.* **2003**, *125*, 13680-13681. b) Ogoshi, T.; Takashima, Y.; Yamaguchi, H.; Harada, A. *J. Am. Chem. Soc.* **2007**, *129*, 4878-4879.
9. a) Murata, K.; Aoki, M.; Suzuki, T.; Harada, T.; Kawabata, H.; Komori, T.; Ohseto, F.; Ueda, K.; Shinkai, S. *J. Am. Chem. Soc.* **1994**, *116*, 6664-6676. b) Lucas, L. N.; van Esch, J.; Kellogg, R. M.; Feringa, B. L. *Chem. Commun.* **2001**, 759-760. c) Yagai, S.; Karatsu, T.; Kitamura, A. *Chem. Eur. J.* **2005**, *11*, 4054-4063. d) De Jong, J. J. D.; Hania, P. R.; Pugzlys, A.; Lucas, L. N.; De Loos, M.; Kellogg, R. M.; Feringa, B. L.; Duppen, K.; van Esch, J. H. *Angew. Chem. Int. Ed.* **2005**, *44*, 2373-2376. e) Sakai, H.; Orihara, Y.; Kodashima, H.; Matsumura, A.; Ohkubo, T.; Tsuchiya, K.; Abe, M. *J. Am. Chem. Soc.* **2005**, *127*, 13454-13455. f) Ketner, A. M.; Kumar, R.; Davies, T. S.; Elder, P. W.; Raghavan, S. R. *J. Am. Chem. Soc.* **2007**, *129*, 1553-1559.
10 a) Irie, M.; Kunwatchakun, D. *Macromolecules* **1986**, *19*, 2476-2480. b) Mamada, A.; Tanaka, T.; Kungwatchakun, D.; Irie, M. *Macromolecules* **1990**, *23*, 1517-1519. c) Frkanec, L.; Jokic, M.; Makarevic, J.; Wolsperger, K.; Zinic, M. *J. Am. Chem. Soc.* **2002**, *124*, 9716-9717. d) Hirakura, T.; Nomura, Y.; Aoyama, Y.; Akiyoshi, K. *Biomacromolecules* **2004**, *5*, 1804-1809. e) Haines, L. A.; Rajagopal, K.; Ozbas, B.; Salick, D. A.; Pochan, D. J.; Schneider, J. P. *J. Am. Chem. Soc.* **2005**, *127*, 17025-17029. f) Tomatsu, I.; Hashidzume, A.; Harada, A. *Macromolecules* **2005**, *38*, 5223-5227.
11. a) Shinkai, S.; Ogawa, T.; Nakaji, T.; Kusano, Y.; Manabe, O. *Tetrahedron Lett.* **1979**, *20*, 4569-4572. b) Shinkai, S. *Pure. Appl. Chem.* **1987**, *59*, 425-430. c) Koumura, N.; Zijlstra, R. W. J.; van Delden, R. A.; Harada, N.; Feringa, B. L. *Nature* **1999**, *401*, 152-155. d) Balzani, V.; Credi, A.; Raymo, F. M.; Stoddart, J. F. *Angew. Chem. Int. Ed.* **2000**, *39*, 3349-3391. e) Irie, M. *Chem. Rev.* **2000**, *100*, 1685-1716. f) Brouwer, A. M.; Frochot, C.; Gatti, F. G.; Leigh, D. A.; Mottier, L.; Paolucci, F.; Roffia, S.; Wurpel, G. W. H. *Science* **2001**, *291*, 2124-2128. g) Raymo, F. M. *Adv. Mater.* **2002**, *14*, 401-414. h) Hernandez, J. V.; Kay, E. R.; Leigh, D. A. *Science* **2004**, *306*, 1532-1537. i) Kinbara, K.; Aida, T. *Chem. Rev.* **2005**, *105*, 1377-1400. j) Lehn, J.-M. *Chem. Eur. J.* **2006**, *12*, 5910-5915. k) Browne, W. R.; Feringa, B. L. *Nat. Nanotechnol.* **2006**, *1*, 25-35. l) Mayer, G.; Heckel, A. *Angew. Chem. Int. Ed.* **2006**, *45*, 4900-4921. m) Kay, E. R.; Leigh, D. A.; Zerbetto, F. *Angew. Chem. Int. Ed.* **2007**, *46*, 72-191. n) Balzani, V.; Credi, A.; Venturi, M. *NanoToday* **2007**, *2*, 18. o) Saha. S.; Stoddart, J. F. *Chem. Soc. Rev.* **2007**, *36*, 77-92. p) Credi, A.; Tian, H. *Adv. Funct. Mater.* **2007**, *17*, 679-682.
12. Mundi, C.; Back, M. H. *J. Photochem. Photobiol. A: Chem.* **1992**, *67*, 13-22.
13. a) Mason, T. G.; Weitz, D. A. *Phys. Rev. Lett.* **1995**, *74*, 1250-1253. b) Crocker, J. C.; Valentine, M. T.; Weeks, E. R.; Gisler, T.; Kaplan, P. D.; Yodh, A. G.; Weitz, D. A. *Phys. Rev. Lett.* **2000**, *85*, 888-891. c) Nowak, A. P.; Breedveld, V.; Pakstis, L.; Ozbas, B.; Pine, D. J.; Pochan, D.; Deming, T. J. *Nature* **2002**, *417*, 424-428.
14. Yamaguchi, S.; Matsumoto, S.; Ishizuka, K.; Iko, Y.; Tabata, K. V.; Arata, H. F.; Fujita, H.; Noji, H.; Hamachi, I. *Chem. Eur. J.* **2008**, *14*, 1891-1896.

15. a) Noji, H.; Yasuda, R.; Yoshida, M.; Kinoshita, K. Jr. *Nature* **1997**, *386*, 299-302. b) Yasuda, R.; Noji, H.; Yoshida, M.; Kinoshita, K. Jr.; Itoh, H. *Nature* **2001**, *410*, 898-904. c) Hirono-Hara, Y.; Noji, H.; Nishiura, M.; Muneyuki, E.; Hara, K. Y.; Yasuda, R.; Kinoshita, K. Jr.; Yoshida, M. *Proc. Natl. Acad. Sci. USA.* **2001**, *98*, 13649-13654. d) Itoh, H.; Takahashi, A.; Adachi, K.; Noji, H.; Yasuda, R.; Yoshida, M.; Kinosita, K. Jr. *Nature* **2004**, *427*, 465-468. e) Hirono-Hara, Y.; Ishizuka, K.; Kinosita, K. Jr.; Yoshida, M.; Noji, H. *Proc. Natl. Acad. Sci. USA.* **2005**, *102*, 4288-4293.

16. To examine the heat effect of the light irradiation, a control experiment using the thermal-responsive hydrogel[13] (**3**: GalNAc-suc-glu(*O*-methyl-*cyc*-pentyl)$_2$, 0.35 wt%) instead of the photo-responsive hydrogel **2** was conducted. In order to make this control system absorb the laser light similar to the hydrogel **2**, fumaric acid was mixed with the hydrogel **3** at the equimolar concentration to the gelator **2** (1.5 mM). The rotation of the microbead attached to $F_1$-ATPase in the hydrogel **3** including fumaric acid stopped by the gelation. However, even by the subsequent laser irradiation, the microbeads remained motionless (data not shown). Since the $T_g$ of this hydrogel **3** (48 ± 2 ºC) was lower than that of hydrogel **2** (63 ± 3 ºC), the insufficient heat generation for this control experiment was not realistic. Therefore, it is obvious that the heat effect of the light irradiation can be ruled out from the main factor to cause restart of the microbead rotation.

17. a) Bald, D.; Noji, H.; Yoshida, M.; Hirono-Hara, Y.; Hisabori, T. *J. Biol. Chem.* **2001**, *276*, 39505. b) Liu, H.; Schmidt, J. J.; Bachand, G. D.; Rizk, S. S.; Looger, L. L.; Hellinga, H. W.; Montemagno, C. D. *Nat. Mater.* **2002**, *1*, 173.

18. Rondelez, Y.; Tresset, G.; Nakashima, T.; Kato-Yamada, Y.; Fujita, H.; Takeuchi, S.; Noji, H. *Nature* **2005**, *433*, 773.

19. a) Hess, H.; Clemmens, J.; Qin, D.; Howard, J.; Vogel, V. *Nano lett.* **2001**, *1*, 235. b) Kocer, A.; Walko, M.; Meijberg, W.; Feringa, B. L. *Science* **2005**, *309*, 755. c) Muramatsu, S.; Kinbara, K.; Taguchi, H.; Ishii, N.; Aida, T. *J. Am. Chem. Soc.* **2006**, *128*, 3764. d) Volgraf, M.; Gorostiza, P.; Numano, R.; Kramer, R. H.; Isacoff, E. Y.; Trauner, D. *Nat. Chem. Biol.* **2006**, *2*, 47.

20. Ionov, L.; Stamm, M.; Diez, S. *Nano lett.* **2006**, *6*, 1982.

21. Kiyonaka, S.; Shinkai, S.; Hamachi, I. *Chem. Eur. J.* **2003**, *9*, 976-983.

22. Bald, D.; Noji, H.; Yoshida, M.; Hirono-Hara, Y.; Hisabori, T. *J. Biol. Chem.* **2001**, *276*, 39505-39507.

23. Itoh, H.; Takahashi, A.; Adachi, K.; Noji, H.; Yasuda, R.; Yoshida, M.; Kinosita, K. Jr. *Nature* **2004**, *427*, 465-468.

# Conclusion and Future Directions

## Conclusion

This thesis discussed about the development of the external-stimuli responsive supramolecular hydrogels and the application studies toward the smart biomaterials.

In Chapter 1, a pH-responsive volume change function has been successfully introduced into a supramolecular hydrogel consisting of glycol-lipid based hydrogelator by simple mixing with an appropriate structure and amount of amphiphilic carboxylic acid. In the 1:1 mol/mol mixture, the swollen hydrogel formed under neutral pH conditions, and it shrunk to almost half its original volume under acidic pH conditions. The structure and pH response of the mixed hydrogel were characterized by XRD, CLSM, TEM, SEM, and FT-IR spectroscopy. It is clear that well-developed fibers are self-assembled and entangled to form a stable hydrogel and the resultant gel fibers are densely packed along with charge neutralization of the carboxylic acid terminal (from carboxylate anion) under acidic conditions. This strategy could be applied for the development of the basic pH-responsive hydrogel composed with the hydrogelator and pyridine-tethered additive. Using this macroscopic pH response, not only the pH-triggered release of bioactive substances but also gel-to-gel communication systems consisting with enzymatic reaction have been carried out. In this mixed supramolecular hydrogel, the hydrogelator provides a stable hydrogel structure and the additives act as a commander sensitive to an environmental pH signal. The present supramolecular copolymerization strategy should be useful for the construction of novel stimuli-responsive soft-materials.

In Chapter 2, a new photo-responsive hydrogel composed of self-assembled small molecules (gelators) was described. This supramolecular hydrogel showed a light-induced gel-to-sol phase transition, resulting in a drastic change of mechanical toughness and aggregation morphology due to the trans/cis photo-isomerization of the double bond unit of the gelator. As well as the bulk gel formation, photo-responsive gel droplets having nano- or pico-L volume that showed photo-induced gel/sol transition were successfully developed, in which the inter-droplet mass transport and the subsequent enzymatic reactions in the interior of the gel droplets were photo-triggered. Focused laser light irradiation allows one to spatially and temporarily regulate the stepwise fusion of the gel droplets mediating a precisely controlled inter-droplet reaction. A novel supramolecular container with such photo-responsiveness might be promising as one of the attractive semi-wet biomaterials.

Chapter 3 described that a few of photo-responsive supramolecular hydrogelators, containing the gelator used in Chapter 2, were newly discovered, not only the gel-sol but also sol-gel transition of which was pseudo-reversibly induced by light among a focused library of glycolipid-based hydrogelators bearing a fumaric amide unit as a trans-cis photo-switching module. The entanglement of the supramolecular fibers produced the nano-meshes the size of which was roughly evaluated to be about 250 nm by the confocal laser scanning microscopy observation for the size dependent Brownian motion of the nano-beads in the supramolecular hydrogel. It was clearly shown that such nano-meshes became a physical obstacle to capture the sub-micro to micro meter sized substrates such as the beads, or *E. Coli* bacteria. On the benefit

of the photo-responsive property of the supramolecular nano-meshes, using a focused laser light, we succeeded in the off-on switching of the bacteria movement and the rotary motion of the beads-tethered $F_1$-ATPase, a bimolecular motor protein, at a single molecular level in the supramolecular hydrogel matrix.

I believe that the present studies from a molecular level to the self-assembled materials in water contribute to the design of external stimuli responsive hydrogels, and moreover the demonstration of the supramolecular hydrogels as sophisticated biomaterials may lead to create new possibilities in gel sciences.

## Future Directions

In the future of nanotechnologies, developments of biomaterials which can encapsulate, isolate, and manipulate biomolecules such as DNA, RNA, protein, and cell at a single molecule level should be more emphasized. Supramolecular architectures constructed by hierarchically assembly of small molecules, in particular, supramolecular hydrogels are attractive materials because they display various aggregate morphologies in mesoscopic scales. Although various supramolecular materials have been developed, it is doubted whether these materials have been useful to the biosciences in the mesoscopic regions. This is because regulation systems of the developed supramolecular aggregates in this scale have not sufficiently been established. To overcome this problem, the author believes that micro-fluidic devices will become one of powerful tools to precisely control molecular aggregates. In deed, several researchers very recently reported reproducible techniques to prepare femto-liter sized W/O emulsions able to capsulate a single biomolecule by using micro fluidic systems. The applications of this strategy to produce supramolecular microgels, as mentioned at chapter 2, should be intriguing. In addition, concerning the manipulation method of the microgel, the usages of nonlinear optical effects such as two-photon stimuli will be effective in pico- or femto-litter sized 3D-fabrications in a microgel, so that this photo-manipulation can not only regulate the communication between microgels or maicrogel/bulk media, but also facilitate to manipulate a biomolecule at a single molecule level in a microgel.

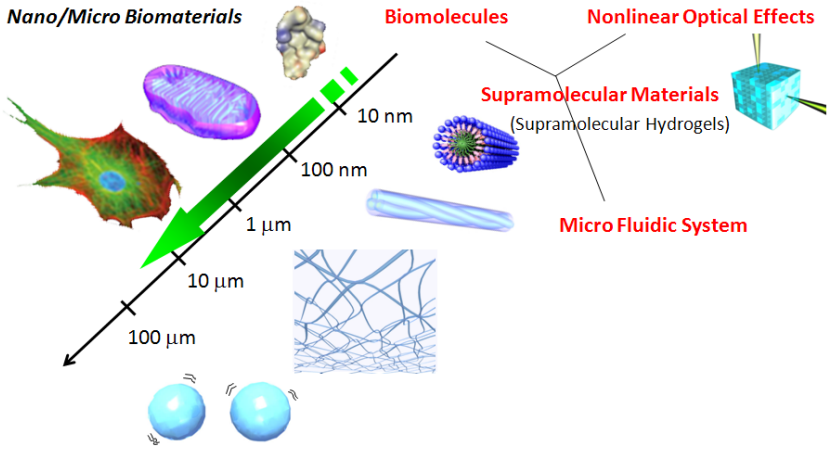


For such promising future, I believe that time has come to enjoy and join the essence of molecular- and bio-nanotechnologies in many ways.

## List of Publications

**Chapter 1** pH-Responsive Shrinkage/Swelling of Supramolecular Hydrogel Composed of Two Small Amphiphilic Molecules

Shan-Lai Zhou, **Shinji Matsumoto**, Huai-Dong Tian, Hiroki Yamane, Akio Ojida, Shigeki Kiyonaka,and Itaru Hamachi

*Chemistry – A European Journal* **2005**, *11*, 1130-1136.

**Chapter 2** Photo-responsive gel droplet as a nano- or pico-litre container comprising a supramolecular hydrogel

**Shinji Matsumoto**, Satoshi Yamaguchi, Atsuhiko Wada, Harunobu Komatsu, Masato Ikeda, and Itaru Hamachi

*Chemical Communications,* "Hot Article", **2008**, in press. (DOI**:** 10.1039/b719004b)

**Chapter 3** Thermally responsive supramolecular nano-meshes for on/off switching of the rotary motion of $F_1$-ATPase at a single molecular level

Satoshi Yamaguchi, **Shinji Matsumoto**, Koji Ishizuka, Yuko Iko, Kazuhito V. Tabata, Hideyuki Arata, Hiroyuki Fujita, Hiroyuki Noji, Itaru Hamachi

*Chemistry – A European Journal*, **2008**, *14*, 1891-1896.

Photo Gel-Sol/Sol-Gel Transition and Its Patterning of a Supramolecular Hydrogel as Stimuli-responsive Biomaterials

**Shinji Matsumoto**, Satoshi Yamaguchi, Shiori Ueno, Harunobu Komatsu, Masato Ikeda, Koji Ishizuka, Yuko Iko, Kazuhito V. Tabata, Hiroyuki Aoki, Shinzaburo Ito, Hiroyuki Noji and Itaru Hamachi

*Chemistry – A European Journal*, **2008**, in press. (DOI: 10.1002/chem.200701904)

## Other Publications

**1.** Urea-functionalized Resorcinarenes: Preparation, Self-folding, and Their CD Phenomena Caused by Chiral Urea Termini through Intramolecular Hydrogen Bonding Interactions
Osamu Hayashida, Jun-ichi Ito, **Shinji Matsumoto**, and Itaru Hamachi
*Chemistry Letters* **2004**, *33*, 994-995.

**2.** Preparation and unique circular dichroism phenomena of urea-functionalized self-folding resorcinarenes bearing chiral termini through asymmetric hydrogen-bonding belts
Osamu Hayashida, Jun-ichi Ito, **Shinji Matsumoto** and Itaru Hamachi
*Organic & Biomolecular Chemistry* **2005**, *3*, 654-660.

**3.** Globular Self-aggregates Formed with a Urea-functionalized Resorcinarene Derivative in Chloroform
Osamu Hayashida, **Shinji Matsumoto**, and Itaru Hamachi
*Chemistry Letters* **2005**, *34*, 1276-1277.

**4.** The Supramolecular Hydrogel Toward "The Smart Biomaterials"
**Shinji Matsumoto** and Itaru Hamachi
*Dojin News* **2006**, *118*, 1-16.

## List of Presentations

### *International Symposium*

**1.** "pH-Responsive Volume Change of Supramolecular Hydrogel Composed of Two Components of Amphiphilic Small Molecules"
**Shinji Matsumoto**, Shan-Lai Zhou, Shigeki Kiyonaka, and Itaru Hamachi.
1st International Symposium on Functional Innovation of Molecular Informatics, Fukuoka, October 2004.

**2.** "A Novel Photo Responsive Supramolecular Hydrogel"
**Shinji Matsumoto**, Satoshi Yamaguchi, and Itaru Hamachi.
The International 21st Century COE Symposium of BINDEC Chemistry Network-BINDEC2005, Osaka, October 2005.

### *Domestic Symposium*

**1.** "Novel Supramolecular Aggregates-1: Preparation and Aggregation Behavior of a Macrocyclic Compound Bearing Eight Urea Residues"
**Shinji Matsumoto**, Osamu Hayashida, and Itaru Hamachi.
83rd Annual Meeting of Chemical Society of Japan, Tokyo, March 2003.

**2.** "Polar Domain Constructed by Self-Assembly of Macrocyclic Molecules toward Anion Recognition Sites."
**Shinji Matsumoto**, Osamu Hayashida, and Itaru Hamachi.
40th Symposium on Affiliated Chemical Society in Kyushu, Fukuoka, July 2003.

**3.** "The Construction of Semi-wet Protein/Peptide Array with Supramolecular Hydrogel"
**Shinji Matsumoto**, Shigeki Kiyonaka, Nobuo Kato, and Itaru Hamachi.
18th Symposium on Biofunctional Chemistry, Kumamoto, October 2003.

**4.** "Novel Supramolecular Hydrogel-1: The Conferment of pH Responsive Functionalization by Copolymerization"
**Shinji Matsumoto**, Shan-Lai Zhou, Shigeki Kiyonaka, and Itaru Hamachi.
84th Annual Meeting of Chemical Society of Japan, Hyogo, March 2004.

**5.** "Novel Supramolecular Semi-wet Materials (1): The Development of Photo Responsive Supramolecular Hydrogel Based on Glycosylated Amino Acid"
**Shinji Matsumoto**, Shigeki Kiyonaka, and Itaru Hamachi.
85th Annual Meeting of Chemical Society of Japan, Kanagawa, March 2005.

**6.** "Exploitation of a Photo-Responsive Supramolecular Hydrogel and a Novel Photo Patterning with Its "Gel-Sol" Transition"
**Shinji Matsumoto**, Satoshi Yamaguchi, and Itaru Hamachi.
20th Symposium on Biofunctional Chemistry, Nagoya, September 2005.

**7.** "Smart Biomaterials (2): Immobilization of Biomolecules into Photo Responsive Supramolecular Hydrogel"
**Shinji Matsumoto**, Satoshi Yamaguchi, and Itaru Hamachi.
86th Annual Meeting of Chemical Society of Japan, Chiba, March 2006.

**8.** "Development of the Supramolecular Smart Materials (2): Development of Photo-Responsive Supramolecular Hydrogel toward Nano-Bio Materials"
**Shinji Matsumoto**, Satoshi Yamaguchi, Koji Ishizuka, Yuko Iko, Kazuhito V. Tabata, Hideyuki Arata, Hiroyuki Aoki, Shinzaburo Ito, Hiroyuki Fujita, Hiroyuki Noji, and Itaru Hamachi.
87th Annual Meeting of Chemical Society of Japan, Osaka, March 2007.

**9.** "Regulation of Biomolecular Motions Using Stimuli-Responsive "Nano-Meshes""
**Shinji Matsumoto**, Satoshi Yamaguchi, Koji Ishizuka, Yuko Iko, Kazuhito V. Tabata, Hideyuki Arata, Hiroyuki Aoki, Shinzaburo Ito, Hiroyuki Fujita, Hiroyuki Noji, and Itaru Hamachi.
56th SPSJ Symposium on Macromolecules, Nagoya, September 2007.

## List of Honors

**1.** Presentation Award
87th Annual Meeting of Chemical Society of Japan, Osaka, March 2007.